CHALMERS
UNIVERSITY OF TECHNOLOGY

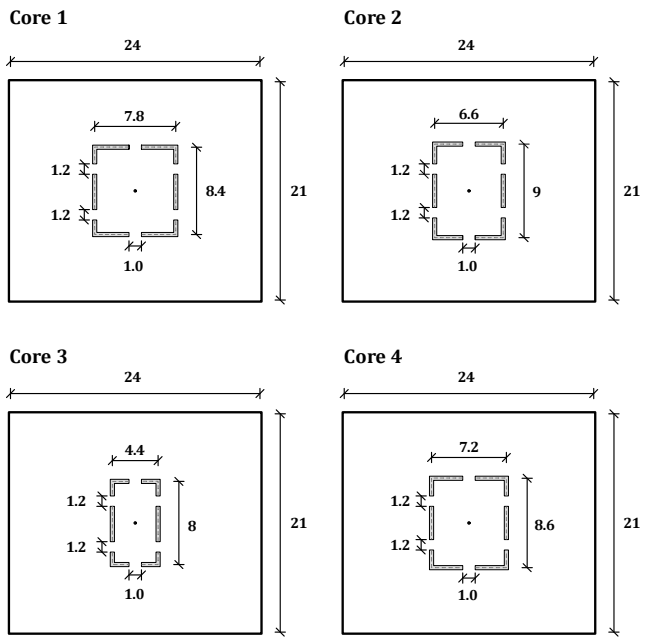

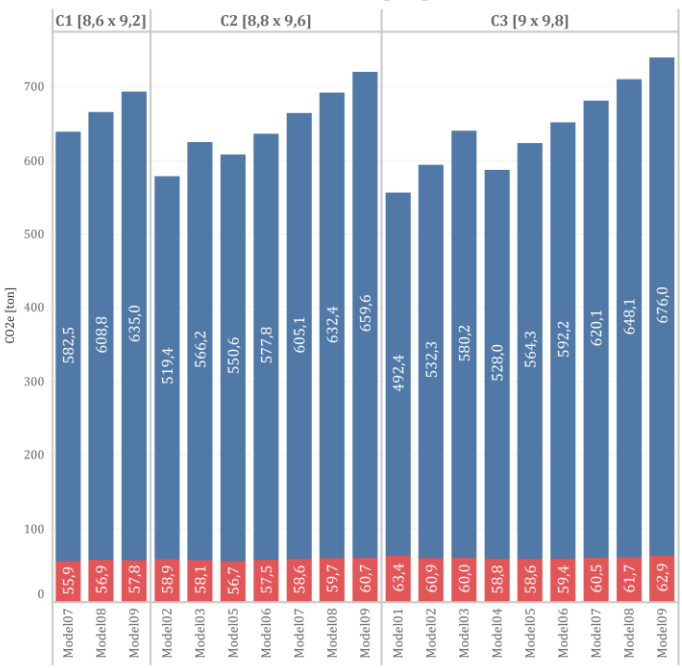

Parametric Design of Efficient High-Rise Buildings

Development of a Design and Analysis Tool for the Early Design Stages

Master's thesis in Structural Engineering and Building Technology

SAMIRA SARRESHTEDARI

DEPARTMENT OF ARCHITECTURE AND CIVIL ENGINEERING

CHALMERS UNIVERSITY OF TECHNOLOGY
Gothenburg, Sweden 2023
www.chalmers.se

MASTER'S THESIS 2023

Parametric Design of Efficient High-Rise Buildings

Development of a Design and Analysis Tool for the Early Design Stages

SAMIRA SARRESHTEDARI

CHALMERS
UNIVERSITY OF TECHNOLOGY

Department of Architecture and Civil Engineering
Research group for Architecture and Engineering
CHALMERS UNIVERSITY OF TECHNOLOGY
Gothenburg, Sweden 2023

Parametric Design of Efficient High-Rise Buildings
Development of a Design and Analysis Tool for the Early Design Stages

Master's Thesis in Structural Engineering and Building Technology

SAMIRA SARRESHTEDARI

Supervisors: Daniel Jonsson & Andreas Lindelöf, VBK Konsulterande Ingenjörer
Examiner: Mats Ander, Department of Architecture and Civil Engineering,
Chalmers University of Technology

Department of Architecture and Civil Engineering
Research group for Architecture and Engineering
Chalmers University of Technology
SE-412 96 Gothenburg
Sweden
Telephone: + 46 (0)31-772 1000

Cover:
Illustration of different core models with a corresponding bar chart showing the CO2e of the different models.

Department of Architecture and Civil Engineering
Gothenburg, Sweden, 2023

Parametric Design of Efficient High-Rise Buildings

Development of a Design and Analysis Tool for the Early Design Stages

Master's Thesis in Structural Engineering and Building Technology

SAMIRA SARRESHTEDARI

Department of Architecture and Civil Engineering
Research group for Architecture and Engineering
Chalmers University of Technology

Abstract

High-rise buildings have become increasingly popular during the past few decades. They have a large potential in providing more floor area for the same building footprint. However, high-rise buildings also require more material in their structural systems to withstand the wind loads that they are subjected to due to their height. High-rise buildings are therefore generally regarded as an unsustainable building type, making it even more important to analyze and optimize their structural systems in early design stages to minimize their environmental impact.

This thesis investigates how a parametric design and analysis tool can be developed and utilized in the early design stages of a high-rise building. By parametrizing a FE-model of the core, the tool computes data on the structural performance and climate impact of several designs. This allows for evaluation of an optimal structural design in regard to low climate impact while fulfilling the structural requirements.

The tool development consists of an intuitive tool for the very early design stages in Rhinoceros 3D and Grasshopper, as well as an in-depth analysis tool in ETABS with scripting in Excel and VBA. The aim with the Rhino/Grasshopper tool is to obtain preliminary dimensions and understand the structural behavior of the core. The tool in ETABS computes data on the structural performance and CO2e of several designs, allowing to make informed design decisions based on a set of evaluation criteria.

The outcome of this thesis indicates that there is a significant possibility of reducing the material usage and climate impact of the core of a high-rise building. The most important factor is to reduce the amount of concrete in the core, which is preferably achieved by increasing the dimensions of the core and decreasing the core wall thicknesses. Lastly, the thesis concludes that the utilization of parametric tools in the construction industry is a valuable asset in decreasing the climate impact of high-rise buildings.

Key words: High-rise buildings, tall buildings, optimization, CO2e, parametric design, grasshopper, octopus, python, ETABS, VBA, tableau

Preface

This thesis marks the end of my 6.5 years of studies at the Architecture and Engineering program at Chalmers University of Technology, graduating with a double degree in architecture and structural engineering.

In this thesis, a design and analysis tool has been developed to parametrically design and evaluate the structural design of a core of a high-rise building. The thesis was performed as a collaboration between the Department of Architecture and Civil Engineering, Chalmers University of Technology and VBK Konsulterande Ingenjörer. The extensive part of the work was carried out at VBK during the fall of 2023.

I would like to thank Andreas Lindelöf for giving me the opportunity to do this thesis and customizing the project to my interest in high-rise buildings and parametric design. I would also like to express my gratitude to my supervisor Daniel Jonsson and examiner Mats Ander for all their invaluable guidance and support throughout the thesis. Moreover, I would like to thank my colleagues at VBK who have provided me with helpful advice and cheered me on. Lastly, thank you to my opponents Linnéa Gabrielsson and Maria Karlsson for valuable feedback.

Gothenburg, January 2024

Samira Sarreshtedari

Contents

Nomenclature

Below are the notations of parameters and variables that have been used in this thesis.

Greek lower case letters

γ_d	Partial coefficient depending on safety class [-]
ρ_{air}	Air density [kg/m^3]
ρ	Material density [kg/m^3]
α_n	Reduction factor for multistory buildings [-]
ψ_i	Load reduction factor for variable loads [kg/m^3]

Roman upper case letters

A_c	Cross-section area of concrete [m^2]
E	Young's modulus [GPa]
G_k	Characteristic permanent load [kN]
I	Second moment of inertia [mm^4]
M_x	Moment around x-axis [Nm]
M_y	Moment around y-axis [Nm]
$Q_{d,SLS}$	Load combination in SLS [kN/m^2]
$Q_{d,ULS}$	Load combination in ULS [kN/m^2]
Q_k	Characteristic variable load [kN]
T	Shear force [N]

Roman lower case letters

b	Building width perpendicular to the direction of the wind speed [m]
C_0	Orography factor [-]
c_{dir}	Directional factor [-]
c_e	Exposure factor [-]
C_p	Windward/leeward coefficient [-]
$c_{pe,10}$	Pressure coefficient [-]
$CsCd$	Structural factor [-]
c_{season}	Seasonal factor [-]

f_{ck}	Characteristic compressive strength of concrete [MPa]
f_{yk}	Characteristic yield stress of steel [MPa]
g_k	Characteristic permanent load [kN/m^2]
h	Building height [m]
$k1$	Turbulence factor [-]
k_r	Terrain factor [-]
n	Number of stories above the loaded element [-]
q_b	Basic velocity pressure [kN/m^2]
q_k	Characteristic variable load [kN/m^2]
q_p	Peak velocity pressure [kN/m^2]
s_k	Characteristic snow load on the ground based on geographical location [kN/m^2]
t	Cross-section thickness [-]
u_{max}	Maximum horizontal displacement at the top of a building [mm]
v_b	Reference wind speed [m/s]
$v_{b,0}$	Fundamental reference wind speed [m/s]
w_e	External wind load [kN/m^2]
z	Observed building height [m]
z_{max}	Building height [m]
z_{min}	Minimum building height [m]
z_0	Roughness length [m]
$z_{0,II}$	Roughness length for terrain category II [m]

Acronyms

Below is a list of acronyms that have been used in this thesis.

API	Application Programming Interface
CO2e	Carbon dioxide equivalent
EC	Eurocode
EKS	Europeiska Konstruktionsstandarder
FE	Finite Element
LCA	Life Cycle Assessment
SDL	Superimposed Dead Load
SLS	Serviceability Limit State
SS	Svensk Standard
ULS	Ultimate Limit State
VBA	Visual Basic for Application

List of Figures

List of Tables

1 Introduction

This chapter introduces the problem statement that will be researched as well as the aim, scope and method of the thesis.

1.1 Background

High-rise buildings have become increasingly popular during the past decades. In Sweden, the number of high-rise buildings during the past few years has significantly increased (CTBUH, 2024). With growing populations around the world, there is an increasing need for more habitable space in city centers. High-rise buildings have a massive potential in generating space vertically from a smaller piece of land, arguably making them a fundamental part of growing cities.

By increasing the number of stories in a high-rise building, more floor area is provided for the same building footprint, which increases the profit of the building. However, high-rise buildings also require more material in their structural systems to withstand the wind loads that they are subjected to due to their height (Yeang, 2007). This leaves less occupiable space and increases material usage. High-rise buildings are therefore generally regarded as an unsustainable building type, making it even more important to analyze and optimize their structural systems in early design stages to minimize their climate impact.

During the past years, the construction company VBK Konsulterande Ingenjörer has been involved in the design of several new high-rise buildings in Sweden, including the 247 m tall building Karlatornet that is situated in Gothenburg. A methodology for finding efficient structures based on stiffness relationships has been developed by VBK, where the workflow allows for a parametric approach to enable numerous combinations being evaluated and compared at an early design stage. Although already proven its worth, the workflow still has a lot of unfulfilled potential and need for further development. This thesis will therefore focus on developing the workflow and extending it to include an additional tool in Rhino/Grasshopper.

1.2 Aim

The aim of this thesis is to gain an understanding of how parametric design can be utilized during early design stages of high-rise buildings. This is achieved by developing a design and analysis tool, useful for both architects and structural engineers. In addition, the thesis aims to lead to in-depth knowledge of the structural behavior and complexity of high-rise buildings.

The aim of the tool development itself is to obtain preliminary dimensions of the core. Furthermore, the tool will perform FE-analyses and compute data on the structural performance of the core of a high-rise building, making a preliminary structural design for each given set of parameters. Visualizations in tables, graphs and diagrams will show the structural performance and climate impact of

several designs, allowing for evaluation of an optimal structural design of the core based on a set of evaluation criteria.

1.2.1 Objectives

The aim of this thesis will be achieved by fulfilling the following objectives:

- Identification of key parameters that affect the structural stability of high-rise buildings and relevant standards through a literature study.
- Tool development and optimization in Rhinoceros 3D, Grasshopper and Karamba3D to understand how a high-rise building behaves and to obtain preliminary dimensions of the core.
- Tool development and optimization in ETABS, Excel/VBA and Tableau to compute and iterate several structural designs of the core.
- Collection of computed data and visualizations in tables, graphs and diagrams for analysis and evaluation of different structural designs with regard to climate impact.

1.3 Method

The thesis initiates with a comprehensive literature study on high-rise buildings and commonly used structural systems. The literature study is conducted to gain an understanding of the research field and identify the key parameters that affect the structural stability of high-rise buildings. In addition, the literature study aims to showcase the complexity of high-rise buildings and how a parametric approach can be beneficial in the early design stages.

In the following phase, the tool development will be performed in two steps:

- **Rhino/Grasshopper Tool:** An intuitive tool in Rhino using Grasshopper and Karamba3D where the aim is to give the user an understanding of how the core of a high-rise building behaves. Preliminary dimensions of the core will also be obtained from the tool. The Rhino/Grasshopper tool is further explained in chapter 1.3.2.1.

- **ETABS/VBA Tool:** Tool development in ETABS, Excel/VBA and Tableau where FE-analysis of the core is performed, and data of the structural performance is extracted and visualized. The development will focus on parametrization of the core of a high-rise building. The ETABS/VBA tool is further explained in chapter 1.3.2.2.

Lastly, through the literature study, tool development and analysis of the results, an evaluation regarding the usefulness of the developed tool in terms of time efficiency and savings in environmental impact will be made. A discussion of the optimal structural design in regard to the design that has the lowest climate impact while fulfilling the maximum allowed horizontal displacement will also be provided.

1.3.1 Previous Workflow

The previous workflow at VBK consisted of manually creating a FE-model of a high-rise building in the finite element software ETABS. The model could then be modified to a certain extent by using a script in Excel through VBA, utilizing the ETABS API. The previous possible modifications were changes in the thickness of the core walls at different stories.

The FE-analyses were performed in ETABS and data was extracted from ETABS and stored in Excel. The data was then visualized in Tableau, allowing the structural behavior of the different alternative designs to easily be analyzed and compared.

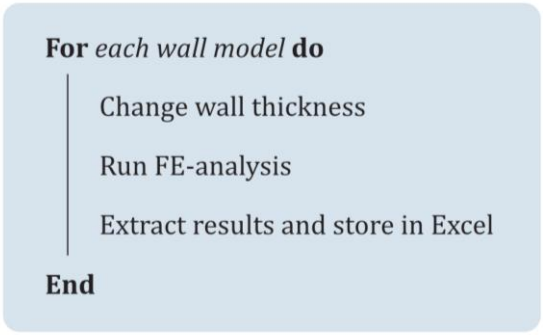

Figure 1.1: Pseudo-code describing the previous workflow at VBK.

1.3.2 Tool Development

1.3.2.1 Rhino/Grasshopper Tool

The aim of the Rhino/Grasshopper tool is to act as an intuitive tool at very early design stages to obtain an understanding of the structural behavior of a high-rise building. In addition, the tool will output preliminary dimensions of the core based on certain displacement criteria. The preliminary core dimensions will serve as a guide to set the domain of core dimensions in the ETABS/VBA tool. A link between Grasshopper and ETABS will not be developed as it is judged to be more efficient for the workflow as well as more user friendly to keep all input in Excel rather than in both Grasshopper and Excel.

The Rhino/Grasshopper tool will use the plug-in Karamba3D for structural analysis. A high-rise building will be modelled in Grasshopper where the dimensions of the core and building footprint will be parametrized. The tool will output the wind load distribution, moment and shear force distribution and the maximum horizontal displacement of the core.

1.3.2.2 ETABS/VBA Tool

The ETABS/VBA tool will consist of further developing the previous workflow at VBK. The main addition to the workflow will consist of parametrizing the dimensions of the core. This will allow several core models with different dimensions to test different wall thickness according to a set amount of wall models. Additionally, the number of openings of the core and positions of the openings will also be parametrized. The extension to the workflow is illustrated in red in Figure 1.2 below.

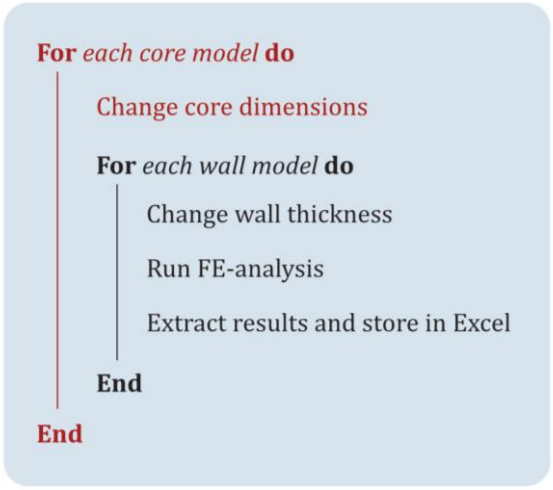

Figure 1.2: Pseudo-code describing the extension of the previous workflow marked in red.

The building will be partially modelled in ETABS and partially modelled through Excel/VBA. In addition to the core walls, slabs and columns will also be modelled through Excel/VBA. This is to allow for easy changes in geometrical properties, number of columns, column positions and stiffness modifiers.

The aim of the ETABS/VBA tool is to perform in-depth analyses of a high-rise building in the early design stages. The FE-analysis in the ETABS/VBA tool will be more detailed and reliable than the FE-analysis in the Rhino/Grasshopper tool. This is due to ETABS having more features and properties, allowing for an analysis of a model that is much more refined and closer to the behavior of a building in reality.

In contrast to the scope of the Rhino/Grasshopper tool, the ETABS/VBA tool will compute parameters such as required amounts of reinforcement and CO2e of the different structural designs. This will be achieved by developing an extension to the script for the previous workflow as well as computing post-calculations of the results. The data from the FE-analysis will be extracted from ETABS and stored in Excel for visualization in Tableau. The visualizations will show the structural performance of several designs, allowing to make informed design decisions based on a set of evaluation criteria.

1.4 Scope

The tool will consider a given high-rise building typology consisting of an 80-130 m tall building with a rectangular concrete core and columns at the facade. The addition of outriggers or other stiffening systems are not considered. Rather, the shear walls of the core are assumed to provide all horizontal stiffness. Other types of structural systems or materials will not be considered as the high-rise building defined above is the most common in its structural system for its height. It is therefore the most relevant case to investigate to make the tool as applicable as possible.

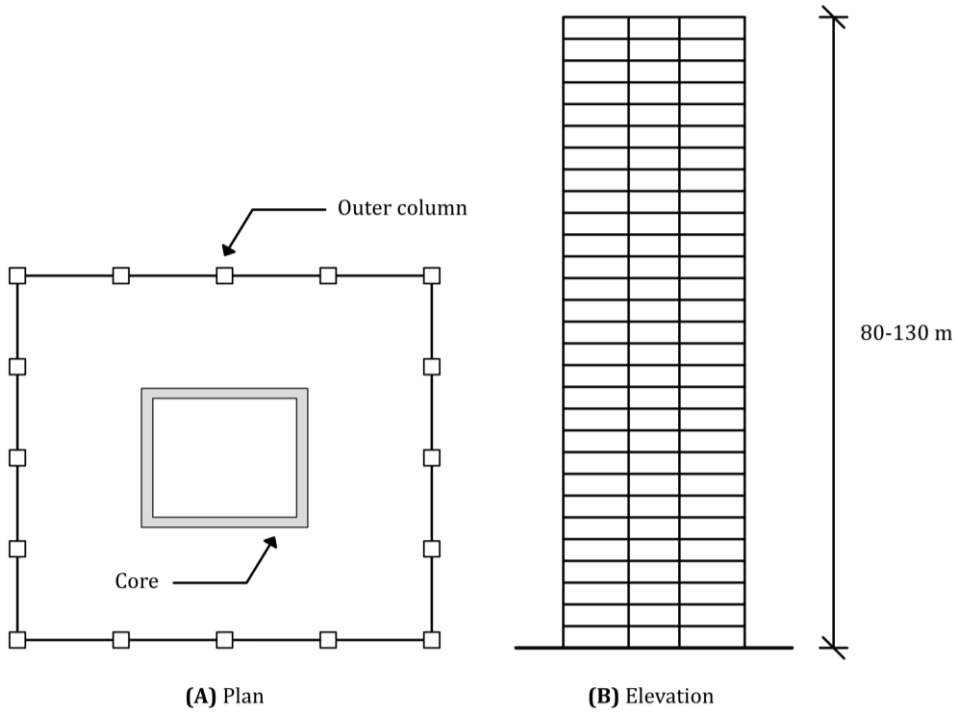

Figure 1.3: Illustration of the high-rise building typology that will be considered in this thesis.

The tool is to be used in Sweden and therefore the preliminary dimensioning will be based on the European standards Eurocode SS-EN 1991 together with additional standards by the Swedish Annex EKS 12 (BFS 2022:4).

The foundation conditions and piles are of great importance for the structural stability of high-rise buildings. Ultimately, all loads acting on the building are transferred down to the foundation. However, since the foundation design is another type of investigation, this will not be included in this thesis. To obtain fair results, piles will be included in the model in the ETABS/VBA tool and their type and properties will be based on reference projects. Furthermore, the seismic or dynamic performance of the core will not be considered.

1.4.1 Limitations

The limitations of the thesis are the following:

- Wind loads will be calculated according to SS-EN 1991-1-4:2005 for the Rhino/Grasshopper tool and auto-generated in ETABS according to EC for the ETABS/VBA tool.
- The core will be placed in the center of the building and only one core will be considered.
- The structural performance of the columns at the facade will not be considered. Rather, they will only be modelled stiff enough to handle the vertical loads acting on the building.
- Long-term effects such as creep, shrinkage and differential settlements will not be considered.
- No inner core walls will be modelled as their configuration depends on the architectural requirements of the core. The inner core walls are much less stiff than the core walls, thus their exclusion will not have a significant effect on the structural performance of the core.
- Since the acceleration of an 80-130 m tall high-rise building is rarely the dimensioning factor over the maximum allowed displacement at the top of the building, the dynamic performance of the building will not be studied.

1.5 Ethical, Ecological and Social Impact

The ecological impacts of this thesis are linked to the United Nations' Goals for Sustainable Development, in particular goal 11 *Sustainable Cities and Communities* (United Nations, n.d.). By developing a tool that can be used to develop and iterate the structural system of a high-rise building, more sustainable choices in terms of material usage and CO2e can be made in early design stages, reducing the overall environmental impact of the building at later stages. The tool will aid in visualizing the differences in climate impact of different structural designs, ultimately showing that informed design decisions in early design stages can have a large impact in the final carbon footprint of the building.

Ethical and social aspects are not considered in this thesis as the focus is on the structural design of high-rise buildings at early design stages.

1.6 Reading Advice

This thesis is divided into several chapters that are built upon each other. A brief description of the content of each chapter is given below.

1. Introduction
Presents the background of the chosen field of research along with the aim, method and scope of the thesis.

2. Theory
Provides theory about high-rise buildings, structural systems in high-rise buildings and the potential of utilizing parametrization when performing FE-analyses of high-rise buildings.

3. Digital Tools
Introduces the digital tools that are used in this thesis to develop the Rhino/Grasshopper and ETABS/VBA tool.

4. Rhino/Grasshopper Tool
Introduces the development of the Rhino/Grasshopper tool and a case study to evaluate the tool.

5. Reference Building
Introduces the reference building that the ETABS/VBA tool will be based on along with relevant input data.

6. ETABS/VBA Tool
Introduces the development of the ETABS/VBA tool as well as outcome and results of the tool.

7. Discussion
Analysis and discussion of the two developed tools, identifying strengths and weaknesses of each tool.

8. Conclusions
Concludes the thesis with a summary and reflections on future research.

2 Theory

This chapter presents an overview of high-rise buildings and the complexity of their structural design, identifying the need for parametrization in early design stages.

2.1 Definitions

In general, a high-rise building is considered to be a structure that has multiple floors and is notable for its height (Cortese, 2018). There is no precise definition of the number of floors or height required to be considered a high-rise building, but there are some guidelines that are widely accepted.

One definition of a high-rise building is that if the building aspect ratio is more than 5:1, then the building may be considered tall (The Concrete Centre, 2014). The building aspect ratio is the height divided by the lowest lateral dimension. For a building to be considered a skyscraper, the structure must be self-supporting, at least 50 % of its height must be occupiable and the height should rise to a minimum of 150 meters (Cortese, 2018). The Council on Tall Buildings and Urban Habitat has defined two other categories to distinguish remarkably tall structures from other skyscrapers (CTBUH, n.d.). These include supertall and megatall buildings. Supertall buildings have a minimum height of 300 m, while megatall buildings have a minimum height of 600 m.

2.2 History of High-Rise Buildings

The first generation of high-rise buildings appeared in the 1880's in Chicago and New York (Marshall, 2015). Designed by architect and engineer William Le Baron Jenney in 1884, Chicago's Home Insurance Building is considered to be the first tall building of the industrial era. At a height of 42 m, a load-bearing metal structural frame design was utilized which did not only make the structure fire resistant, but it also weighed a third as much by using iron and steel rather than stone or masonry. This allowed the building to reach taller heights without being limited by the strength of its outer walls.

Chicago's Home Insurance Building ignited an architectural movement called the Chicago School (Marshall, 2015). The Chicago School developed innovative tall buildings in a commercial style, driving America's technological advancement forward during the late 19th and early 20th centuries. Some recognizable features of the Chicago School include the use of steel-frame structures with masonry cladding in commercial buildings.

From the 1960s, the Second Chicago school emerged from the work of architect Ludwig Mies van der Rohe and structural engineer Fazlur Khan (Condit et al., 1980). While working for Skidmore, Owings & Merill, Khan introduced a new structural concept of framed tubes in high-rise buildings, which first appeared in the Dewitt Chestnut Apartments in 1965. His concept used the exterior wall perimeter of a building to simulate a thin-walled tube structure formed by closely spaced exterior columns of reinforced concrete. This revolutionized the

high-rise building design and laid the groundwork for future tube-framed structures such as Chicago's John Hancock Center, New York's World Trade Center and Kuala Lumpur's Petronas Towers.

2.3 Why High-Rise Buildings?

There are several reasons why high-rise buildings are built and have been built over the years. Historically, tall structures such as the pyramids of Giza and the Eiffel Tower were built as icons representing a city and symbolizing power. High-rise buildings were also developed as a response to technological advancements, increasing land prices and a high demand to live and work in city centers (Al-Kodmany, 2012). Today, high-rise buildings are built as a combination of these reasons where urbanization and growing populations are major factors.

According to the UN, 55 % of the world's population currently live in urban areas (UN, n.d.). This proportion is expected to increase to 68 % by 2050. The increase in urbanization and rapid growth of the population worldwide sets demands on already highly dense cities to provide even more habitable space. To accommodate large populations in urban areas, high-rise buildings have become more common in both low-rise and high-rise cities (Al-Kodmany, 2012). In high-rise cities such as New York and Singapore, the geographical boundaries limit the horizontal growth of the city, leading to a necessity of expanding the city vertically. In low-rise cities in Europe, the limited space in urban areas and interest in promoting a city has made high-rise buildings more popular.

2.4 High-Rise Buildings in Sweden

Sweden is generally not known as a high-rise country. Over the years, high-rise buildings in Sweden have had a height of around 50-80 m (CTBUH, 2024). Some buildings include the first Gothia Tower (Gothenburg, 1988) with a height of 79.5 m and Kronprinsen (1964, Malmö) with a height of 82 m. During the past decade, there has been an increase in the number of high-rise buildings with a height of around 80-130 m. Some examples include The Point (2019, Malmö) with a height of 110 m and Victoria Tower (2011, Stockholm) with a height of 117.6 m. The two tallest buildings in Sweden are Turning Torso (2005, Malmö) with a height of 190 m and Karlatornet (2024, Gothenburg) with a height of 247 m. The height of high-rise buildings being built in the near future in Sweden is expected to be around 80-130 m, which motivates the scope of this thesis.

2.5 Structural Design of High-Rise Buildings

The choice of structural system is fundamental when designing high-rise buildings and needs to be considered in early design stages to reduce the risk of wasted floor area and increased costs (The Concrete Centre, 2014). The main difference in designing high-rise buildings compared to low-rise buildings is the influence of lateral loads coming from wind forces, which usually governs the design of the core, columns and foundation.

2.5.1 The Core

The core of a high-rise building is the most fundamental part to consider during early design stages, since for most high-rise buildings, the core will resist a large proportion of the vertical and lateral loads (The Concrete Centre, 2014). Usually, the core will also house vertical transportation throughout the building by integrating lifts, staircases and other vertical service shafts within and around the core.

Today, reinforced concrete is a leading material used in cores due to its strength, construction techniques and properties such as sound insulation and fire resistance (The Concrete Centre, 2014). In contrast to cast-in-situ concrete, precast concrete enables a quicker construction phase although requiring more cranage to lift the precast concrete at high levels.

The core can be positioned in different configurations in a building, and it is also possible to have several cores. With regard to structural efficiency, a core placed in the center of a building is the best choice. This is due to a central core being less affected by torsion. Two eccentric cores are less structurally efficient than a centrally placed core, but more structurally efficient than one eccentric core. A core positioned eccentric to the center of the building gives rise to torsional loads and is therefore the worst choice.

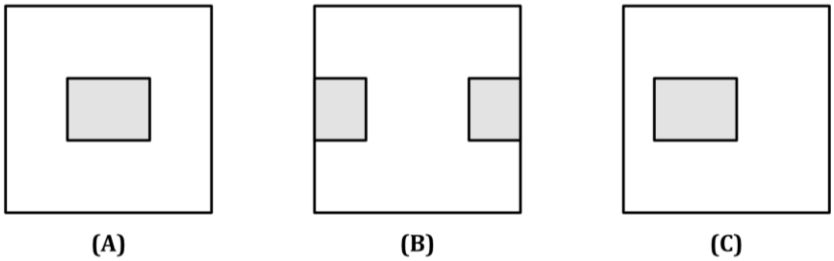

Figure 2.1: Plan views showing different positions of the core. (A) Central core. (B) Two eccentric cores. (C) One eccentric core.

2.5.2 Structural Frames and Tubes

The choice of structural frame for a high-rise building depends on many factors, including aesthetics, building height and intended use of the building. Depending on which kind of lateral load-bearing system a building has, the structural frames can be divided into interior and exterior structures. Interior structures are created by placing columns and beams, shear walls or trusses in the building that resist wind forces. In exterior structures, the lateral load-bearing elements are placed at the perimeter of the building, forming a rigid tube that is as strong as a core but has the potential to weigh less.

2.5.2.1 Frame System

The frame system is suitable for buildings up to approximately 75 m in height and utilizes beams and columns that are rigidly connected to each other, forming a moment-resisting frame (The Concrete Centre, 2014). The frames are typically placed in two perpendicular directions to ensure lateral stability of the building. The strength from the frame is derived from the moment interaction between the beams and columns.

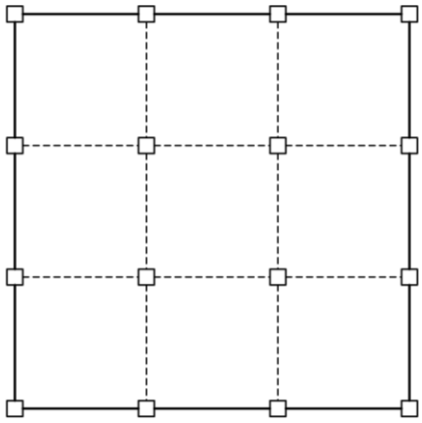

Figure 2.2: Illustration of the frame system.

2.5.2.2 Shear Wall System

The shear wall system is suitable for buildings up to 120 m in height and consists of thin shear walls designed to resist lateral forces that are preferably placed at the center of the building (The Concrete Centre, 2014). This allows the shear walls to act as a vertical cantilever that is fixed to the ground, designed to transfer lateral loads to the foundation through shear and flexural action. Additional shear walls can also be evenly distributed throughout the floor plan of the building. As the shear walls are much stiffer laterally compared to the columns, this ensures that the lateral loads are resisted by the shear walls, leaving the columns to only resist dead loads.

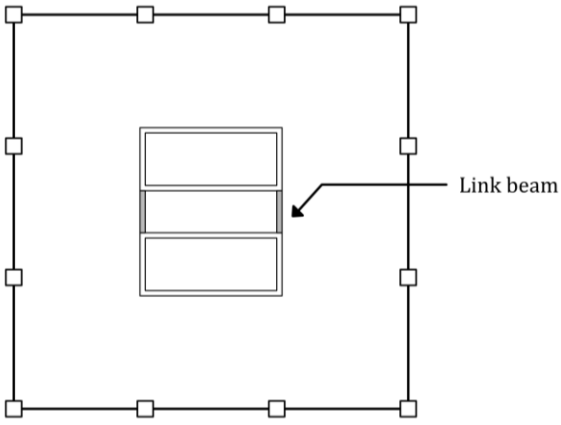

Figure 2.3: Illustration of the shear wall system.

2.5.2.3 Framed Tube System

The framed tube system is suitable for buildings up to around 150-170 m in height and consists of a hollow tube by placing closely spaced columns at intervals of 2-4 m at the perimeter of the building (The Concrete Centre, 2014). The columns are connected to beams to create rigid frames around the perimeter, forming a tube that acts as a vertical cantilevered box.

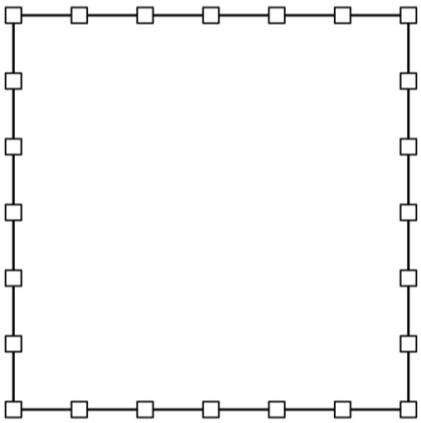

Figure 2.4: Illustration of the framed tube system.

An unavoidable phenomenon in any tube structure loaded laterally is shear lag, making the tube not work as an ideal cantilever (Jayachandran, 2009). Shear lag occurs due to the flexibility of the beams, leading to non-uniform stress distribution over the columns where corner columns are subjected to higher stresses than middle columns. By introducing braces to the frame, wider columns or smaller spacing between columns, the stresses are redistributed from the higher stressed corner columns to the lower stressed middle columns.

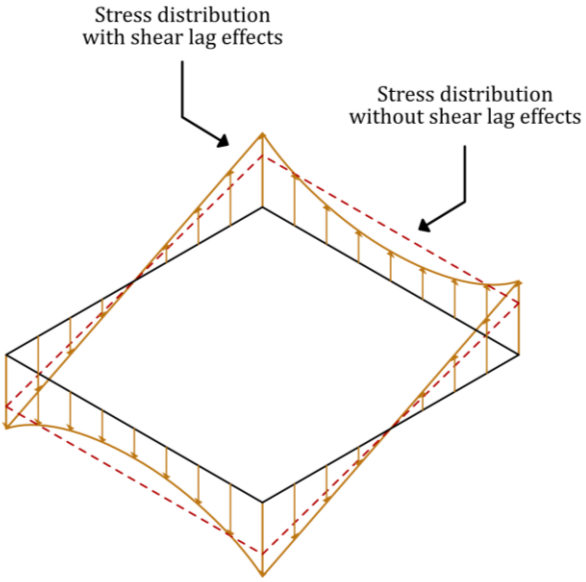

Figure 2.5: Illustration of the shear lag effect in framed tube systems

2.5.2.4 Tube-In-Tube System

The tube-in-tube system is suitable for buildings up to roughly 180-200 m in height and consists of a combination of a framed tube at the perimeter and internal core walls (The Concrete Centre, 2014). This makes the building perform in a similar manner to the shear wall and framed tube system, but with a considerably increased stiffness against lateral loads.

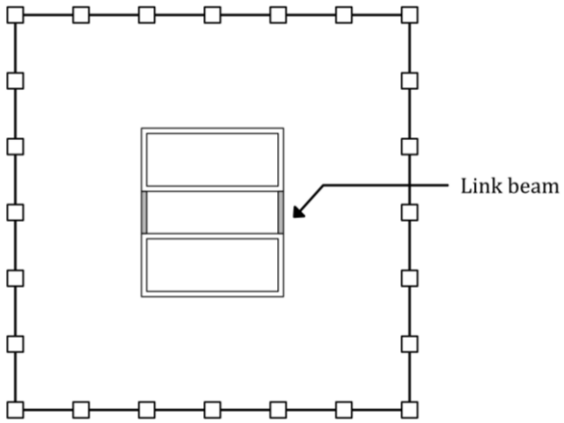

Figure 2.6: Illustration of the tube-in-tube system.

2.5.2.5 Bundled Tube System

The bundled tube system is suitable for buildings with a height greater than 200 m or for supertall buildings (The Concrete Centre, 2014). This system consists of a series of smaller tube systems, essentially splitting the plan into numerous modules. The modules are connected to each other through wall or frame elements, significantly increasing the stiffness of the building.

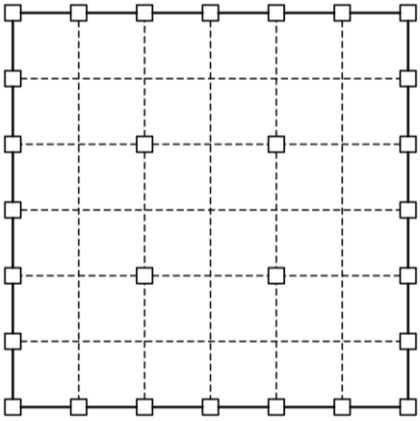

Figure 2.7: Illustration of the bundled tube system.

2.5.2.6 Braced Tube System

The braced tube system is suitable for buildings with a height up to and greater than 300 m and consists of a framed tube with additional diagonal bracing added to the perimeter frame (The Concrete Centre, 2014). The bracing elements transfer lateral loads to the foundation along with redistributing the dead loads from the higher stressed columns to the lower stressed columns. This increases the tube system's stiffness and allows larger column spacing at the perimeter of the building, allowing for more area for glazing at the facade. The diagonal bracing elements will largely dictate the visual appearance of the building.

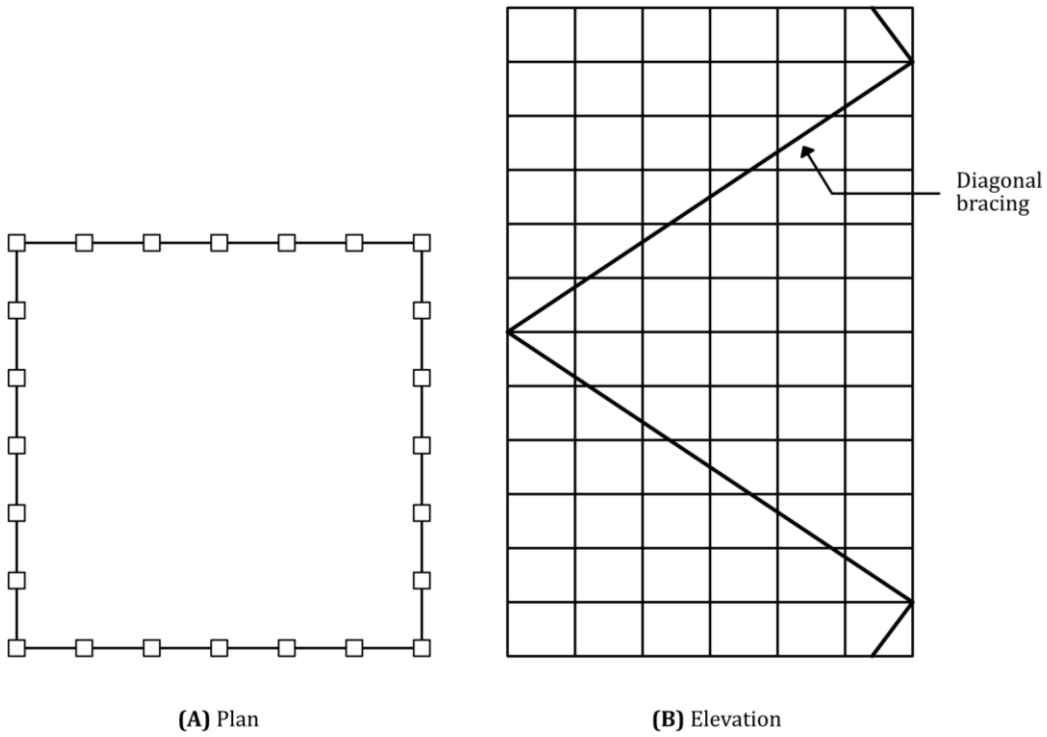

Figure 2.8: Illustration of the braced tube system.

2.5.2.7 Outrigger Braced System

The outrigger braced system is suitable for buildings up to and greater than 350 m in height, although outriggers can also be used in much shorter buildings (The Concrete Centre, 2014). This system introduces horizontal outrigger elements, often trusses, that connect the core with the perimeter columns. The outriggers are often one or two stories high and there could be one or multiple outrigger levels in a building. The outriggers redistribute horizontal loads from the core to the perimeter columns, allowing the columns to act as vertical load couples with a large lever arm. Thereby, the outriggers reduce the moment induced by wind loads from the core.

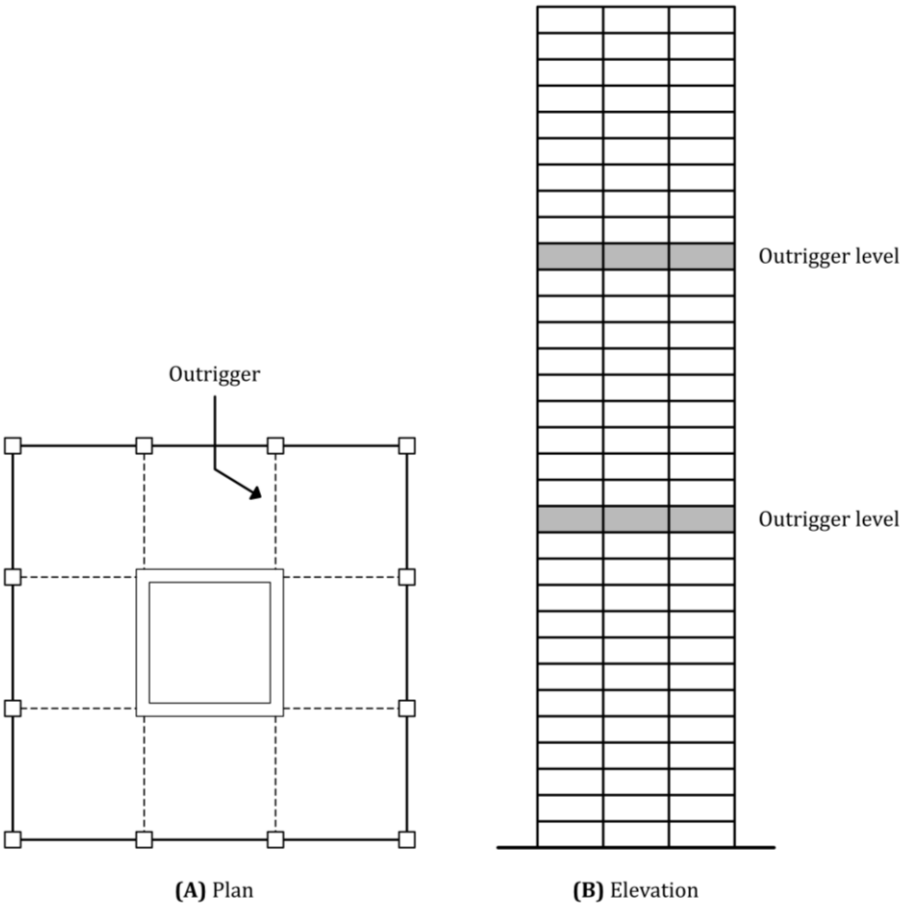

Figure 2.9: Illustration of the outrigger braced system.

2.5.3 Loads according to Eurocode

2.5.3.1 Permanent Loads

Permanent loads are loads that vary very little over time and are therefore assumed to be constant (Al-Emrani, 2019). Permanent loads include the self-weight, also known as dead load, of structural elements as well as installations and are known by the characteristic term G_k [kN] or g_k [kN/m^2]. In FE-softwares such as ETABS, the self-weights of structural elements can be calculated automatically after assigning materials to structural elements. Reference values for different structural elements and materials can also be found in EKS 12 (BFS 2022:4).

2.5.3.2 Imposed Loads

Variable loads are loads that vary over time and consist of imposed loads, snow loads and wind loads (Al-Emrani et al., 2019). Variable loads are known by the characteristic term Q_k [kN] or q_k [kN/m^2]. Imposed loads arise due to people and moveable objects during usage of the building, leading to load concentrations. When applying imposed loads to a building model, they are usually applied as distributed loads. For buildings with multiple stories, evenly distributed imposed loads should be applied to all floors. However, due to low probability of maximum loading on all floors at the same time, the imposed load can be reduced by applying the reduction factor α_n.

For a multistorey building, all floors except for the first two floors and the roof may be reduced by α_n according to Equation 2.1.

$$\alpha_n = \frac{2 + (n-2) \cdot \psi_0}{n} \tag{2.1}$$

where:

α_n = reduction factor for multistory buildings [-]

n = number of stories above the loaded element [-]

ψ_0 = reduction factor for variable loads, see Table 2.2 [-]

Depending on the use of the building, different characteristic values of imposed loads are given in SS-EN 1991-1-1, see Table 2.1 below.

Table 2.1: Characteristic values of imposed loads for different building usages according to SS-EN 1991-1-1.

Imposed Loads	q_k [kN/m²]	Q_k [kN]
Residential	2.0	2.0
Office	2.5	3.0
Retail	4.0	4.0
Department Store	5.0	7.0

Load reduction factors, ψ_i, are applied to variable loads when calculating load combinations. This is due to the low probability of all variable loads acting at the same time and with full load. The recommended load reduction factors according to EKS 12 (BFS 2022:4) are presented in Table 2.2.

Table 2.2: Recommended load reduction factors for variable loads according to EKS 12 (BFS 2022:4).

Load Reduction Factors	ψ_0	ψ_1	ψ_2
Office	0.7	0.5	0.3
Residential	0.7	0.5	0.3
Snow $2.0 \leq s_k < 3.0$ kN/m² $1.0 \leq s_k < 2.0$ kN/m²	 0.7 0.6	 0.4 0.3	 0.2 0.1
Wind	0.3	0.2	0.0

2.5.3.3 Wind Loads

Wind loads are also variable loads and since they govern the design of high-rise buildings, the impact of wind loading on high-rise buildings will be further elaborated on in this sub-chapter.

Wind acts on a building either through pressure or suction depending on the building geometry, wind direction and air turbulence (Poulos, 2017). Wind interacts with the surrounding terrain and creates air turbulence whose character and intensity changes with increasing height. The wind pressure acting on the windward side of the building is positive, while for the leeward side the pressure, or suction, is negative. These two components combine, resulting in a net wind force acting on the building.

When wind acts on a high-rise building, two different wind responses can be observed; along-wind and cross-wind (Fu, 2018). Along-wind consists of positive wind pressure from the windward side, while cross-wind consists of suction on the leeward side perpendicular to the direction of the wind. The along-wind motion is usually governing for the design of the core and foundation, whereas the cross-wind motion is usually critical for the facade and vibrations.

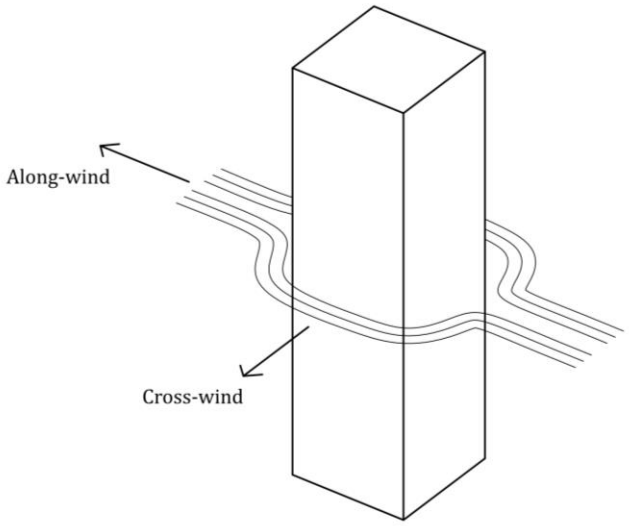

Figure 2.10: Illustration showing the along-wind and cross-wind motion.

The cross-wind causes vortex shedding, where the initially parallel along-wind forces are displaced on either side of the building, resulting in spiral vortices breaking away from the surface of the building (Fu, 2018). When the vortices are shed on both sides of the building, an impulse is applied in the perpendicular direction. At low wind velocities, shedding occurs simultaneously on either side of the building, causing no oscillation of the building in the transverse direction. However, at high wind speeds, the vortices are shed alternately from each side of the building, giving rise to impulses in both the along-wind direction and cross-wind direction. If the frequency of vortex shedding is close to the natural frequency of the building, the structure will vibrate significantly.

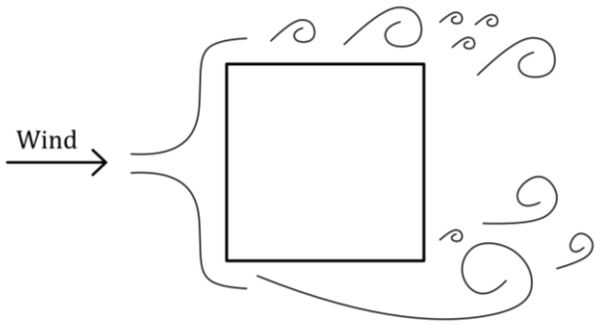

Figure 2.11: Illustration showing vortex shedding.

Since the velocity of the wind depends on the geographical location and surrounding terrain and buildings, the wind load acting on a specific building needs to be uniquely studied. The velocity of the wind is low close to the ground and successively increases as the height increases (Taranath, 2005), as shown in Figure 2.12. At a certain height, the velocity of the wind ceases to increase and reaches its maximum value. The height at which the maximum wind velocity is achieved depends on the surrounding terrain. In city outskirts where there are less obstacles, the maximum wind velocity is achieved at lower heights compared to city centers where surrounding buildings block the wind and force it upwards, resulting in a maximum wind velocity at taller heights.

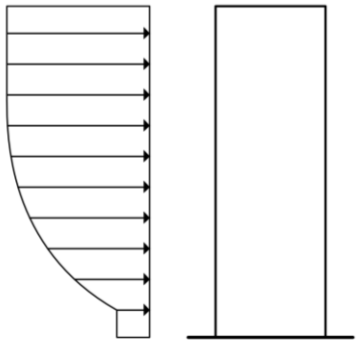

Figure 2.12: Illustration showing the variation of wind velocity with height.

Apart from the geographical location, the geometry of the building has a significant impact on the portion of wind that will be caught by the building. Therefore, the shape of the building can be modified to control the wind actions. This can be achieved in different ways such as rounding corners, tapering the width of the building with increasing height, twisting the building shape or designing openings in the building allowing wind to pass through (Poulos, 2017).

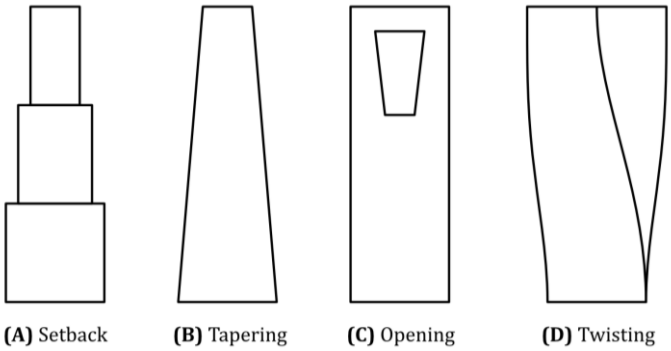

Figure 2.13: Illustration showing the different methods of aerodynamic optimizations.

2.5.3.3.1 Wind Load Calculations

For buildings up to 200 m, wind loads can be calculated according to SS-EN 1991-1-4:2005. For buildings exceeding a height of 200 m, wind tunnel tests are utilized to obtain the wind loads. A wind tunnel test consists of a physical model of the building along with models of all surrounding buildings within a radius of 800 m (Ascher, 2011). The wind is simulated by fans blowing on the models and the wind pressure on the model is measured.

Compared to building codes, wind tunnel tests are more accurate and less conservative as they consider more factors such as aerodynamics of the building, torsional loading and neighboring buildings. This could justify the costs of performing a wind tunnel test as the results are more favorable and will most likely minimize material usage. However, in this thesis, the wind loads will be obtained from SS-EN 1991-1-4:2005. The procedure of calculating the wind loads according to SS-EN 1991-1-4:2005 is presented in the following pages.

The reference wind speed v_b depends on the geographical location of the building, the season of construction and direction of the wind. It is calculated according to Equation 2.3. Values for the reference wind speed in different regions in Sweden are given in EKS 12 (BFS 2022:4), ranging between 21-26 m/s.

$$v_b = c_{dir} \cdot c_{season} \cdot v_{b,0} \tag{2.3}$$

where:

v_b = reference wind speed [m/s]

c_{dir} = directional factor, recommended value is 1.0 [-]

c_{season} = seasonal factor, recommended value is 1.0 [-]

$v_{b,0}$ = fundamental reference wind speed [m/s]

The fundamental reference wind speed $v_{b,0}$ corresponds to the characteristic average wind velocity 10 m above ground in an open terrain during a 10-minute period.

The reference wind speed is then used to calculate the basic velocity pressure q_b according to Equation 2.4.

$$q_b = \frac{\rho_{air} \cdot {v_b}^2}{2} \tag{2.4}$$

where:

q_b = basic velocity pressure [kN/m^2]

ρ_{air} = air density, 1.25 kg/m^3 [kg/m^3]

v_b = fundamental reference wind speed [m/s]

In SS-EN 1991-1-4:2005, different terrain categories are defined that describe different topographies of the location of the studied building. The roughness length z_0 and minimum building height z_{min} are related to the terrain category and given in Table 2.3 below.

Table 2.3: Terrain categories and values related to the different terrain categories according to SS-EN 1991-1-4:2005.

Terrain Category		z_0 [m]	z_{min} [m]
0	Sea or coastal area exposed to the open sea.	0.003	1
I	Lakes or flat and horizontal area with negligible vegetation and without obstacles.	0.01	1
II	Area with low vegetation such as grass and isolated obstacles (trees, buildings) with separations of at least 20 obstacle heights.	0.05	2
III	Area with regular cover of vegetation or buildings or with isolated obstacles with separation of maximum 20 obstacles heights (such as villages, suburban terrain, permanent forest).	0.3	5
IV	Area in which at least 15 % of the surface is covered with buildings and their average height exceeds 15 m.	1.0	10

Once the terrain category is determined, the terrain factor k_r can be calculated according to Equation 2.5.

$$k_r = 0.19 \cdot \left(\frac{z_0}{z_{0,II}} \right)^2 \tag{2.5}$$

where:

k_r = terrain factor [m]

z_0 = roughness length [m]

$z_{0,II}$ = roughness length for terrain category II [m]

The exposure factor $c_e(z)$ is then calculated according to Equation 2.6. The exposure factor relates to the building height z and terrain category, where the value is higher for lower terrain categories.

$$c_e(z) = \left[k_r \cdot \ln \left(\frac{z}{z_0} \right) \right]^2 \cdot \left[1 + \frac{7}{\ln \left(\frac{z}{z_0} \right)} \right] \tag{2.6}$$

where:

$c_e(z)$ = exposure factor [-]

k_r = terrain factor [-]

z = observed building height [m]

z_0 = roughness length [m]

Equation 2.6 is valid for $z_{min} \leq z \leq z_{max}$, whereas for $z \leq z_{min}$ the exposure factor is $c_e(z_{min})$. z_{max} is the height of the building.

The variation of $c_e(z)$ with height and for the different terrain categories are shown in Figure 2.14 below.

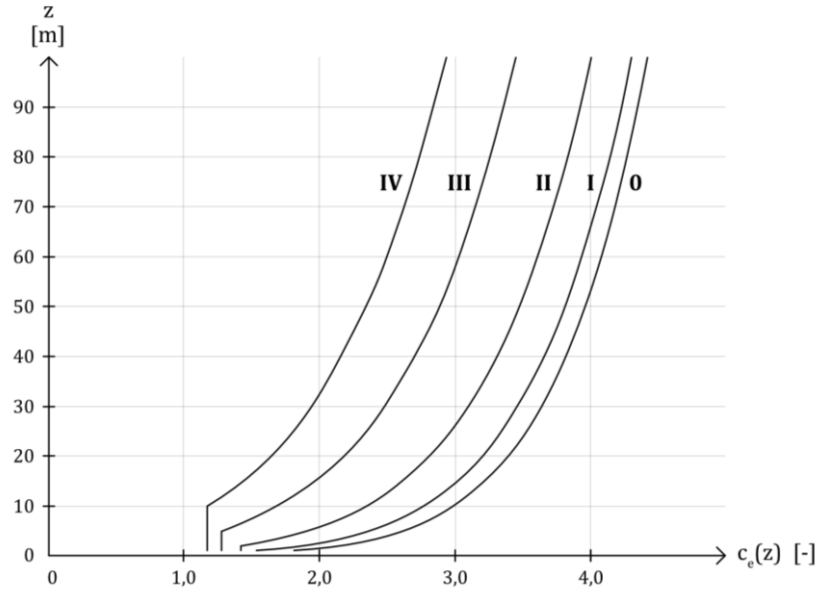

Figure 2.14: Graph showing how the exposure factor $c_e(z)$ depends on the building height z for the different terrain categories.

For buildings where $h > 2b$, the peak velocity pressure varies along the height of the building and is therefore calculated according to a strip method. The peak velocity pressure is constant at the bottom and top part of the building. To calculate the peak velocity pressure in the middle part of the building, the middle part of the building needs to be divided into strips where the peak velocity pressure at the corresponding height of each strip is calculated. This method is illustrated in Figure 2.15 below.

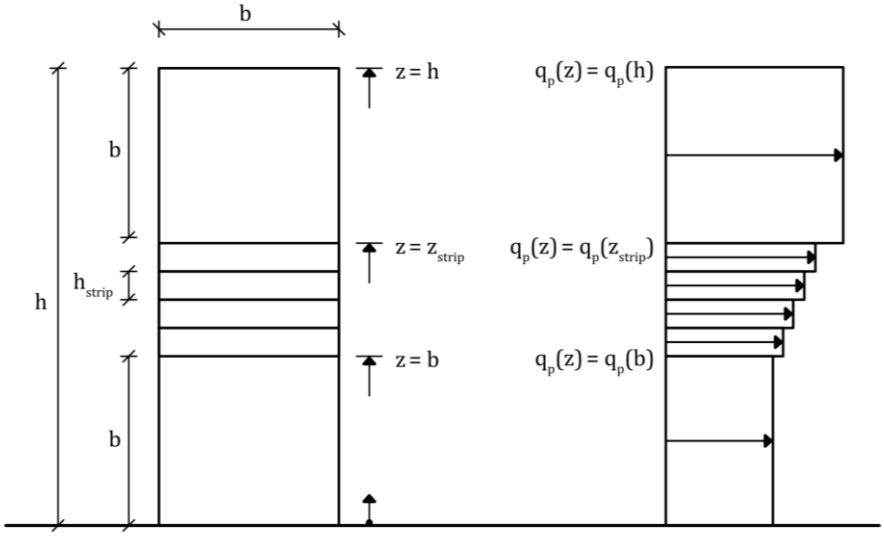

Figure 2.15: Diagram showing the wind load distribution of a building model where $h > 2b$.

The peak velocity pressure $q_p(z)$ is calculated according to Equation 2.7, by multiplying the exposure factor $c_e(z)$ with the basic velocity pressure q_b.

$$q_p(z) = c_e(z) \cdot q_b \tag{2.7}$$

where:

$q_p(z)$ = peak velocity pressure [kN/m^2]

$c_e(z)$ = exposure factor [-]

q_b = basic velocity pressure [kN/m^2]

Once the peak velocity pressure is calculated, pressure coefficients need to be determined. The pressure coefficients reduce the peak velocity pressure since the full load is assumed to not act on the entire external walls of the building. The pressure coefficients vary for different zones of the external walls. In this thesis, only zone D and E are relevant to study since the along-wind motion is governing for the design of the core.

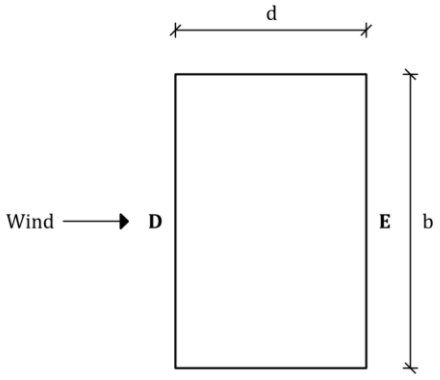

Figure 2.16: Illustration showing zone D and E of the external walls.

The pressure coefficients for zone D and E are presented in Table 2.4. According to EC, if the zone lies above h/d, further calculations need to be made to determine the pressure coefficients. Since the further calculations have a minimal effect on the resulting pressure coefficients, an assumption is made in this thesis that the pressure coefficients are the same for $h/d = 5$ as for $h/d > 5$.

Table 2.4: Pressure coefficients $c_{pe,10}$ for zone D and E of external walls.

Zone	**D**	**E**
≥ h/d	$\boldsymbol{c_{pe,10}}$	$\boldsymbol{c_{pe,10}}$
5	+ 0.8	- 0.7
1	+ 0.8	- 0.5
≤ 0.25	+ 0.7	- 0.3

Finally, the external wind load w_e is calculated according to Equation 2.8, by multiplying the peak velocity pressure with the net pressure coefficients.

$$w_e = q_p(z) \cdot (c_{pe,10,D} - c_{pe,10,E}) \tag{2.8}$$

where:

w_e = external wind load [kN/m^2]

$q_p(z)$ = peak velocity pressure [kN/m^2]

$c_{pe,10,D}$ = pressure coefficient for zone D [-]

$c_{pe,10,E}$ = pressure coefficient for zone E [-]

2.5.3.4 Load Combinations

When applying loads to a structure, load combinations are defined in ULS and SLS. ULS is a state where the structure no longer has the capacity to carry the loads and is on the verge of collapse (Al-Emrani et al., 2019). SLS is a state where the normal usage of the structure is no longer fulfilling its requirements to function. In SLS, deflections and long-term behavior of a structure are studied.

Since the wind load is dimensioning in this project, the ULS load combination where the wind load is the worst load case is relevant to study. The load combination ULS according to EKS 12 (BFS 2022:4) is given in Equation 2.9.

$$Q_{d,ULS} = \sum_{j \geq 1} \gamma_d \cdot 0.89 \cdot 1.35 \cdot G_{k,j} + \gamma_d \cdot 1.5 \cdot Q_{k,1} + \sum_{i>1} \gamma_d \cdot 1.5 \cdot \psi_{0,i} \cdot Q_{k,i} \tag{2.9}$$

where:

γ_d = partial coefficient depending on safety class, 1.0 for safety class 1 which is used in this thesis [-]

$G_{k,j}$ = permanent loads [kN/m^2]

$Q_{k,1}$ = main variable load [kN/m^2]

$\psi_{0,i}$ = load reduction factor [-]

$Q_{k,i}$ = interacting variable loads [kN/m^2]

When evaluating the deflections of a high-rise building, the characteristic deformations are relevant to study since the recommended deformations are characteristic values. The characteristic load combination in SLS according to EKS 12 (BFS 2022:4) is given in Equation 2.10.

$$Q_{d,SLS} = \sum_{j \geq 1} G_{k,j} + Q_{k,1} + \sum_{i>1} \psi_{0,i} \cdot Q_{k,i} \tag{2.10}$$

2.5.4 Wind Induced Vibrations

Initially, it is important to design high-rise buildings in regard to strength and safety requirements in ULS to ensure the structure's stability under wind loading (Fu, 2018). Secondly, the effect of wind induced vibrations needs to be considered in SLS to ensure the occupants' comfort. Most occupants in high-rise buildings will to a certain extent sense motion due to wind loads acting on the building. With increasing magnitude and frequency of wind induced motion, this may negatively affect the comfort of the occupants.

If the frequency of the wind induced motion is close to the natural frequency of the building, the structure will vibrate significantly. This is due to the building being in a resonance condition, resulting in high accelerations in the building due to increased amplitude of the vibrations.

2.5.5 Deformations

Deformations in high-rise buildings are considered when designing in SLS and consist of vertical and horizontal displacements both locally and globally in the building. Local deformations consider vertical displacements of floors and columns due to axial shortening while global deformations mainly consider differential vertical shortening and horizontal deformations at the top of the building. Global deformations are critical when considering the stability of the building, whereas local deformations are critical in structural elements such as facade and roof elements.

2.5.5.1 Horizontal Deformations

Today, there are no building codes that limit the maximum allowed horizontal deformation of a high-rise building. Instead, there are recommendations in SS-EN-1990-2023 where the maximum horizontal displacement of a multistory non-industrial building is limited by the height of the building divided by 500 according to Equation 2.11. This is the maximum allowed horizontal displacement that will be used in this thesis.

$$u_{max} \leq \frac{h}{500} \tag{2.11}$$

where:

u_{max} = maximum horizontal displacement at the top of the building [m]

h = height of the building [m]

2.5.6 Reinforced Concrete

2.5.6.1 Material Properties

Concrete is the most commonly used material in high-rise buildings as it has many advantages compared to other building materials (The Concrete Centre, 2014). These include high stiffness and mass, cheaper construction costs and better fire resistance. Concrete consists of a mix of cement, water, aggregates and potentially admixtures, where the composition of materials influences the material properties of the concrete (Al-Emrani, 2013). In general, a higher amount of cement results in stronger concrete. On the contrary, the production of cement is very energy intensive and emits large amounts of CO_2.

Concrete has a high compressive strength compared to its tensile strength (Al-Emrani, 2013). To increase the tensile strength of concrete and achieve equilibrium after cracking, rebars of reinforcing steel are added to the concrete, creating reinforced concrete. Furthermore, concrete is divided into different classes corresponding to their characteristic compressive strength f_{ck}. The strength and deformation properties of different concrete classes can be found in EC.

2.5.6.2 Long-Term Effects

In reinforced concrete high-rise buildings, the effect of long-term deformations such as creep and shrinkage have an impact on the vertical displacements of the structure. Creep is a physical property where the concrete undergoes slow deformation under constant load, leading to increased deformations over time (Al-Emrani, 2013). Shrinkage occurs due to moisture loss from drying of concrete, which leads to contractions and change of volume of the concrete structure.

In concrete vertical members such as columns and walls, deformations due to time dependent effects of creep and shrinkage are larger than the elastic deformations from initial axial loading (The Concrete Centre, 2014). Since the core and columns have different levels of axial stress and undergo long-term shortening at different rates, differential axial shortening occurs between the core walls and columns. For the floor slabs that are supported by columns, this leads to altering distribution of moments and shear forces and affects the levelness of floors. Similar problems can occur if using different materials in different structural elements, as different materials have different long-term effects.

2.5.7 Climate Impact

The climate impact of a building can be calculated by performing a life cycle assessment (LCA). LCA considers a building's climate impact during the entire life cycle of the building, from resources being extracted to the demolition of the building (Boverket, 2019). The assessment is divided into several stages of the life cycle of the building, as depicted in Figure 2.17. For this thesis, the relevant stages are A1-A5, that is the product and construction stages.

A1-A3 Product Stage	**A1**	Raw supply material
	A2	Transport
	A3	Manufacturing
A4-A5 Construction Stage	**A4**	Transport
	A5	Construction installation
B1-B7 Operational Stage	**B1**	Usage
	B2	Maintenance
	B3	Repair
	B4	Replacement
	B5	Refurbishment
	B6	Operational energy usage
	B7	Operational water usage
C1-C4 End of Life Stage	**C1**	Deconstruction demolition
	C2	Transport
	C3	Water processing
	C4	Disposal

Figure 2.17: The stages in an LCA.

For each stage and type of material used in that stage, there is a corresponding climate factor that is multiplied by the total mass or volume of the material used to obtain the mass of carbon dioxide equivalent, CO2e, that is emitted. For this thesis, the climate impact studies will be included in the ETABS/VBA tool for the total amount of concrete and reinforcement that is used in each design. The climate factors for the relevant materials are shown in Table 2.5.

Table 2.5: Climate factors for concrete and steel reinforcement according to Boverket's climate database (version 02.04.000).

	ρ [kg/m³]	**A1-A5 [kg CO2e/m³ material]**
Concrete C50/60	2350	0.173
Steel Reinforcement	5885	0.75

2.6 Parametric Design

Parametric design in architecture is a design method where key parameters are identified and fed into algorithms that shape building elements. This allows the user to make changes in the model interactively by inputting different parameters. Parametric design is a powerful tool in exploring and evaluating numerous design options, resulting in more efficient and optimized designs.

When a certain task needs to be repeated several times, such as calculating loads when the dimensions of a building changes, parametric design is a powerful tool in saving time by automating the workflow. In addition, parametric design is useful when dealing with optimization of structures. Optimization often deals with minimizing the amount and dimensions of structural elements, which in turn saves costs and CO_2 emissions. Performing optimizations manually is often too time-consuming, but by automating the workflow, the computer performs several iterations in one go.

The typology of a high-rise building often consists of a repetition of multiple stories, making parametric workflows a suitable tool when working with them. The amount of data computed from a FE-analysis of a high-rise building can quickly become difficult to manage, particularly if several iterations are performed. By recognizing patterns and storing data appropriately, the data can be visualized in graphs and diagrams, giving the user a comprehensive and informative overview of the structural performance of several designs.

2.7 Optimization

Optimization is about finding an optimal solution to a problem by obtaining the maximum, minimum or residual value of one or several objectives (Savic, 2002). Single-objective optimization optimizes against one goal, while multi-objective optimization optimizes against several goals. For single-objective optimization, there is only one optimal solution. However, by optimizing with respect to a single objective, the solution can be unfavorable with respect to other objectives that have not been considered. In multi-objective optimization, a collection of compromised solutions is identified. In this thesis, multi-objective optimization will be used.

In multi-objective optimization, a large range of solutions are found, where the set of efficient solutions are considered to be on the Pareto front (Jahan et al., 2016). The solutions at the Pareto front are considered to be optimal, meaning that there is no action that makes one individual better without making another worse. In order to find a single solution from the set of Pareto solutions, the subjective preferences need to be satisfied by a decision maker.

In Figure 2.18, an example of multi-objective optimization and the Pareto front is shown. The objectives that the solutions are optimized against are f_1 and f_2. The position of the solutions, indicated by the blue boxes, show how well they fit the objectives f_1 and f_2. The solutions A and B are not dominated by any other solution and therefore lie on the Pareto front. A decision maker needs to

determine the preferred solution or solutions from the Pareto front. In the case of minimizing the objectives, the Pareto front lies close to the axes and low values are preferred to higher ones.

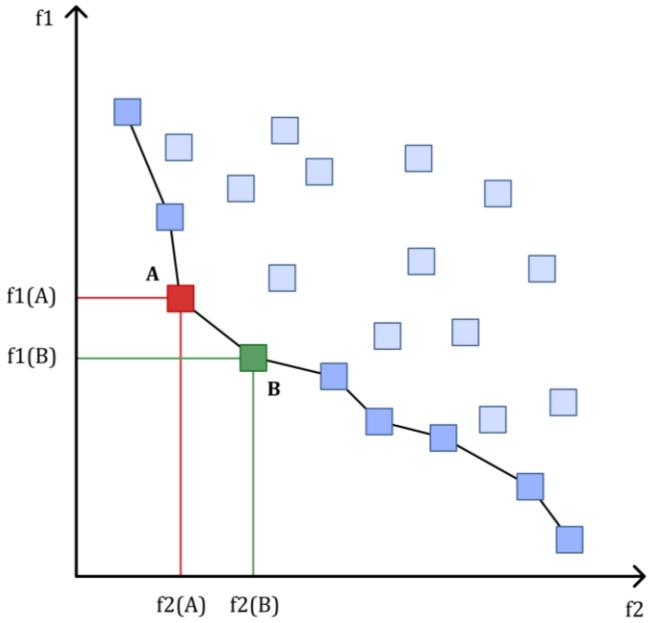

Figure 2.18: Example of multi-objective optimization and the Pareto front.

2.7.1 Genetic Algorithm

Optimization can be performed by using various algorithms. In multi-objective optimization, genetic algorithms are particularly suited (Rutten, 2011). Genetic algorithms mimic the principle of natural selection. The algorithm is based on a population of individuals, commonly referred to as solutions, that are controlled by a set of genes. The genes are allowed to change, and each combination of genes result in a unique solution. By altering the genes, the fitness of the corresponding solutions with respect to the objectives increases or decreases.

The initial step of the algorithm is to populate a random collection of solutions based on the different combinations of genes (Rutten, 2011). The algorithm then evaluates the fitness of each solution and the most fitted ones are selected. These solutions are then bred to create a new and improved generation of solutions. This process is repeated until a chosen maximum number of generations is reached.

2.7.2 Structural Optimization

Structural optimization means to design a structural system that manages the applied loads in an optimal way according to a set of goals (Christensen et al., 2010). A goal could be to make the structural system as light or stiff as possible, where constraints are required to achieve well-defined solutions. For example, to maximize the stiffness of a structure, there may be a constraint on the material usage. Otherwise, the structure can contain an excessive amount of material and achieve a high stiffness, but this would not be a well-defined solution. Requirements on displacements, geometry and stresses are usually limiting factors in structural optimization.

For example, a structural optimization problem could be formulated as the following:

> **Goal:** Maximize the stiffness of a structural system.
> **Objectives:** Maximum allowed horizontal deflection and minimum material usage.
> **Genes:** Dimensions of structural elements and material properties.

The goal of the optimization is to find a structural system that is as stiff as possible while restricting the deflections and material usage. Each combination of material property (e.g. concrete class) and dimensions of structural elements (e.g. thickness) results in a unique solution. Each solution corresponds to a certain material usage and horizontal deflection. The goal of the solver is to find the appropriate dimensions and material properties which results in the maximum allowed horizontal deflection and minimum material usage.

3 Digital Tools

In this chapter, the digital tools that are used to develop the two tools in this thesis are introduced.

3.1 Rhinoceros 3D

Rhinoceros 3D, or Rhino for short, is a 3D modelling software developed by Robert McNeel & Associates (Robert McNeel & Associates, n.d.). The geometries created in Rhino are based on non-uniform rational basis splines, commonly abbreviated as NURBS.

3.1.1 Grasshopper

Grasshopper is an add-on for Rhino where the user can parametrically program geometries by using visual scripting language. Grasshopper opens in a separate window and is directly linked to Rhino, allowing the user to interactively see the changes in the model in Rhino when scripting in Grasshopper. Visual programming is performed by connecting predefined components to each other. Custom components can also be created by scripting in C# or Python. In Grasshopper, data is stored in a hierarchical structure in data trees. A data tree contains branches, which are essentially lists containing data. A data tree could therefore be considered as a list of lists.

3.1.2 Octopus

To perform multiple-objective optimization in Grasshopper, an add-on needs to be installed. For this thesis, Octopus is installed and used. Octopus can only maximize or minimize objectives. In order to optimize against a specific target value, the difference between the achieved value and target value, also called the residual, can be minimized. The user can analyze the solutions at the Pareto front and either determine a set of reasonable solutions or find a single optimal solution that satisfies the preferences of the user.

3.1.3 Karamba3D

Karamba3D is an add-on to Grasshopper where real-time FE-analysis (Ottosen et al., 1992) can be performed on the parametric models that are modelled in Grasshopper and displayed in Rhino. Karamba3D is particularly useful in early design stages, where for example load distributions, deflections and material utilizations are visualized interactively when changes are made to the structural elements in Grasshopper.

3.2 ETABS

ETABS is a FE-software (Ottosen et al., 1992) that is particularly useful for the design and analysis of multistory buildings (Computers & Structures, 2023). ETABS has an API that allows users to automate workflows in ETABS. The API

consists of a library containing functions that can be used in a script outside of ETABS and build, analyze and design models in ETABS. The API is compatible with most major programming languages, including for example Visual Basic, C# and Python.

3.3 Excel/VBA

Excel is a spreadsheet editor developed by Microsoft. It features basic operations as well as functions by using a grid of cells arranged in columns and rows. The data in the cells can be visualized in tables, graphs and diagrams. In the Windows version of Excel, it is possible to program through VBA, which is a dialect of Visual Basic. VBA allows the user to automate processes, manipulate spreadsheets and control other applications.

3.4 Tableau

Tableau is an interactive data visualization program that allows users to manage and display large sets of data. Once a database file is linked to Tableau, different labels (e.g. a column in Excel) containing data can be visualized in graphs, diagrams and tables using a drag and drop technique. It is also possible to perform basic and logical operations in Tableau, similar to the possible operations in Excel.

3.5 Flow Chart of Digital Tools

The implementation of the different digital tools presented in this chapter are visualized in Figure 3.1 below for the Rhino/Grasshopper and ETABS/VBA tool respectively.

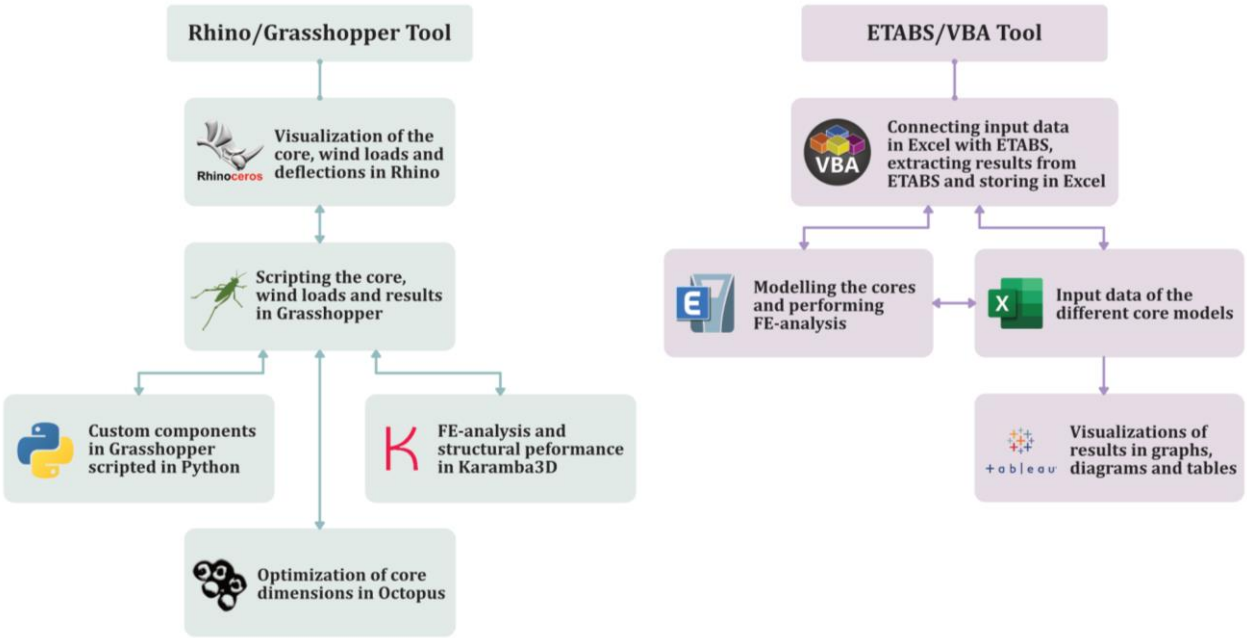

Figure 3.1: Flow chart of the implemented digitals tools for the Rhino/Grasshopper and ETABS/VBA tool.

4 Rhino/Grasshopper Tool

The Rhino/Grasshopper tool is intended to be used in an early conceptual design phase. The aim is to give the user an understanding of the behavior of the core subjected to wind load. The tool also outputs preliminary dimensions of the core based on maximum allowed displacements and minimum required core area. This chapter presents an overview of the developed tool as well as a verification and analysis of the tool by two case studies.

The type of structural system that can be modelled and analyzed in the Rhino/Grasshopper tool is a shear wall system where shear walls are positioned at the center of the building. No outriggers are included in the model, thus the wind loads are assumed to be resisted entirely by the core and not the building envelope. Therefore, the wind loads are only applied to the core walls. The wind loads are the only loads that are considered and applied in this tool, although vertical loads could easily be added if desirable.

4.1 Definitions

A high-rise building is parametrically modelled in Grasshopper by defining a core and a building footprint, both consisting of surfaces that are regarded as shells. The dimensions of the building footprint, story height, number of stories and dimensions of the core are parametrized and can therefore be set by the user. Wind properties such as reference wind speed, terrain category and direction of the wind can also be set by the user.

As the width and length of the building footprint affects the wind load distribution based on which side the wind is blowing from, the width *w* and length *l* are defined according to Figure 4.1 below. The width *w* always aligns with the predefined X-axis in Rhino, while the length *l* always aligns with the Y-axis.

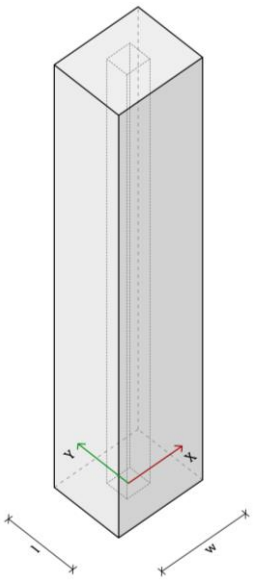

Figure 4.1: Diagram showing the orientation of the modelled building in relation to the X- and Y-axis in Rhino.

The wind can blow from any of the four sides of the building, therefore the four facades of the building footprint are defined according to Figure 4.2.

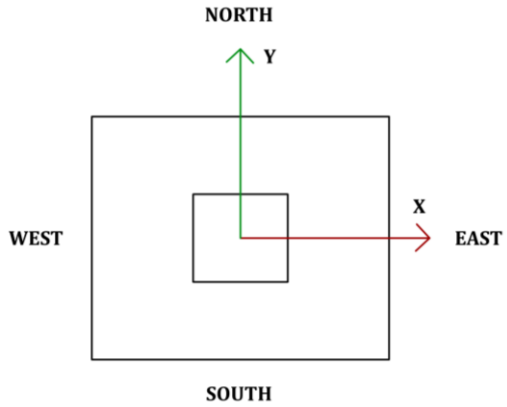

Figure 4.2: Diagram showing the definitions of the facades of the modelled building.

The tool only allows to model a rectangular building and core. The core can only be placed in the center of the building footprint, although this could easily be modified if desired. All core walls have uniform thicknesses over the height of the building.

4.2 Flow Chart of the Rhino/Grasshopper Tool

Figure 4.3 shows a flow chart of the Rhino/Grasshopper tool. Further instructions on the interface and how the tool works can be found in Appendix A. The sizing optimization is performed in Octopus, where the user evaluates optimization graphs of the different solutions to find the optimal solution. This is further explained in chapter 4.6.

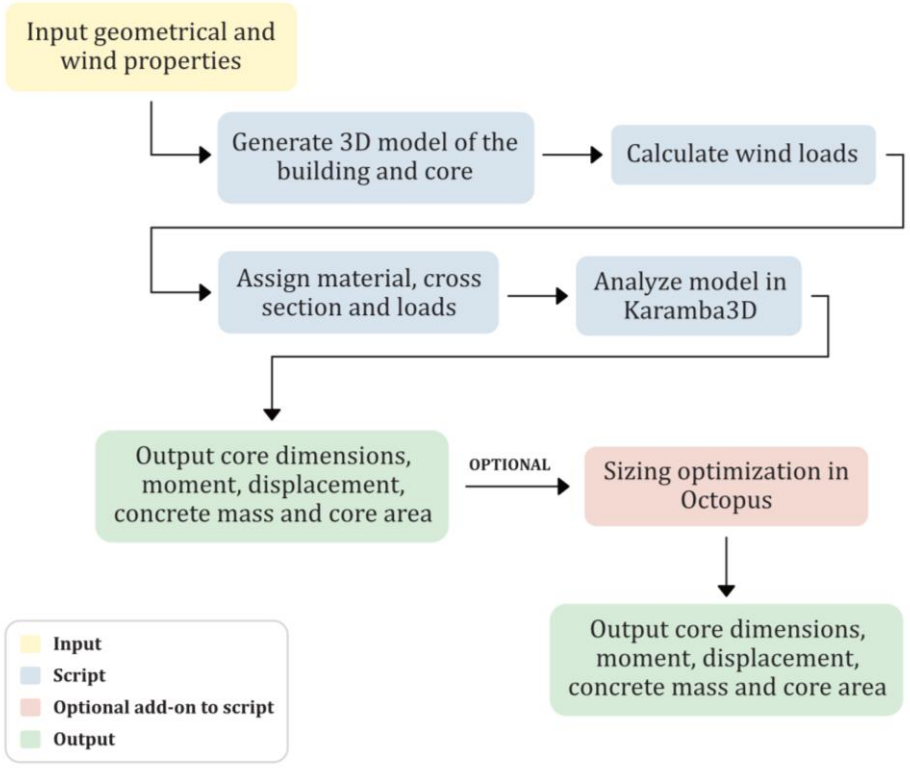

Figure 4.3: Flow chart explaining the Rhino/Grasshopper tool.

4.3 Input Data

The input data that can be set by the user in Grasshopper is defined according to Table 4.1 to Table 4.5. The data varies from geometrical input to properties of the wind acting on the building.

Table 4.1: Core Dimensions.

Core Dimensions	Description
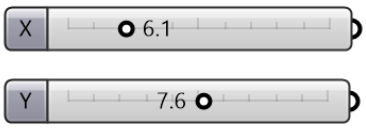	Sliders *X* [m] and *Y* [m] control the length and width of the core.

Table 4.2: Story Height.

Story Height	Description
	Slider *h* [m] controls the story height.

Table 4.3: Number of Levels.

Number of Levels	Description
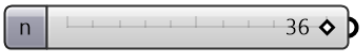	Slider *n* [-] controls the number of levels of the building.

Table 4.4: Building Envelope Dimensions.

Building Envelope Dimensions	Description
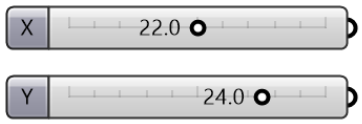	Sliders *X* [m] and Y [m] control the length and width of the building envelope.

Table 4.5: Wind Properties.

Wind Properties	Description
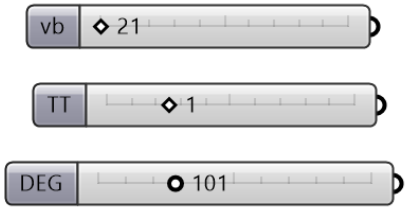	Sliders controlling the wind properties reference wind speed vb [m/s], terrain type TT [-] and wind direction DEG [°]. The wind direction is defined according to the angle of the wind direction, see Figure 4.6 for definition of the angle. $21 \leq vb \leq 26$ $0 \leq TT \leq 4$

4.4 Wind Load Calculations

The wind loads acting on the building are calculated by the custom components presented in Table 4.6 and 4.7. These components are scripted in Python by the author of the thesis.

The component *Wind Load Calc X- and Y-DIR* inputs geometrical information of the building as well as wind properties. The script utilizes Equations 2.3-2.8 to calculate the wind loads acting on the facades in both X- and Y-direction. The wind load values are calculated per facade level. Therefore, the component outputs a data tree with four branches, one for each facade. Each branch contains *n* wind load vectors, one for each facade level. The wind load data tree is then converted into wind load vectors per core wall level by multiplying the area of each facade level and dividing by the area of each core wall level.

Table 4.6: Wind load calculator for wind acting in X- and Y-direction.

Wind Load Calculator X-DIR and Y-DIR	Description
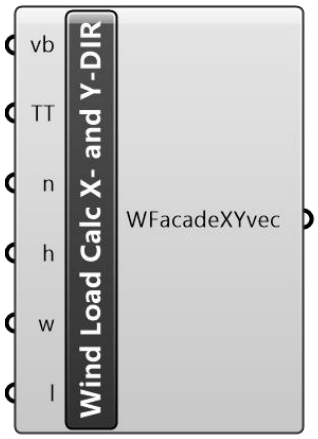	Inputs the reference wind speed *vb* [m/s], terrain type *TT* [-], number of levels *n* [-], level height *h* [m], width *w* [m] and length *l* [m] of building envelope. Outputs a data tree *WFacadeXYvec* [kN/m^2] with wind load vectors acting on each facade level in X- and Y-direction. Organized as a tree with four branches, one branch for each facade. Each branch contains n items, one vector for each facade level.

The initial loading state of the building is presented in Figure 4.4, where all facades of the building are loaded with wind loads. This is merely for simplicity before using the *Wind Load Calc Any Angle* component.

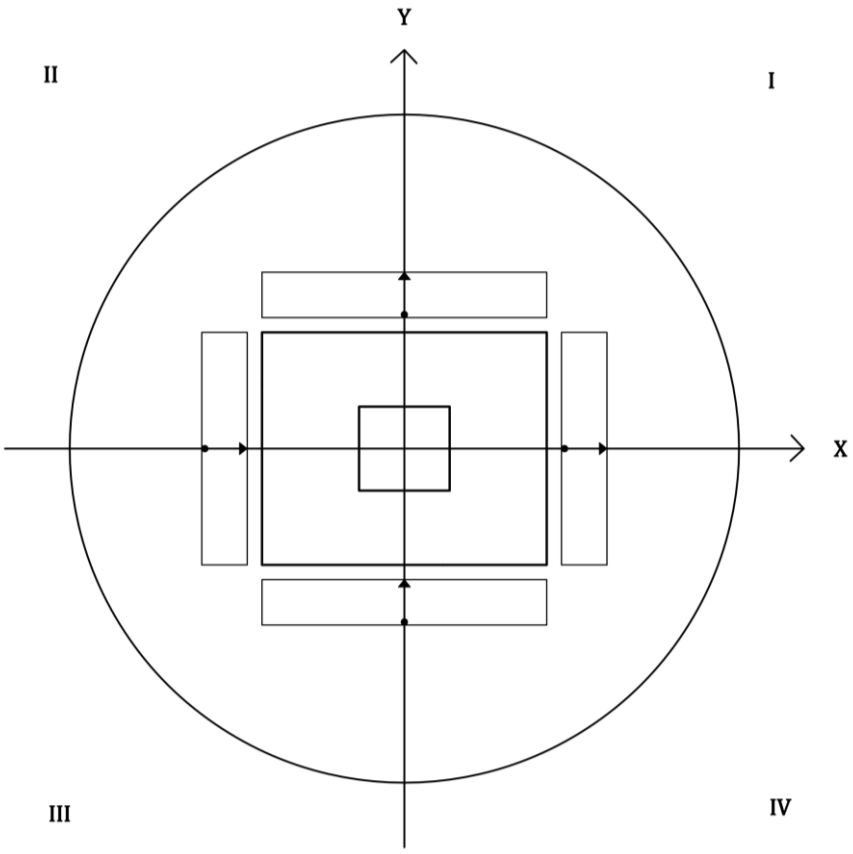

Figure 4.4: Diagram showing the initial loading state of the building before using the *Wind Load Calc Any Angle* component.

The component *Wind Load Calc Any Angle* inputs the angle of the wind, number of levels and a data tree containing the wind load vectors per core wall level.

Table 4.7: Wind load calculator for any given angle of the wind direction.

Wind Load Calculator Any Angle	Description
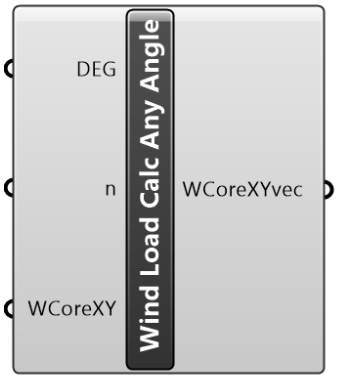	Inputs the angle *DEG* [°] of the wind direction, number of levels *n* [-] and a data tree *WCoreXY* [kN/m²] containing wind load vectors acting on each core wall level. *WCoreXY* is organized as a tree with four branches, one branch for each core wall. Each branch contains n items, one vector for each core wall level. Outputs a data tree *WCoreXYvec* [kN/m²] with wind load vectors acting on each core wall level for all core walls North, West, South and East at any wind direction defined by *DEG*. *WCoreXYvec* is organized as a tree with four branches, one branch for each core wall. Each branch contains n items, one vector for each core wall level.

The main function of the *Wind Load Calc Any Angle* component is to manipulate the initial loading state of the building as seen in Figure 4.4 according to the angle of the wind. This is achieved by placing the building in the center of a Cartesian coordinate system, where the axes divide the plane into four quadrants. Depending on the angle of the wind, the wind will always act in one of the four quadrants, defining which facades are loaded by wind.

When the angle of the wind aligns with the axes, only one facade is fully subjected to wind. In contrast, when the angle of the wind is in between two axes, the wind load is split up into its X- and Y-components and loaded to the appropriate facades. This is exemplified in Figure 4.6, where the wind vector W acts in the second quadrant and the X- and Y-components W_x and W_y are therefore placed on the West and North facade. A flow chart of the *Wind Load Calc Any Angle* is shown in Figure 4.5.

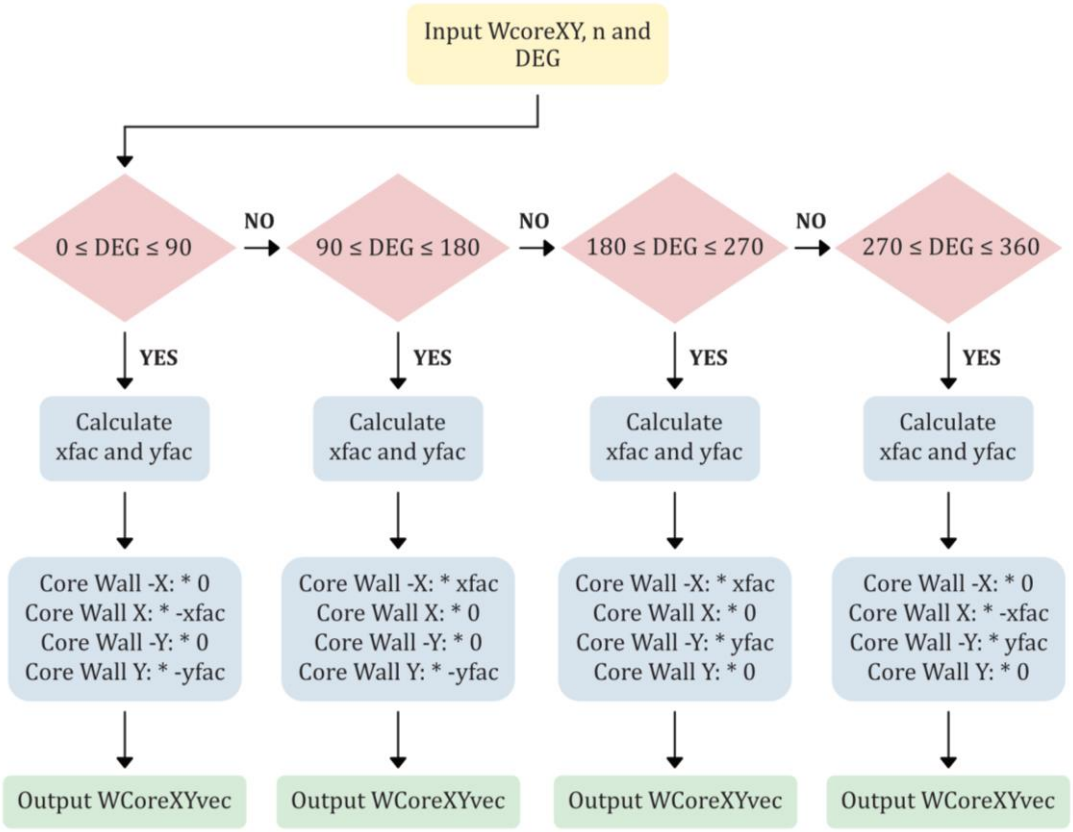

Figure 4.5: Flow chart explaining the *Wind Load Calc Any Angle* component.

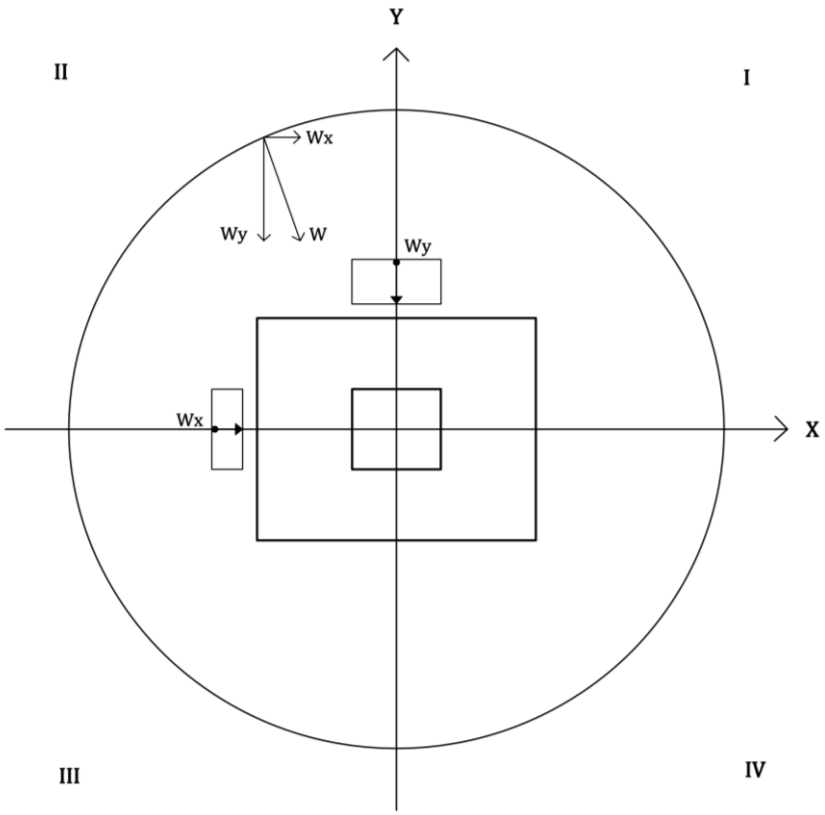

Figure 4.6: Diagram showing how the wind load acting from a certain angle on the building is split into its X- and Y-force components.

4.5 Output Data

The output data that can be extracted from the Rhino/Grasshopper tool are displacements, reaction forces, core dimensions, core wall thickness and the total mass of concrete. The wind load distribution, displacements and moment and shear force distribution of the core are also visualized in Rhino according to Figure 4.7 below.

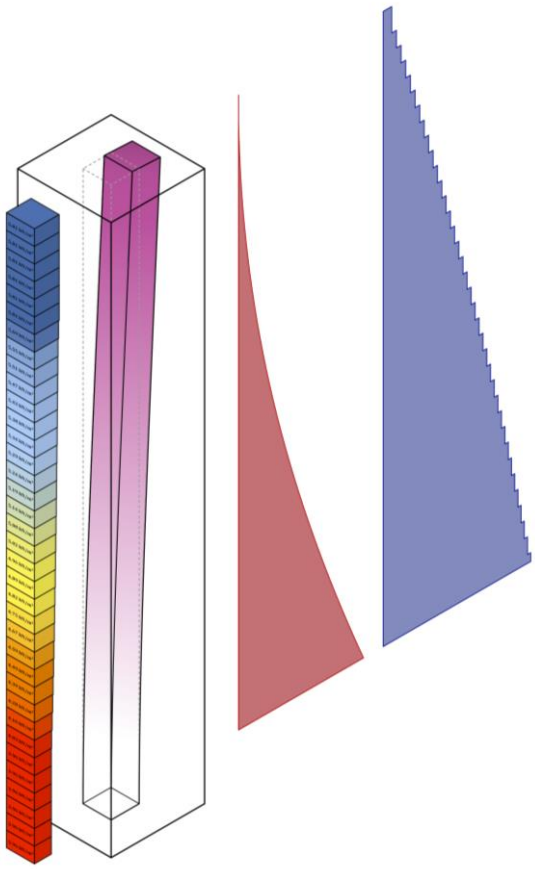

Figure 4.7: Figure showing the modelled core and building envelope in Rhino along with the wind load distribution, displacements of the core and moment and shear force distribution.

4.5.1 Comparison With Hand Calculations

To verify the Rhino/Grasshopper tool, an example building is defined and the moment at the base and horizontal displacement is calculated with the tool and analytically. The properties of the example building and calculations can be found in Appendix C.

Table 4.8: Comparison of displacement and moment from Rhino/Grasshopper tool and hand calculations.

	Displacement [mm]	**Moment** [MNm]
Hand Calculations	389	287.9
Rhino/Grasshopper Tool	250	294.7

The calculated moments are relatively similar, where the moment is slightly higher when calculated from the Rhino/Grasshopper tool. For the displacements, there is a large difference between the calculated values. The displacement is much smaller in the Rhino/Grasshopper tool compared to hand calculations. The hand calculations are based on a cantilever beam as this is how the core is modelled in the Rhino/Grasshopper tool. A beam is rarely around 130 m tall as it is in this case, which could entail that this calculation model isn't fair for calculating deflections of a high-rise building.

To verify this, the deflections have been compared for a 21.6 m tall beam or building, see Appendix C. The Rhino/Grasshopper calculates a displacement of 0.18 mm while hand calculations result in a displacement of 0.20 mm. The difference is minimal, which verifies that the Rhino/Grasshopper can be compared to a cantilever beam for lower heights, but for taller heights the displacement becomes significantly larger for hand calculations and the calculation model isn't fair.

4.6 Optimization

Other than using the sliders of the input data to visualize the behavior of the core and obtain preliminary results of the reaction forces and displacements, the Rhino/Grasshopper tool can also be utilized to perform an optimization of the core. The goal with the optimization is to make the core as small as possible while still fulfilling the requirements on deformations. By making the core as small as possible, the occupiable area of the building increases and thus leads to increased profit.

The objectives are to reach the maximum allowed horizontal displacement and to minimize the core area. To reach the target value of the maximum allowed horizontal displacement, the objective needs to be reformulated into a minimum or maximum problem. In this case it is appropriate to minimize the difference between the achieved value and the target value to obtain solutions that are as close as possible to the maximum allowed horizontal displacement.

The genes that can be changed to obtain unique solutions consist of the X- and Y-dimensions of the core (corresponding to the length and width) and thickness of the core walls. When performing the optimization, these three different genes are combined to form solutions that are evaluated against the objectives.

Two different cases, A and B, are defined in the following chapters where the goal is to optimize the core area for a square building envelope (Case A) and a rectangular building envelope (Case B). The wind angle is the only difference between Case A1/B1 and Case A2/B2, to analyze the effect on the core area depending on the wind angle.

4.6.1 Case A

In Case A, the building envelope consists of a square, where the wind load angle is 180° for Case A1 and 135° for Case A2. All other geometrical input data of the building envelope and wind properties are kept the same between Case A1 and A2. The dimensions and wind angle of Case A1 and A2 are depicted in Figure 4.8 below.

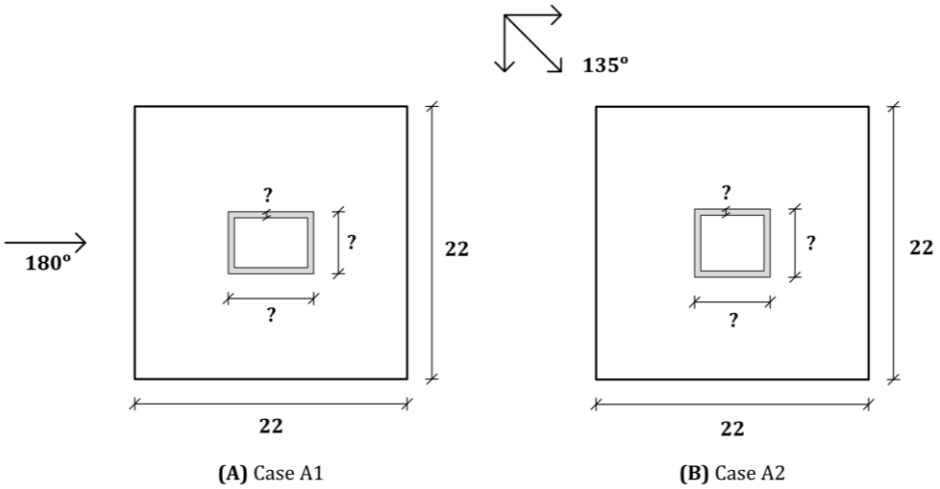

Figure 4.8: Dimensions in meters and wind angle of Case A1 and A2.

The input data for Case A1 and A2 are summarized in Table 4.9 below.

Table 4.9: Input data for Case A1 and A2.

	Case A1	**Case A2**
Number of Levels	36	36
Level Height	3.6 m	3.6 m
Building Height	129.6 m	129.6 m
Building Envelope	22 x 22 m	22 x 22 m
Concrete Class	C30/37	C30/37
Reference Wind Speed v_b	21 m/s	21 m/s
Terrain Category	II	II
Wind Angle	180°	135°

The results of the optimization for Case A1 are depicted as red boxes at the Pareto front in Figure 4.9 below. The blue-marked solution is identified as the most optimal solution, fulfilling the smallest core area while achieving a displacement that is 2.0 mm smaller than the maximum allowed displacement. The green, dashed line corresponds to the maximum allowed displacement, where positive values consist of solutions that exceed the maximum allowed displacements. Accordingly, negative values consist of solutions with displacements smaller than the maximum allowed displacement. The red boxes are Pareto solutions, where the blue-marked box is identified as the most optimal solution.

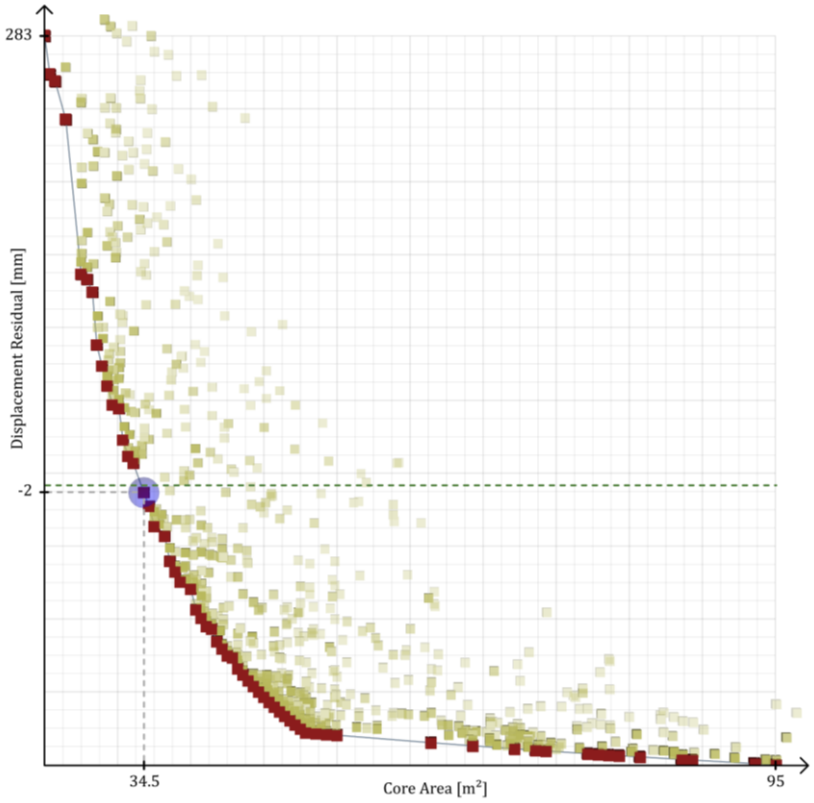

Figure 4.9: Optimization graph for Case A1.

The results of the optimization for Case A2 are depicted as red boxes at the Pareto front in Figure 4.10 below. The most optimal solution achieves a displacement that is 0.7 mm smaller than the maximum allowed displacement.

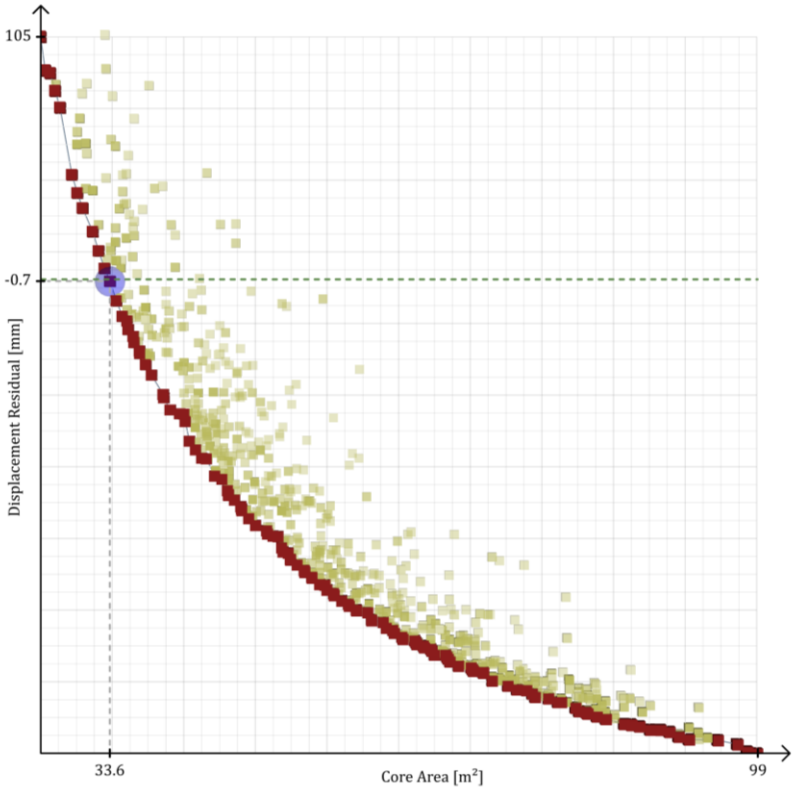

Figure 4.10: Optimization graph for Case A2.

The output data in terms of core dimensions, concrete mass, displacements and moment at the supports for Case A1 and A2 are summarized in Table 4.10 below.

Table 4.10: Output data for Case A1 and A2.

	Case A1	**Case A2**
Core Dimensions	6.9 x 5 m	6.1 x 5.5 m
Core Wall Thickness	0.49 m	0.5 m
Core Area	34.5 m^2	33.55 m^2
Concrete Mass	3778.5 ton	3758.4 ton
Displacement	257.2 mm	258.5 mm
Moment	M_y = 294.7 MNm	M_y = 147.4 MNm M_x = -147.4 MNm

The Rhino/Grasshopper tool displays the wind load distribution, deflection and moment and shear force distribution of the core according to Figure 4.11. This allows the user to visualize the distribution of forces and the bending behavior of the core depending on the loading conditions. The visual displacement of the core is scaled by a factor of 20 in Figure 4.11.

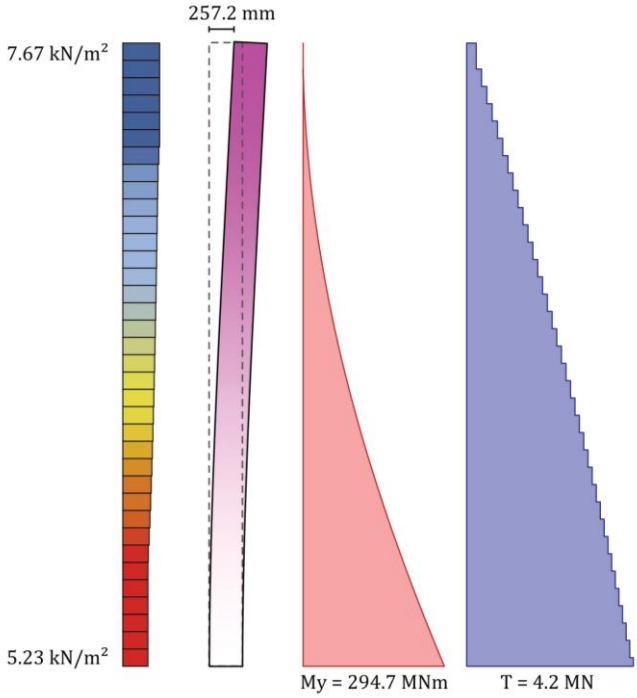

Figure 4.11: Wind load distribution, displacement, moment and shear force distribution for Case A1.

The wind load distribution, deflections and moment and shear force distribution for Case A2 is presented in Figure 4.12 below.

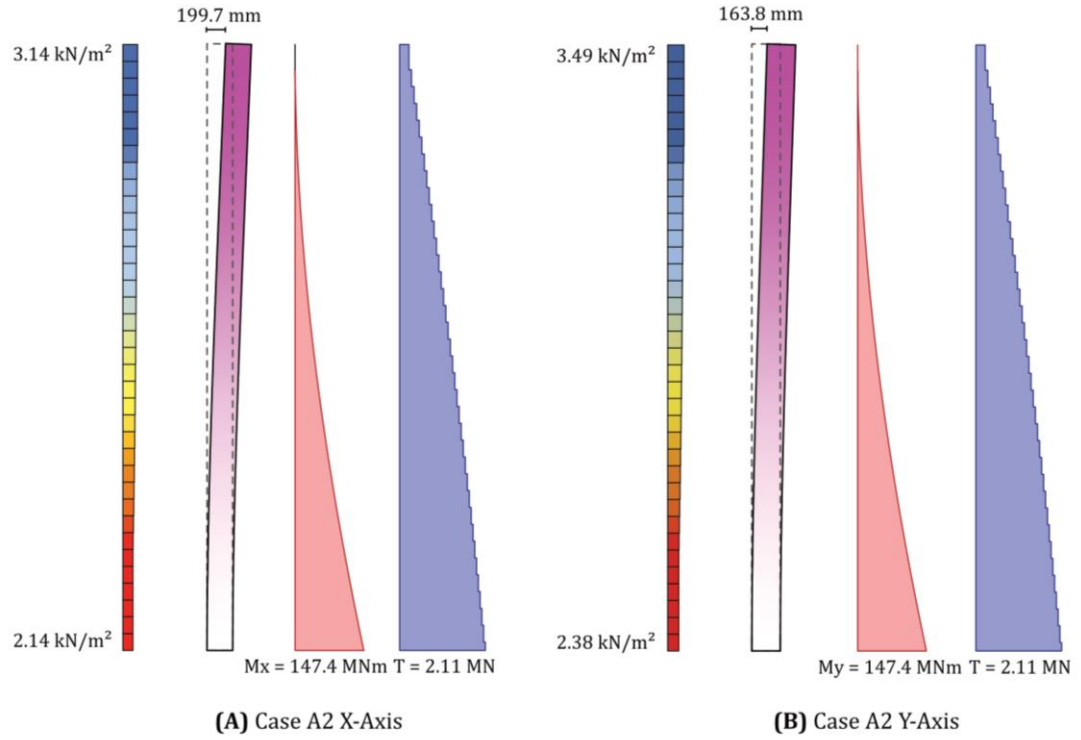

Figure 4.12: Wind load distribution, displacement, moment and shear force distribution for Case A2.

The results show that a smaller core is sufficient when the wind load angle is 135° compared to when the wind load angle is 180°. This is expected as the building is fully loaded on the west facade when the wind load angle is 180°. When the wind blows diagonally, the wind load is divided on the north and west facade. This means that the north and west facades are less loaded in Case A2 compared to when the west facade is fully loaded in Case A1. Despite this, the displacement at the top of the building is slightly higher in Case A2 than in Case A1. This is due to the building bending diagonally when the wind blows diagonally, making the resulting displacement the hypothenuse of a right-angled triangle.

Furthermore, a square core is more beneficial when the wind blows diagonally, whereas a rectangular core is more beneficial when the wind blows from one direction. When the wind blows diagonally, all four edges of the core are activated, resulting in a square core being the best choice. In contrast, when the wind blows in one direction, two parallel edges of the core are activated, resulting in a rectangular core with the strong bending axis placed in the wind direction being the best choice.

4.6.2 Case B

In Case B, the building envelope is rectangular, where the wind load angle is 180° for Case B1 and 135° for Case B2. All other geometrical input data of the building envelope and wind properties are kept the same between Case B1 and B2. The dimensions and wind angle of Case B1 and B2 are depicted in Figure 4.13 below.

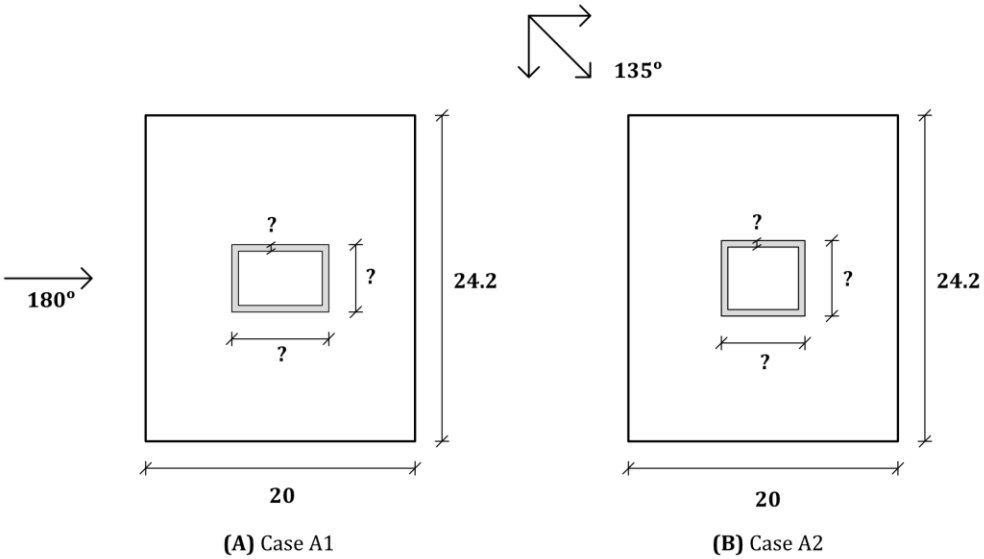

Figure 4.13: Dimensions in meters and wind properties of Case B1 and B2.

The input data for Case B1 and B2 are summarized in Table 4.11 below.

Table 4.11: Input data for Case B1 and B2.

	Case B1	**Case B2**
Number of Levels	36	36
Level Height	3.6 m	3.6 m
Building Height	129.6 m	129.6 m
Building Envelope	20 x 24.2 m	20 x 24.2 m
Concrete Class	C30/37	C30/37
Reference Wind Speed v_b	21 m/s	21 m/s
Terrain Category	II	II
Wind Angle	180°	135°

The results of the optimization for Case B1 are depicted as red boxes at the Pareto front in Figure 4.14 below. The most optimal solution achieves a displacement that is 4.6 mm smaller than the maximum allowed displacement.

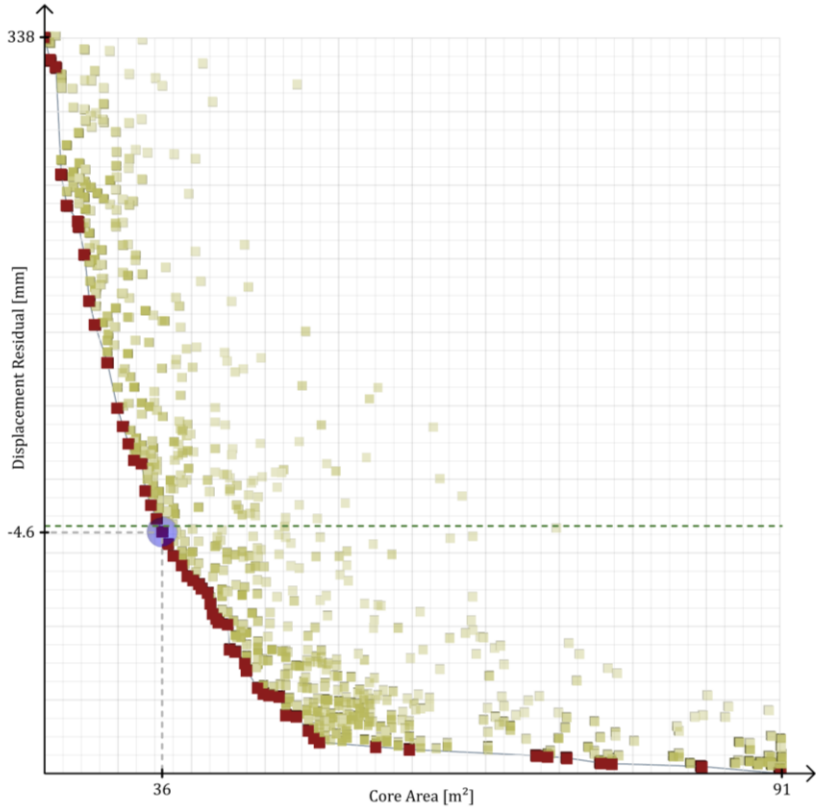

Figure 4.14: Optimization graph for Case B1.

The results of the optimization for Case B2 are depicted as red boxes at the Pareto front in Figure 4.15 below. The most optimal solution achieves a displacement that is 5.4 mm smaller than the maximum allowed displacement.

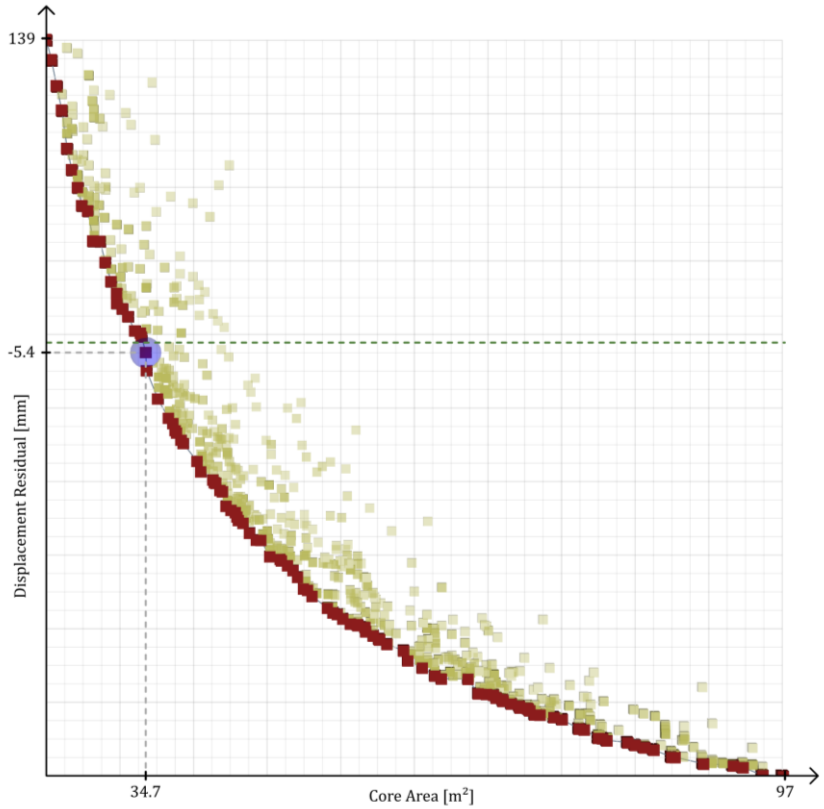

Figure 4.15: Optimization graph for Case B2.

The output data in terms of core dimensions, concrete mass, displacements and moment at the supports for Case B1 and B2 are summarized in Table 4.12 below.

Table 4.12: Output data for Case B1 and B2.

	Case B1	**Case B2**
Core Dimensions	7.2 x 5 m	6.2 x 5.6 m
Core Wall Thickness	0.49 m	0.48 m
Core Area	36 m^2	34.72 m^2
Concrete Mass	3873.7 ton	3670.3 ton
Displacement	254.6 mm	253.8 mm
Moment	M_y = 324.4 MNm	M_y = 162.2 MNm M_x = -133.7 MNm

The wind load distribution, deflections and moment and shear force distribution for Case B1 is presented in Figure 4.16 below.

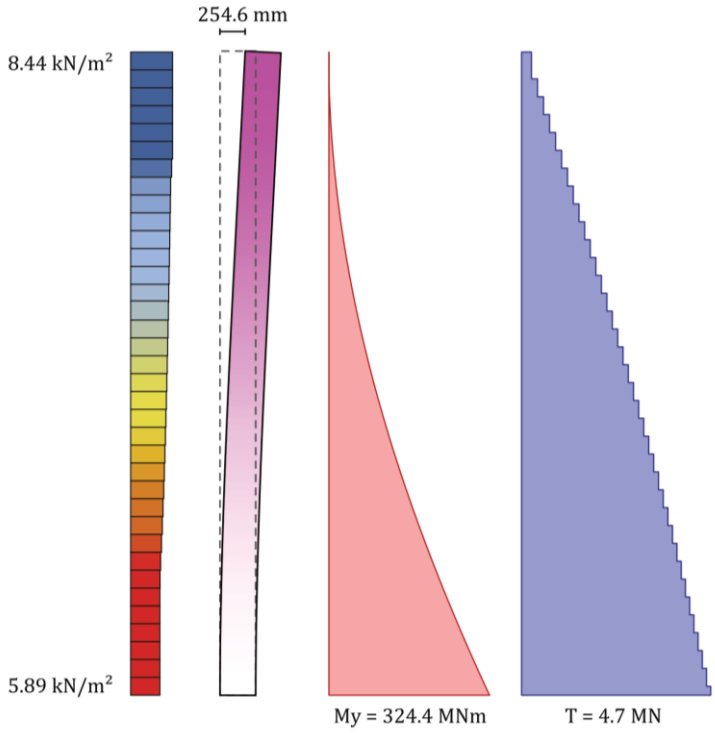

Figure 4.16: Wind load distribution, displacement, moment and shear force distribution for Case B1.

The wind load distribution, deflections and moment and shear force distribution for Case B2 is presented in Figure 4.17 below.

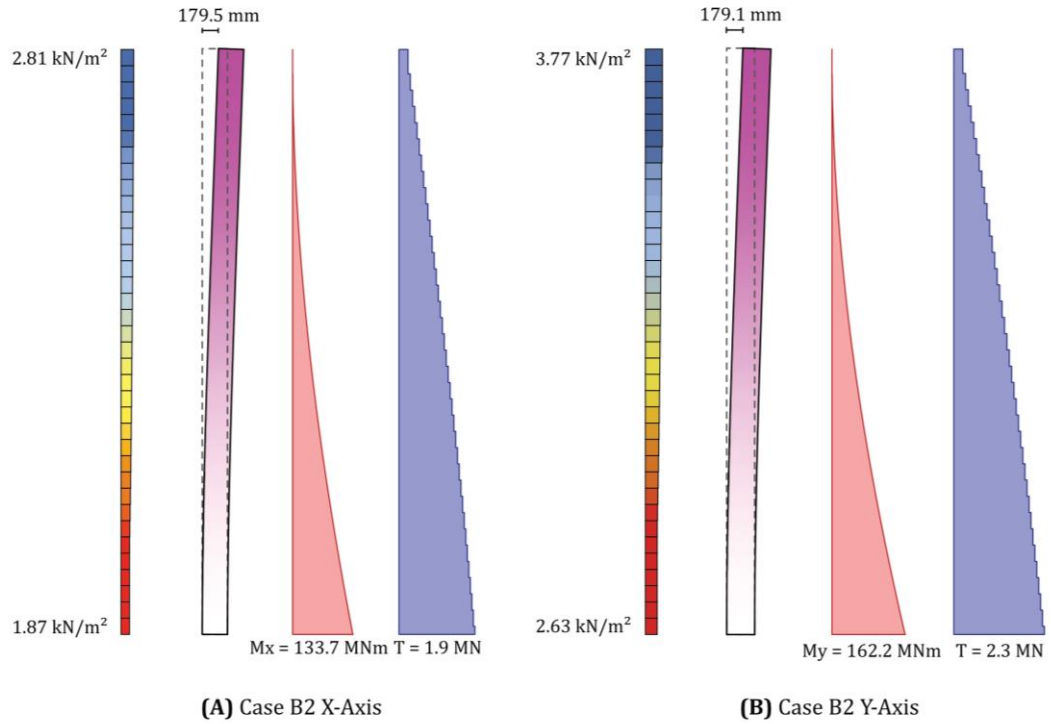

Figure 4.17: Wind load distribution, displacement, moment and shear force distribution for Case B2.

The results from Case B show that a smaller core is sufficient when the wind load angle is 135° compared to when the wind load angle is 180°. The results from both optimizations show that a smaller core is needed when the wind blows diagonally compared to when the wind blows in one direction. Furthermore, it seems that a square core is more beneficial when the wind blows diagonally whereas a rectangular core is more beneficial when the wind blows from one direction.

Compared to Case A, the displacement at the top of the building is slightly lower in Case B2 than in Case B1. Since the building footprint is rectangular, the wind load is distributed over a larger area on the west facade in Case B2 compared to Case A2. Due to this, the effect on the core is a slightly lower total displacement at the top of the building.

5 Reference Building

The development of the ETABS/VBA tool is implemented for analysis of a reference building that is planned to be built in Gothenburg in the coming years. In this chapter, the reference building will be introduced along with all relevant input data. The structural system of the building, material properties and load combinations in SLS and ULS are also presented.

5.1 Centralstaden, Gothenburg

Gothenburg is the second largest city in Sweden and is growing with several new high-rise buildings that have been and are planned to be built in the near future. In the city center close to the central station, a new neighborhood is planned called Centralstaden (Göteborgs Stad, n.d.). The central station is currently a region where traffic and congestion dominate the area. The extensive development with Centralstaden aims to turn the area into accessible and attractive neighborhoods with a vibrant city life.

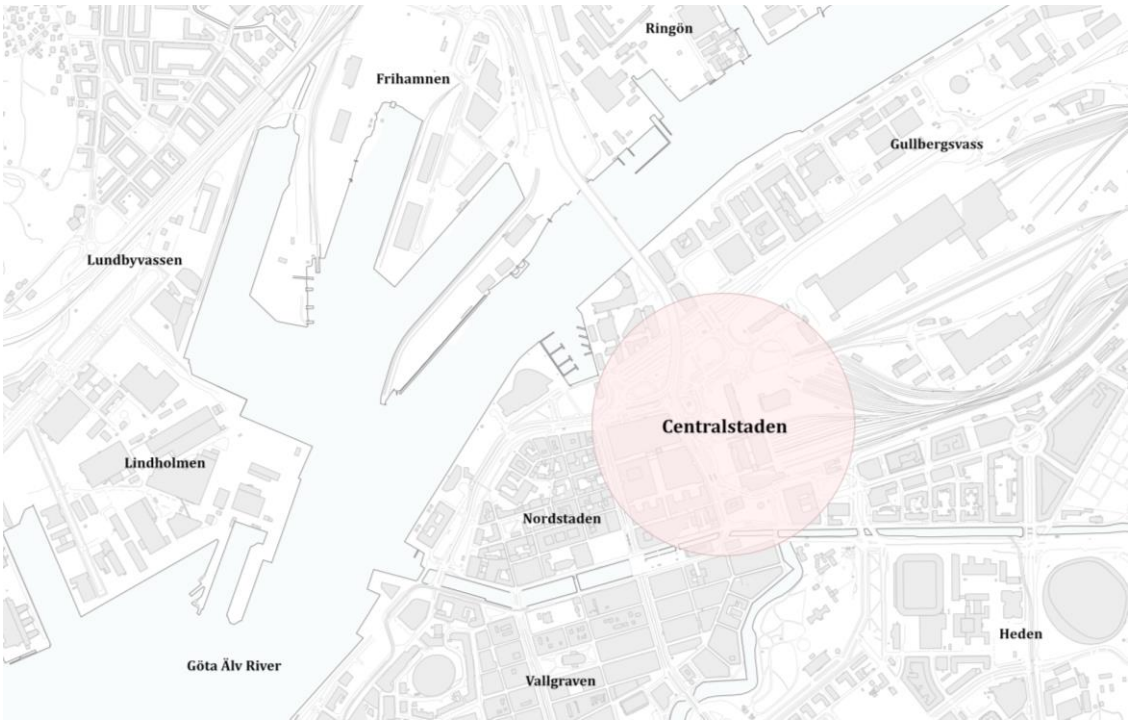

Figure 5.1: Map of Gothenburg showing the area of interest, Centralstaden, marked in red.

The buildings within Centralstaden are planned to have a height between 80-130 m and will consist of offices, residential and public buildings. The building in question for this thesis will primarily be a residential building with a height between 110-130 m. This building is used to gain relevant measures from a real project, however, due to copyright reasons only generic data is presented in this thesis.

5.2 Input Data

5.2.1 Geometry

The building has a rectangular footprint with dimensions of 24 x 21 m. The height is not determined yet but will be between 110-130 m. In this thesis, the height is assumed to be 128.4 m spread over 40 stories. The first three stories have a height of 4.8 m while all other stories have a height of 3.0 m. The core dimensions will be iterated until dimensions that fulfill the requirement on maximum horizontal deflection are found. The core will have one opening on the south and north sides and two openings on the west and east sides. The openings have a height of 2.3 m and a width of 1.0 m for the sides with two openings and 1.2 m for the sides with one opening.

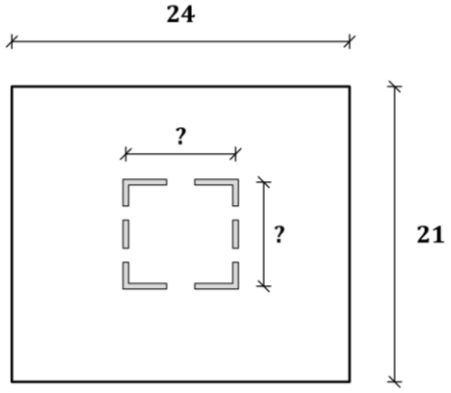

Figure 5.2: Simplified floor plan of the reference building with dimensions in meters of the building envelope.

5.2.2 Structural System

The structural system of the building will consist of a shear wall system with a rectangular cast-in-situ concrete core in the center of the building. Columns will be placed at the facades, but they will only handle vertical loads and not wind loads. This assumption is reasonable since the core is much stiffer than the columns and the building has no outriggers.

5.2.3 Material Properties

The different materials and their properties of the structural elements in the building are presented in Table 5.1 below.

Table 5.1: The relevant materials and their properties of the structural elements in the building.

Structural Element	Material	Property	Section
Base	Concrete	C50/60	t = 2000 mm
Slabs	Concrete	C50/60	t = 250 mm
Core Walls	Concrete	C50/60	200 ≤ t ≤ 600
Columns	Steel	S355	VKR 400x400x20
Piles	Steel/Concrete	C50/60	RD320x12+Concrete

5.2.4 Loads

The building will be subjected to both permanent and variable loads. The permanent loads include the dead weights of slabs and columns as well as installations and partition walls. The variable loads include wind load and imposed load, where snow load is neglectable in this case. The horizontal wind load will act on the core whereas the vertical loads acting on the slabs will be distributed and transferred to the columns and core.

Table 5.2: The permanent and variable loads acting on the building, excluding the dead loads from the structure and wind loads.

Loads	[kN/m^2]
Imposed Load (Residential)	2.0
Superimposed Dead Load (SDL)	1.5

5.2.4.1 Wind Loads

Since the building will be situated in Gothenburg, the reference wind velocity v_b is 25 m/s. The building is assumed to be in terrain category IV. The wind loads are assumed to decrease when a wind tunnel test is performed on the building, making terrain category IV a conservative choice.

To obtain the worst loading case, the wind is applied diagonally and perpendicular to all sides of the building, resulting in a total of eight wind directions. The relevant wind load properties are presented in Table 5.3 below.

Table 5.3: Wind load properties.

Wind Load	
Wind Velocity [v_b]	25 m/s
Terrain Category	IV
Windward Coefficient [C_p]	0.8
Leeward Coefficient [C_p]	0.5
Air Density [ρ_{air}]	1.25 kg/m^3
Orography Factor [$Co(z)$]	1
Structural Factor [$CsCd$]	1
Turbulence Factor [$K1$]	1
Direction Angles	0^o, 45^o, 90^o, 135^o, 180^o, 225^o, 270^o, 315^o

5.2.5 Load Combinations

The following load combinations in Equation 5.1-5.5 are defined in ETABS and the structural performance of the core for each load combination will be calculated. No load reduction factor is applied on the imposed load for multiple stories as that is more relevant in later design stages for fine tuning.

$$\mathrm{ULS_{WLML}} = 1.2 \cdot g_{dead} + 1.5 \cdot q_{wind} + 1.5 \cdot \psi_{0,imposed} \cdot q_{imposed} \quad (5.1)$$

$$\mathrm{ULS_{LLML}} = 1.2 \cdot g_{dead} + 1.5 \cdot q_{imposed} + 1.5 \cdot \psi_{0,wind} \cdot q_{wind} \quad (5.2)$$

$$\mathrm{ULS_{WL}} = 1.0 \cdot g_{dead} + 1.5 \cdot q_{wind} \quad (5.3)$$

$$\mathrm{SLS_{WL}} = g_{dead} + q_{wind} \quad (5.4)$$

$$\mathrm{SLS_{WLML}} = g_{dead} + q_{wind} + 0.7 \cdot q_{imposed} \quad (5.5)$$

where:

$\mathrm{ULS_{WLML}}$ = load combination in ULS where the wind load is the main load and imposed load is an accompanying load [kN/m^2]

$\mathrm{ULS_{LLML}}$ = load combination in ULS where the imposed load is the main load and wind load is an accompanying load [kN/m^2]

$\mathrm{ULS_{WL}}$ = load combination in ULS where the wind load is the only variable load and the dead loads are favorable [kN/m^2]

$\mathrm{SLS_{WL}}$ = characteristic load combination in SLS where the wind load is the only variable load [kN/m^2]

$\mathrm{SLS_{WLML}}$ = characteristic load combination in SLS where the wind load is the main load and imposed load is an accompanying load [kN/m^2]

$\psi_{0,imposed}$ = 0.7 for imposed load for a residential building [-]

$\psi_{0,wind}$ = 0.3 for wind load [-]

6 ETABS/VBA Tool

This chapter introduces the previous in-place ETABS/VBA tool before being further developed, as well as the development process made as part of this thesis, and outcome of the tool. The tool will be used to optimize the core dimensions, material usage and CO2e of the reference building presented in the previous chapter and can be used for future projects within the practice.

6.1 Overview of the Previous Tool

As previously mentioned in the introduction chapter, the previous ETABS/VBA tool implemented at VBK, before being further developed through this thesis, consisted of manually creating a FE-model of a high-rise building in ETABS. The model could then be modified to a certain extent by using a script in Excel through VBA. The previous possible modifications were changes in the thickness of the core walls at different levels.

The tool benefits from including other modifications of the model through Excel/VBA, including geometrical modifications of the structural elements. By parametrizing geometrical properties, several structural designs can be analyzed in one go, rather than having to manually change the geometry and performing a FE-analysis for each design.

6.2 Development of the ETABS/VBA Tool

6.2.1 Flow Chart

The input, depicted as yellow in Figure 6.1, of the ETABS/VBA tool is given in different worksheets in Excel. Piles, beams, sections, materials, loads and load combinations need to be manually defined in ETABS. Although the slabs and columns are parametrized and defined in Excel, no changes are made to their dimensions or properties during the iterations. Rather, it is only the cores dimensions and wall thicknesses that change during the iterations. Once all input is given, the script can be run through macros in VBA, depicted in blue. The script links the input in Excel with a running instance of ETABS, creating and analysing a set amount of wall models for each core model. A wall model consists of different wall thicknesses over the height of the core, whereas a core model consists of a specific length and width of the core. The results, depicted in green, are extracted and stored in Excel for each iteration. Finally, some post-calculations are made to the results before they are visualized in Tableau. Further instructions on how the tool works can be found in Appendix B.

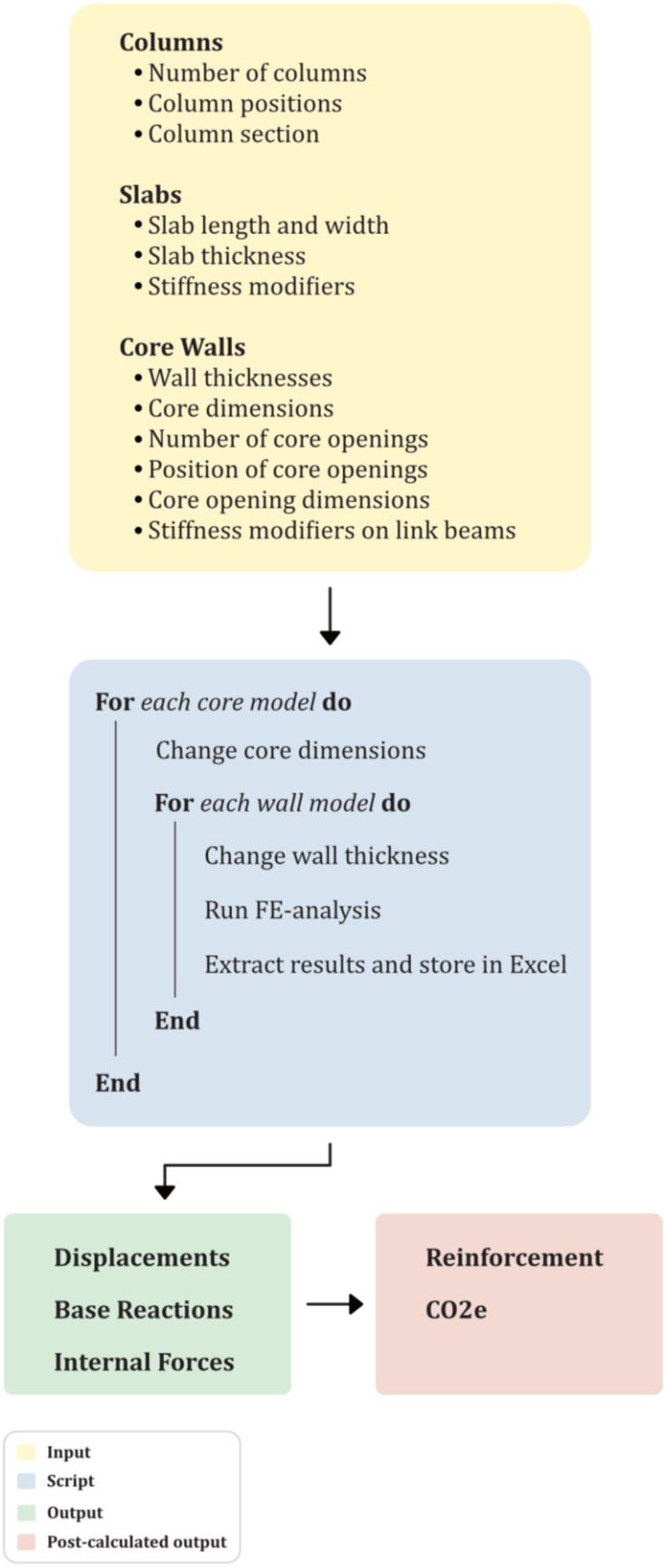

Figure 6.1: Flow chart showing how the ETABS/VBA Tool works.

6.2.2 Parametrization of the Core

To parametrize the dimensions of the core, it is not enough to only define the dimensions of each core model in Excel. Rather, parameters such as the number of core openings and positions of the openings need to be determined. A maximum number of three openings per core edge can be defined in Excel. In the case of three openings at each core edge, this results in a total number of 28 partitions. In Figure 6.2, all 28 core walls are shown where the red, dashed lines depict the core openings.

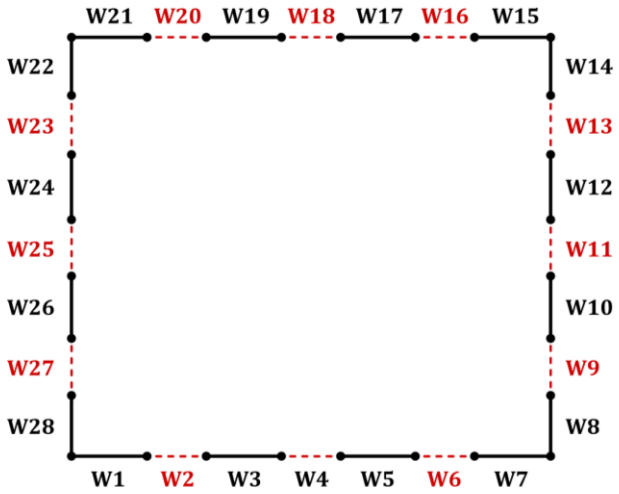

Figure 6.2: Plan view showing how the core wall partitions are defined.

Above the core openings, link beams are placed that link together two adjacent walls. The link beams are assumed to be cracked and therefore need to have stiffness modifiers assigned to them to reduce their stiffness in the FE-model.

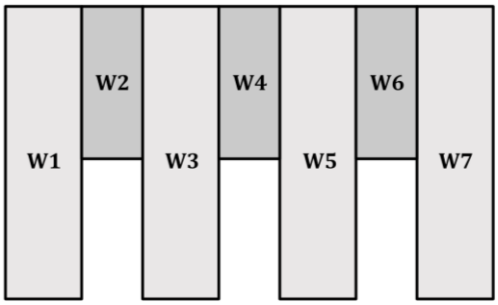

Figure 6.3: Elevation showing one story of core walls W1, W3, W5, W7 and link beams W2, W4, W6.

Once the number of openings is defined, the opening type assigned to each opening needs to be defined. The opening type sets the length and height of the opening. Lastly, the local start coordinates of each opening need to be defined. When the core dimensions of each core model and properties of the openings are defined, all other coordinates of the core walls are automatically calculated in Excel through functions.

Figure 6.4 illustrates the start coordinates of the openings that need to be given by the user in Excel. Only the X-coordinate on the horizontal side needs to be given, whereas on the vertical side only the Y-coordinate needs to be given.

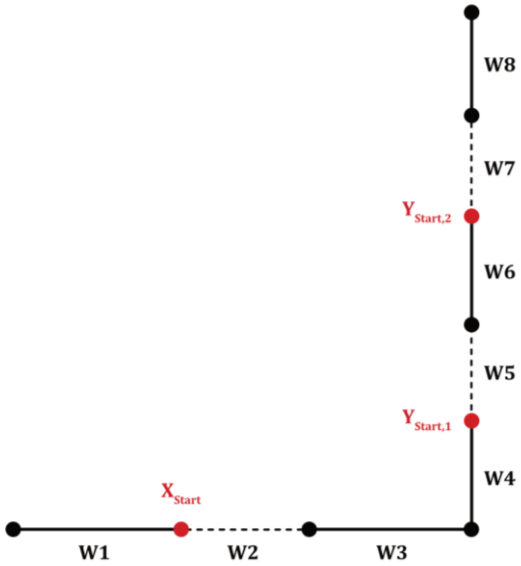

Figure 6.4: Illustration showing the user-defined start coordinates of the core openings.

To reduce the amount of input data that needs to be given by the user, the number of openings and positions of the openings are only defined for the first core model. This means that the number of openings and opening types are the same for all core models, however the positions of the openings change for each core model. This slightly limits the flexibility of the tool as the user has less control over the opening configurations for each iteration, but gives more comparable results.

The change of positions of the openings depends on the difference in core dimensions between core 1 and core *i*. In Figure 6.5, one side of core 1 has a length of 7.8 m and the opening has the starting position X_{start}. The corresponding side of core 2 has a length of 8.0 m. Therefore, the difference in length between the cores is 0.2 m. For core 2, the starting position is added by half the difference as seen in Figure 6.5.

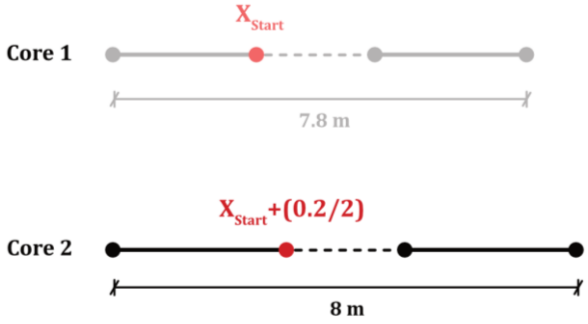

Figure 6.5: Illustration showing how the coordinates of the core walls change when the core dimensions change.

Likewise, if one side of core *i* is smaller than the corresponding edge of core 1, the starting position is subtracted by the difference. The user needs to ensure that the core for all iterations is large enough to enable the defined openings.

Once all input is given in Excel, the script can be run through macros in Excel. The script starts by updating the core wall coordinates for core i in Excel. Since the wall coordinates are defined in local coordinates, they are converted into global coordinates before the walls are modelled in ETABS. Then, names and labels from the walls in ETABS are extracted and stored in Excel. This is to have unique information of each wall to be able to change their wall thickness. A FE-analysis is performed and the results are extracted from ETABS and stored in Excel. This procedure is repeated for the set amount of wall models and core models.

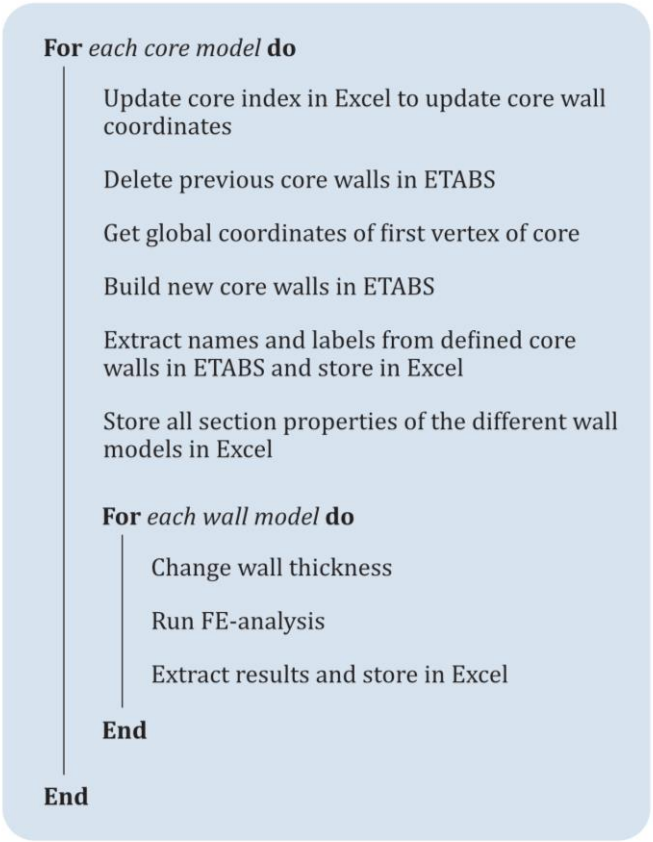

Figure 6.6: Pseudo-code describing the script that links Excel with ETABS through VBA.

6.2.3 Pier Forces

To obtain the internal forces in the core walls, pier labels need to be assigned to each core wall. Through the pier labels, pier forces such as axial and shear forces can be extracted. The pier forces are derived from a column placed centrally in each core wall, meaning that smaller core walls return more accurate internal forces compared to larger core walls. Due to this, the defined core walls in Excel are divided into finer walls through an extension of the script in VBA. The script divides the core walls into a desired length and creates finer core walls in ETABS. For each fine core wall that is created, a new pier label is defined and assigned to the corresponding wall in ETABS. In this way, equally and evenly distributed fine core walls can be obtained around the whole perimeter of the core.

The script for dividing the core walls into finer walls and obtaining the pier forces is intended to be an additional tool for in-depth analysis of the iterations. Since the total amount of core walls increases significantly when creating finer core walls, it becomes much more computationally heavy. Thus, this script has been implemented to run separately from the main script. The red text in Figure 6.8 shows the additional script that is added on top of the main script in black text, where the only difference is that coordinates for the fine core walls are created in VBA and pier labels are defined in ETABS and assigned to each fine core wall.

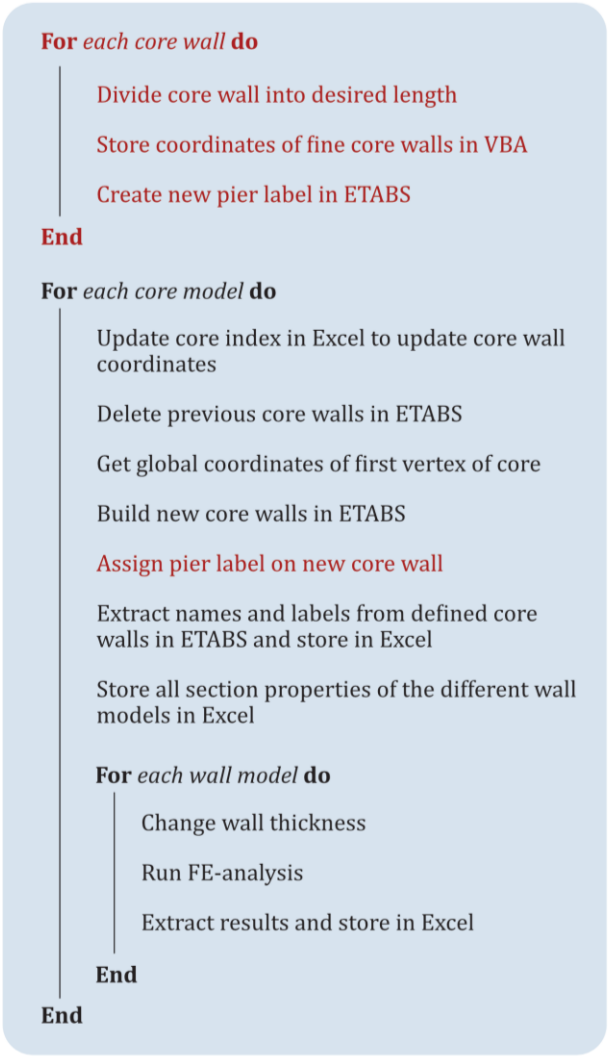

Figure 6.7: Pseudo-code describing the script for obtaining pier forces.

6.2.4 Reinforcement

The pier forces are used for to calculate the required reinforcement amounts based on the normal stress in each core wall. The ETABS/VBA tool is not intended to be used as a tool to obtain an estimation of the required reinforcement amounts since the calculations implemented in the tool are approximations. Rather, the calculated reinforcement amounts can be used as an indication of the amount of reinforcement that is required for each model.

The required amount of tensile reinforcement is dependent on the tensile stress in the walls due to the bending moment caused by wind and is calculated in Tableau for different rebar diameters. The rebar is assumed to have a characteristic yield stress of f_{yk} = 500 MPa.

The required amount of compressive reinforcement depends on the compressive force in the walls due to dead loads and the thickness of the wall. Therefore, the minimum and maximum compressive forces in the walls are calculated in Tableau. These loads have been applied to a meter wide wall of different thicknesses in Strusoft's WIN-Statik software to obtain the required amount of compressive reinforcement. The compressive loads and corresponding reinforcement are then linearly interpolated in order to calculate the compressive reinforcement for the compressive force in each wall. A minimum compressive reinforcement amount of $0.002 \cdot A_c$ is assigned to the walls.

The horizontal reinforcement amount is in this case only determined by the thickness of the wall, where the thinner walls have sparsely spaced rebars in contrast to thicker walls. The horizontal reinforcement amounts that are assigned to each wall thickness are specified in Table 6.1 below and are based on reference values.

Table 6.1: Horizontal reinforcement specification and amount for different wall thicknesses.

Wall Thickness [mm]	Reinforcement [-]
500	Φ16s100
400	Φ16s150
300	Φ16s200
200	Φ12s200

6.3 FE-Modelling

In ETABS, the slabs and core walls are defined as 2D shells with a thickness. The columns and piles are defined as frame objects with a user-defined section. Edge beams without any stiffness or weight are added at the edges of the slabs with the only purpose to add cladding load to them. The position and number of piles were calculated and modelled in the previous workflow prior to this thesis. The piles are concentrated around the core area but will not be positioned directly under the core walls for each core model iteration since the exact positions of the piles are assumed not to have a large effect on the structural performance of the core.

Stiffness modifiers are added to the slabs and link beams to reduce their stiffness and simulate as realistic behavior as possible. The base slab is assumed to be cracked and its stiffness is reduced to 50 % for axial, moment and shear capacity. For the other slabs, their stiffness is reduced to 20 % for axial, moment and shear capacity. This is to ensure that the wind loads are resisted by the core walls and not the slabs. The link beams are also assumed to be cracked and their stiffness is reduced to 45 % for axial capacity. The core walls are assumed to be uncracked and therefore no stiffness modifiers are applied to them.

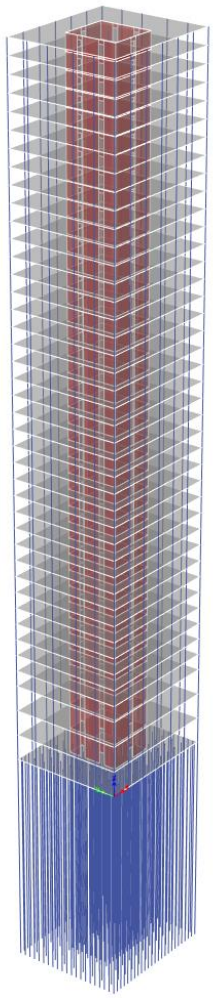

Figure 6.8: FE-model of the building in ETABS.

6.4 Results

6.4.1 Iteration 1

6.4.1.1 Core and Wall Models

The first iteration serves to obtain estimations of the minimum required core dimensions and wall thicknesses. The core dimensions are arbitrarily chosen for six different core models and vary between each core model to analyze a wide range of core dimensions.

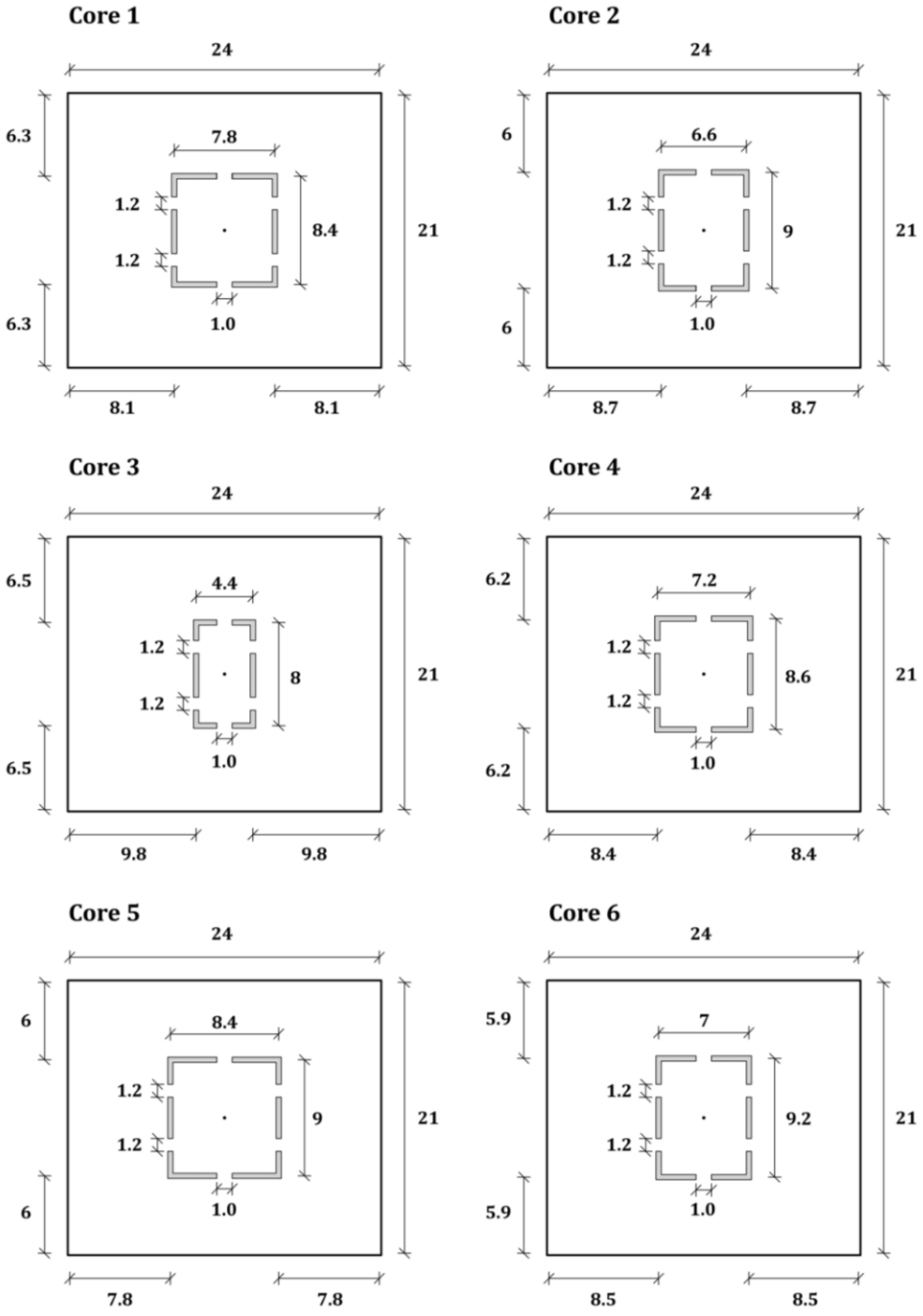

Figure 6.9: The six different core models that have been studied.

The wall thicknesses that have been used in the different core models are shown in Table 6.2 below. The thickness decreases with increasing height as the lower stories need larger wall thicknesses to withstand the maximum moment that is achieved at the base. Since six core models and 21 wall models have been defined, a total number of 126 models are analyzed during the first iteration.

Table 6.2: The 21 different wall models with varying wall thicknesses at each story.

Core Wall Thicknesses [mm]

	Model01	Model02	Model03	Model04	Model05	Model06	Model07	Model08	Model09	Model10	Model11	Model12	Model13	Model14	Model15	Model16	Model17	Model18	Model19	Model20	Model21
Story41	200	200	200	200	200	300	300	300	300	300	400	400	400	400	400	500	500	500	500	500	600
Story40	200	200	200	200	200	300	300	300	300	300	400	400	400	400	400	500	500	500	500	500	600
Story39	200	200	200	200	200	300	300	300	300	300	400	400	400	400	400	500	500	500	500	500	600
Story38	200	200	200	200	200	300	300	300	300	300	400	400	400	400	400	500	500	500	500	500	600
Story37	200	200	200	200	200	300	300	300	300	300	400	400	400	400	400	500	500	500	500	500	600
Story36	200	200	200	200	300	300	300	300	300	400	400	400	400	400	500	500	500	500	500	600	600
Story35	200	200	200	200	300	300	300	300	300	400	400	400	400	400	500	500	500	500	500	600	600
Story34	200	200	200	200	300	300	300	300	300	400	400	400	400	400	500	500	500	500	500	600	600
Story33	200	200	200	200	300	300	300	300	300	400	400	400	400	400	500	500	500	500	500	600	600
Story32	200	200	200	200	300	300	300	300	300	400	400	400	400	400	500	500	500	500	500	600	600
Story31	200	200	200	200	300	300	300	300	300	400	400	400	400	400	500	500	500	500	500	600	600
Story30	200	200	200	200	300	300	300	300	300	400	400	400	400	400	500	500	500	500	500	600	600
Story29	200	200	200	200	300	300	300	300	300	400	400	400	400	400	500	500	500	500	500	600	600
Story28	200	200	200	200	300	300	300	300	300	400	400	400	400	500	500	500	500	500	600	600	600
Story27	200	200	200	300	300	300	300	300	400	400	400	400	400	500	500	500	500	500	600	600	600
Story26	200	200	200	300	300	300	300	300	400	400	400	400	400	500	500	500	500	500	600	600	600
Story25	200	200	200	300	300	300	300	300	400	400	400	400	400	500	500	500	500	500	600	600	600
Story24	200	200	200	300	300	300	300	300	400	400	400	400	400	500	500	500	500	500	600	600	600
Story23	200	200	200	300	300	300	300	300	400	400	400	400	400	500	500	500	500	500	600	600	600
Story22	200	200	200	300	300	300	300	300	400	400	400	400	400	500	500	500	500	500	600	600	600
Story21	200	200	200	300	300	300	300	300	400	400	400	400	400	500	500	500	500	500	600	600	600
Story20	200	200	200	300	300	300	300	300	400	400	400	400	400	500	500	500	500	500	600	600	600
Story19	200	200	200	300	300	300	300	300	400	400	400	400	400	500	500	500	500	500	600	600	600
Story18	200	200	300	300	300	300	300	400	400	400	400	400	500	500	500	500	500	600	600	600	600
Story17	200	200	300	300	300	300	300	400	400	400	400	400	500	500	500	500	500	600	600	600	600
Story16	200	200	300	300	300	300	300	400	400	400	400	400	500	500	500	500	500	600	600	600	600
Story15	200	200	300	300	300	300	300	400	400	400	400	400	500	500	500	500	500	600	600	600	600
Story14	200	200	300	300	300	300	300	400	400	400	400	400	500	500	500	500	500	600	600	600	600
Story13	200	200	300	300	300	300	300	400	400	400	400	400	500	500	500	500	500	600	600	600	600
Story12	200	200	300	300	300	300	300	400	400	400	400	400	500	500	500	500	500	600	600	600	600
Story11	200	200	300	300	300	300	300	400	400	400	400	400	500	500	500	500	500	600	600	600	600
Story10	200	200	300	300	300	300	300	400	400	400	400	400	500	500	500	500	500	600	600	600	600
Story09	200	300	300	300	300	300	400	400	400	400	400	500	500	500	500	500	600	600	600	600	600
Story08	200	300	300	300	300	300	400	400	400	400	400	500	500	500	500	500	600	600	600	600	600
Story07	200	300	300	300	300	300	400	400	400	400	400	500	500	500	500	500	600	600	600	600	600
Story06	200	300	300	300	300	300	400	400	400	400	400	500	500	500	500	500	600	600	600	600	600
Story05	200	300	300	300	300	300	400	400	400	400	400	500	500	500	500	500	600	600	600	600	600
Story04	200	300	300	300	300	300	400	400	400	400	400	500	500	500	500	500	600	600	600	600	600
Story03	200	300	300	300	300	300	400	400	400	400	400	500	500	500	500	500	600	600	600	600	600
Story02	200	300	300	300	300	300	400	400	400	400	400	500	500	500	500	500	600	600	600	600	600
Story01	200	300	300	300	300	300	400	400	400	400	400	500	500	500	500	500	600	600	600	600	600

6.4.1.2 Displacements

The maximum horizontal displacements at the top of the building are shown in Figure 6.10 below. The results show that core 3 with dimensions 4.4 x 8.0 m has the largest horizontal displacements for all wall models. This is reasonable since core 3 has the smallest dimensions. Additionally, the results show that core 5 with dimensions 8.4 x 9.0 m is the only core model that doesn't exceed the maximum allowed horizontal displacement of h/500 for the thicker wall thicknesses. This indicates that the dimensions of core 5 and thicker wall thicknesses are reasonable or a larger core with thinner walls. The second iteration will therefore consist of core models that are similar to the dimensions of core 5.

It can also be seen that there is a minor difference in maximum horizontal displacement between a couple of adjacent wall models. For example, wall models 19-21 have the same displacement value in all core models. Wall model 21 has a wall thickness of 600 mm in all stories, whereas wall model 19 has a wall thickness of 600 mm in stories 1-28 and 500 mm in stories 28-41. Despite this, they have the same displacement value. This suggests that larger wall thicknesses are unnecessary in the top stories, as they have a minor effect on the maximum horizontal displacement.

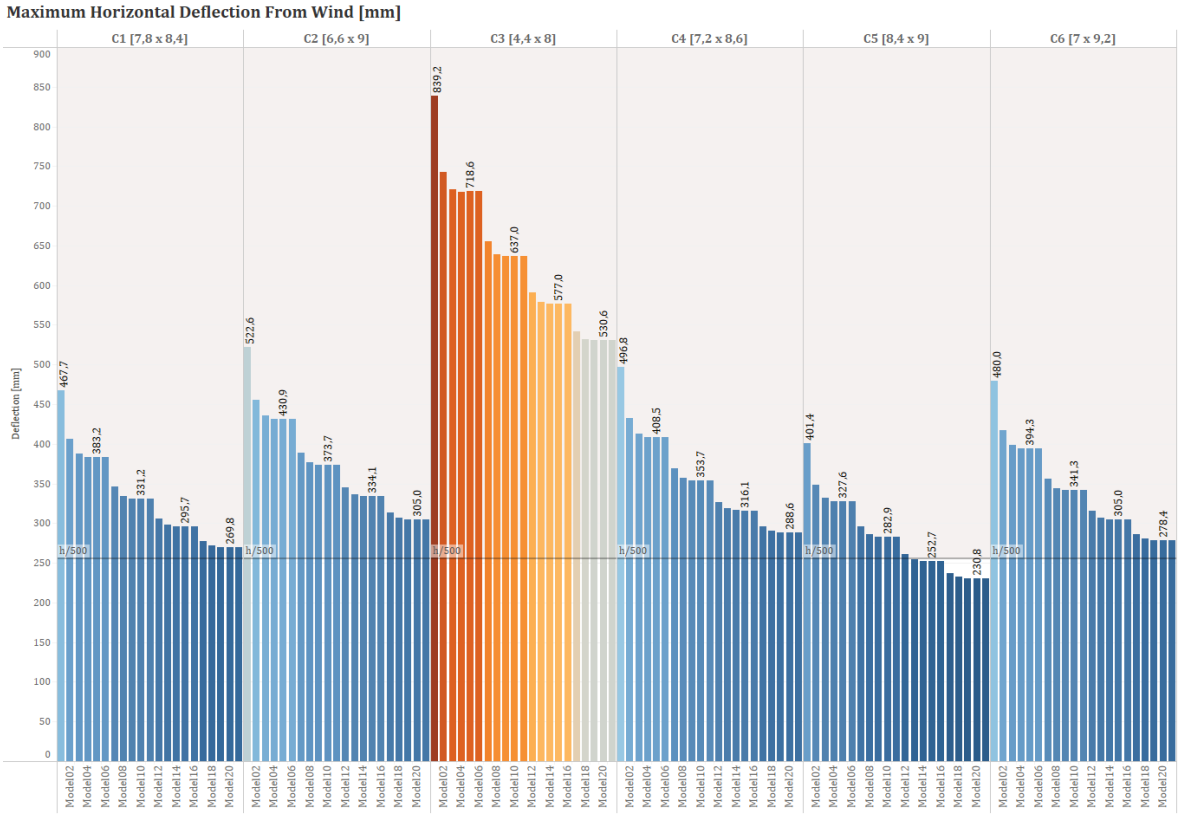

Figure 6.10: Maximum horizontal displacement from wind for the six different cores. C1-C6 denote the core model and Model01-Model21 denote the wall model.

6.4.2 Iteration 2

6.4.2.1 Core and Wall Models

For the second iteration, three different core models are defined along with nine different wall models, resulting in a total number of 27 models that are analyzed. The number of core and wall models are reduced in iteration 2 to simplify the comparison of results from the different models. The dimensions and wall thicknesses are adjusted according to the conclusions drawn from the previous iteration.

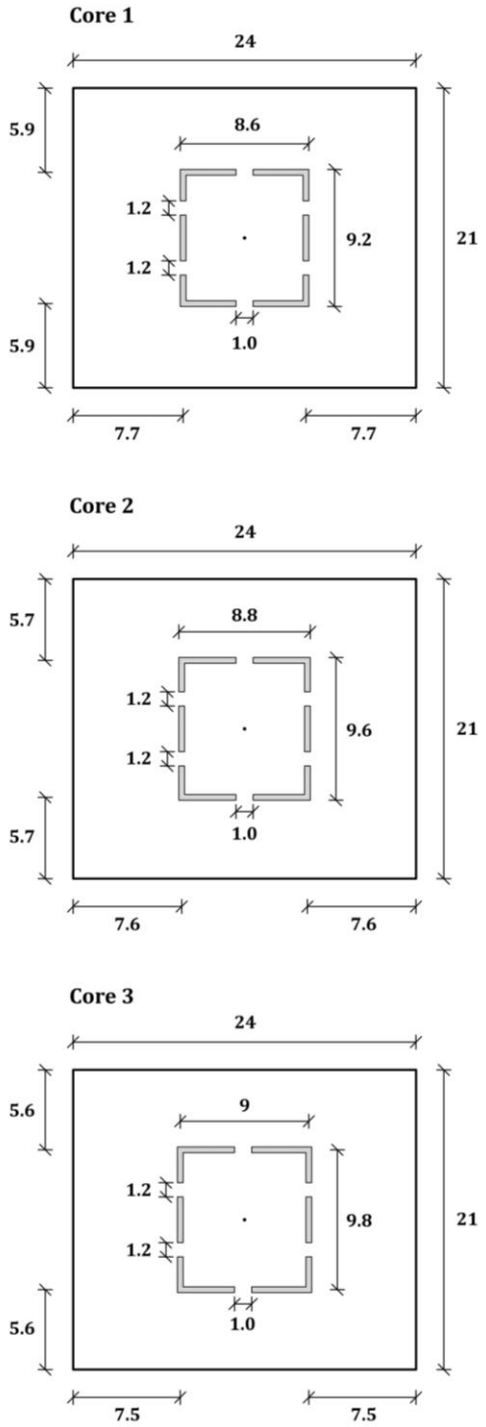

Figure 6.11: The three different core models that have been studied.

As previously concluded, larger wall thicknesses in the top stories have a minor effect on the horizontal displacement of the core. Therefore, the nine wall models in the second iteration all have a wall thickness of 200 mm at stories 36-41. Compared to the wall models in the previous iteration, the wall models in the second iteration have a minimum of three different wall thicknesses with increasing height, which is also more feasible from a building perspective.

Table 6.3: The nine different wall models with varying wall thicknesses at each story.

Core Wall Thicknesses [mm]

	Model01	Model02	Model03	Model04	Model05	Model06	Model07	Model08	Model09
Story41	200	200	200	200	200	200	200	200	200
Story40	200	200	200	200	200	200	200	200	200
Story39	200	200	200	200	200	200	200	200	200
Story38	200	200	200	200	200	200	200	200	200
Story37	200	200	200	200	200	200	200	200	200
Story36	200	200	200	200	200	200	200	200	200
Story35	200	200	200	300	300	300	300	300	300
Story34	200	200	200	300	300	300	300	300	300
Story33	200	200	200	300	300	300	300	300	300
Story32	200	200	200	300	300	300	300	300	300
Story31	200	200	300	300	300	300	300	300	300
Story30	200	200	300	300	300	300	300	300	300
Story29	200	200	300	300	300	300	300	300	300
Story28	200	200	300	300	300	300	300	300	300
Story27	200	300	300	300	300	300	300	300	400
Story26	200	300	300	300	300	300	300	300	400
Story25	200	300	300	300	300	300	300	300	400
Story24	200	300	300	300	300	300	300	300	400
Story23	300	300	300	300	300	300	300	400	400
Story22	300	300	300	300	300	300	300	400	400
Story21	300	300	300	300	300	300	300	400	400
Story20	300	300	300	300	300	300	300	400	400
Story19	300	300	300	300	300	300	400	400	400
Story18	300	300	300	300	300	300	400	400	400
Story17	300	300	300	300	300	300	400	400	400
Story16	300	300	300	300	300	300	400	400	400
Story15	300	300	300	300	300	400	400	400	500
Story14	300	300	300	300	300	400	400	400	500
Story13	300	300	300	300	300	400	400	400	500
Story12	300	300	300	300	300	400	400	500	500
Story11	300	300	500	300	400	400	400	500	500
Story10	300	300	500	300	400	400	400	500	500
Story09	300	300	500	300	400	400	500	500	500
Story08	300	300	500	300	400	400	500	500	500
Story07	300	500	500	400	400	400	500	500	500
Story06	300	500	500	400	400	500	500	500	500
Story05	300	500	500	400	400	500	500	500	500
Story04	500	500	500	400	400	500	500	500	500
Story03	500	500	500	400	500	500	500	500	500
Story02	500	500	500	400	500	500	500	500	500
Story01	500	500	500	400	500	500	500	500	500

6.4.2.2 Displacements

The maximum horizontal displacements at the top of the building are shown in Figure 6.12 below. The maximum displacements occur when the building is only loaded by wind diagonally, where no imposed or dead loads help to resist the moment. The results show that core 3 with dimensions 9.0 x 9.8 m is the only core model that doesn't exceed the maximum allowed horizontal displacement for all wall models. This is expected since core 3 has the largest dimensions. Core 1 with dimensions 8.6 x 9.2 m has acceptable displacement values for wall models 7-9, whereas core 2 with dimensions 8.8 x 9.6 m has acceptable displacement values for wall models 2-3 and 5-9.

To evaluate if a smaller core with larger wall thicknesses that fulfils the maximum allowed horizontal displacement is a better choice in regard to CO2e than a larger core with smaller wall thicknesses, the total amount of required reinforcement needs to be considered.

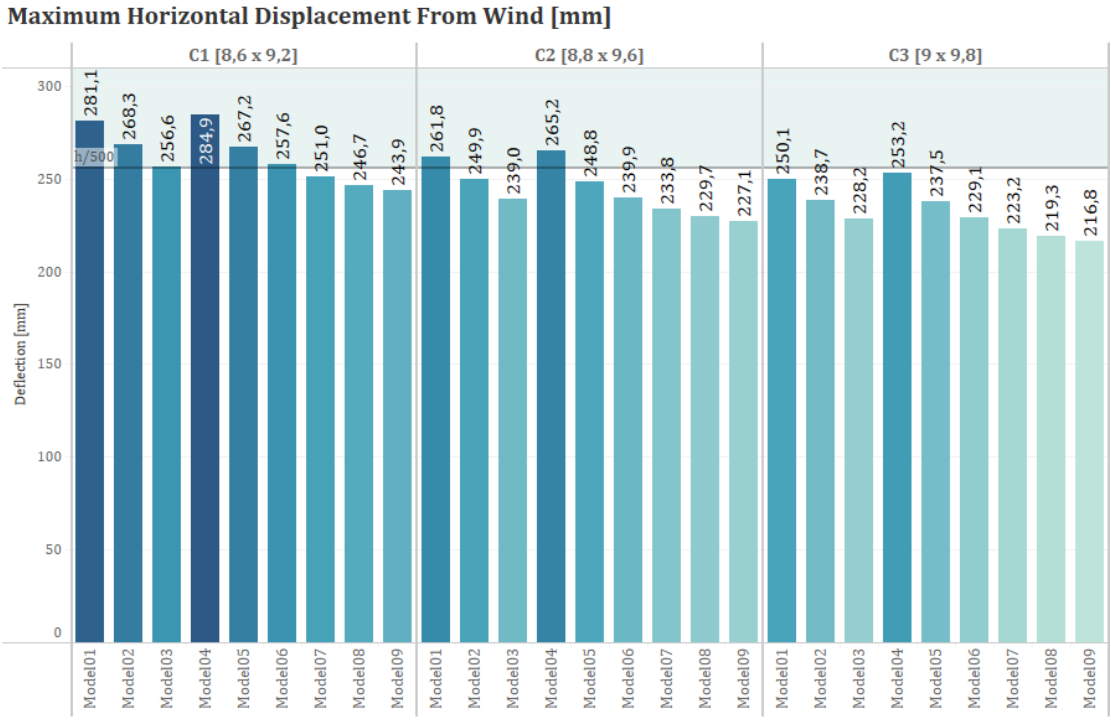

Figure 6.12: Maximum horizontal deflection from wind for the different models.

6.4.2.3 Reinforcement

By utilizing the additional script to the tool as described in chapter 6.2.3 for in-depth analysis, the core walls are divided into finer walls with a width of around 0.8 m to obtain the normal force in each fine wall. Each fine core wall is categorized according to which core side it belongs to. In Figure 6.13, the maximum number of tensile rebars in each fine core wall on all sides and stories are shown for core model 1, wall model 1. The maximum number of tensile rebars is calculated from all ULS load combinations and all wind directions. By doing so, it is accounted for that the maximum number of tensile rebars can occur in different wind directions at different regions of the core.

The results in Figure 6.13 show that the core walls at the edges on the lower stories of the core are most tensioned, as they have the need for tensile rebars. This is reasonable since the stress is linearly distributed over each side of the core, where the maximum stress is located at the edges of the core.

Maximum Number of Tensile Rebars per Wall (ø25)

	South									East									North								West								
	S01	S02	S03	S04	S05	S06	S07	S08	S09	E01	E02	E03	E04	E05	E06	E07	E08	E09	E10	N01	N02	N03	N04	N05	N06	N07	N08	N09	W01	W02	W03	W04	W05	W06	W07	W08	W09	W10
Story41	0	0	0	0	0	0	0	0	0	0	0	0	0	0	0	0	0	0	0	0	0	0	0	0	0	0	0	0	0	0	0	0	0	0	0	0	0	0
Story40	0	0	0	0	0	0	0	0	0	0	0	0	0	0	0	0	0	0	0	0	0	0	0	0	0	0	0	0	0	0	0	0	0	0	0	0	0	0
Story39	0	0	0	0	0	0	0	0	0	0	0	0	0	0	0	0	0	0	0	0	0	0	0	0	0	0	0	0	0	0	0	0	0	0	0	0	0	0
Story38	0	0	0	0	0	0	0	0	0	0	0	0	0	0	0	0	0	0	0	0	0	0	0	0	0	0	0	0	0	0	0	0	0	0	0	0	0	0
Story37	0	0	0	0	0	0	0	0	0	0	0	0	0	0	0	0	0	0	0	0	0	0	0	0	0	0	0	0	0	0	0	0	0	0	0	0	0	0
Story36	0	0	0	0	0	0	0	0	0	0	0	0	0	0	0	0	0	0	0	0	0	0	0	0	0	0	0	0	0	0	0	0	0	0	0	0	0	0
Story35	0	0	0	0	0	0	0	0	0	0	0	0	0	0	0	0	0	0	0	0	0	0	0	0	0	0	0	0	0	0	0	0	0	0	0	0	0	0
Story34	0	0	0	0	0	0	0	0	0	0	0	0	0	0	0	0	0	0	0	0	0	0	0	0	0	0	0	0	0	0	0	0	0	0	0	0	0	0
Story33	0	0	0	0	0	0	0	0	0	0	0	0	0	0	0	0	0	0	0	0	0	0	0	0	0	0	0	0	0	0	0	0	0	0	0	0	0	0
Story32	0	0	0	0	0	0	0	0	0	0	0	0	0	0	0	0	0	0	0	0	0	0	0	0	0	0	0	0	0	0	0	0	0	0	0	0	0	0
Story31	0	0	0	0	0	0	0	0	0	0	0	0	0	0	0	0	0	0	0	0	0	0	0	0	0	0	0	0	0	0	0	0	0	0	0	0	0	0
Story30	0	0	0	0	0	0	0	0	0	0	0	0	0	0	0	0	0	0	0	0	0	0	0	0	0	0	0	0	0	0	0	0	0	0	0	0	0	0
Story29	0	0	0	0	0	0	0	0	0	0	0	0	0	0	0	0	0	0	0	0	0	0	0	0	0	0	0	0	0	0	0	0	0	0	0	0	0	0
Story28	0	0	0	0	0	0	0	0	0	0	0	0	0	0	0	0	0	0	0	0	0	0	0	0	0	0	0	0	0	0	0	0	0	0	0	0	0	0
Story27	0	0	0	0	0	0	0	0	0	0	0	0	0	0	0	0	0	0	0	0	0	0	0	0	0	0	0	0	0	0	0	0	0	0	0	0	0	0
Story26	0	0	0	0	0	0	0	0	0	0	0	0	0	0	0	0	0	0	0	0	0	0	0	0	0	0	0	0	0	0	0	0	0	0	0	0	0	0
Story25	0	0	0	0	0	0	0	0	0	0	0	0	0	0	0	0	0	0	0	0	0	0	0	0	0	0	0	0	0	0	0	0	0	0	0	0	0	0
Story24	0	0	0	0	0	0	0	0	0	0	0	0	0	0	0	0	0	0	0	0	0	0	0	0	0	0	0	0	0	0	0	0	0	0	0	0	0	0
Story23	0	0	0	0	0	0	0	0	0	0	0	0	0	0	0	0	0	0	0	0	0	0	0	0	0	0	0	0	0	0	0	0	0	0	0	0	0	0
Story22	0	0	0	0	0	0	0	0	0	0	0	0	0	0	0	0	0	0	0	0	0	0	0	0	0	0	0	0	0	0	0	0	0	0	0	0	0	0
Story21	0	0	0	0	0	0	0	0	0	0	0	0	0	0	0	0	0	0	0	0	0	0	0	0	0	0	0	0	0	0	0	0	0	0	0	0	0	0
Story20	0	0	0	0	0	0	0	0	0	0	0	0	0	0	0	0	0	0	0	0	0	0	0	0	0	0	0	0	0	0	0	0	0	0	0	0	0	0
Story19	0	0	0	0	0	0	0	0	0	0	0	0	0	0	0	0	0	0	0	0	0	0	0	0	0	0	0	0	0	0	0	0	0	0	0	0	0	0
Story18	0	0	0	0	0	0	0	0	0	0	0	0	0	0	0	0	0	0	0	0	0	0	0	0	0	0	0	0	0	0	0	0	0	0	0	0	0	0
Story17	0	0	0	0	0	0	0	0	0	0	0	0	0	0	0	0	0	0	0	0	0	0	0	0	0	0	0	0	0	0	0	0	0	0	0	0	0	0
Story16	0	0	0	0	0	0	0	0	0	0	0	0	0	0	0	0	0	0	0	0	0	0	0	0	0	0	0	0	0	0	0	0	0	0	0	0	0	0
Story15	0	0	0	0	0	0	0	0	0	0	0	0	0	0	0	0	0	0	0	0	0	0	0	0	0	0	0	0	0	0	0	0	0	0	0	0	0	0
Story14	0	0	0	0	0	0	0	0	0	0	0	0	0	0	0	0	0	0	0	0	0	0	0	0	0	0	0	0	0	0	0	0	0	0	0	0	0	0
Story13	0	0	0	0	0	0	0	0	0	0	0	0	0	0	0	0	0	0	0	0	0	0	0	0	0	0	0	0	0	0	0	0	0	0	0	0	0	0
Story12	0	0	0	0	0	0	0	0	0	0	0	0	0	0	0	0	0	0	0	0	0	0	0	0	0	0	0	0	0	0	0	0	0	0	0	0	0	0
Story11	0	0	0	0	0	0	0	0	0	0	0	0	0	0	0	0	0	0	0	0	0	0	0	0	0	0	0	0	0	0	0	0	0	0	0	0	0	0
Story10	1	0	0	0	0	0	0	0	1	1	0	0	0	0	0	0	0	0	0	0	0	0	0	0	0	0	0	0	0	0	0	0	0	0	0	0	0	1
Story09	1	0	0	0	0	0	0	0	1	1	0	0	0	0	0	0	0	0	0	0	0	0	0	0	0	0	0	0	0	0	0	0	0	0	0	0	0	1
Story08	2	1	0	0	0	0	0	0	1	1	0	0	0	0	0	0	0	0	0	0	0	0	0	0	0	0	0	0	1	0	0	0	0	0	0	0	1	2
Story07	3	1	0	0	0	0	0	1	2	2	1	0	0	0	0	0	0	0	1	1	0	0	0	0	0	0	0	1	1	0	0	0	0	0	0	0	1	3
Story06	4	1	0	0	0	0	0	1	3	3	1	0	0	0	0	0	0	0	1	1	0	0	0	0	0	0	0	1	2	0	0	0	0	0	0	0	2	4
Story05	5	2	0	0	0	0	0	1	4	4	1	0	0	0	0	0	0	0	2	2	0	0	0	0	0	0	0	2	3	1	0	0	0	0	0	0	2	5
Story04	5	3	0	0	0	0	0	2	5	5	2	0	0	0	0	0	0	1	3	3	1	0	0	0	0	0	1	3	3	1	0	0	0	0	0	0	2	6
Story03	6	3	1	0	0	0	1	3	6	6	4	1	0	0	0	0	0	2	4	3	1	0	0	0	0	0	1	4	4	2	0	0	0	0	0	1	4	7
Story02	7	5	2	1	0	0	2	5	6	7	7	1	0	0	0	0	1	4	5	4	2	0	0	0	0	0	3	5	6	5	1	0	0	0	0	2	7	8
Story01	12	6	1	0	0	0	1	5	11	11	3	0	0	0	0	0	0	2	8	8	2	0	0	0	0	0	3	10	10	3	0	0	0	0	0	1	4	12

Figure 6.13: Maximum number of tensile rebars per wall for core 1, wall model 1.

The maximum number of horizontal rebars per wall are calculated according to the thickness of each wall. According to Table 6.1 where the horizontal reinforcement amount for the different wall thicknesses were specified, the thicker walls have larger reinforcement amounts than thinner walls. In Figure 6.14 below, the maximum number of horizontal rebars per wall on all sides and stories are shown for core 1, wall model 1.

The results show that the lower stories need more rebars than the higher stories. This is due to the lower stories having thicker walls, where the wall thicknesses decrease as the height of the core increases. Additionally, the results show that some walls on the same story have different number of rebars. Since the fine core walls do not have equal width, but all fine core walls have a width of around 0.8 m, this results in different number of rebars per fine core wall.

Maximum Number of Horizontal Rebars per Wall (ø25)

	South									East										North									West									
	S01	S02	S03	S04	S05	S06	S07	S08	S09	E01	E02	E03	E04	E05	E06	E07	E08	E09	E10	N01	N02	N03	N04	N05	N06	N07	N08	N09	W01	W02	W03	W04	W05	W06	W07	W08	W09	W10
Story41	2	2	2	2	3	2	2	2	2	2	2	2	2	2	2	2	2	2	2	2	2	2	2	3	2	2	2	2	2	2	2	2	2	2	2	2	2	2
Story40	2	2	2	2	3	2	2	2	2	2	2	2	2	2	2	2	2	2	2	2	2	2	2	3	2	2	2	2	2	2	2	2	2	2	2	2	2	2
Story39	2	2	2	2	3	2	2	2	2	2	2	2	2	2	2	2	2	2	2	2	2	2	2	3	2	2	2	2	2	2	2	2	2	2	2	2	2	2
Story38	2	2	2	2	3	2	2	2	2	2	2	2	2	2	2	2	2	2	2	2	2	2	2	3	2	2	2	2	2	2	2	2	2	2	2	2	2	2
Story37	2	2	2	2	3	2	2	2	2	2	2	2	2	2	2	2	2	2	2	2	2	2	2	3	2	2	2	2	2	2	2	2	2	2	2	2	2	2
Story36	2	2	2	2	3	2	2	2	2	2	2	2	2	2	2	2	2	2	2	2	2	2	2	3	2	2	2	2	2	2	2	2	2	2	2	2	2	2
Story35	2	2	2	2	3	2	2	2	2	2	2	2	2	2	2	2	2	2	2	2	2	2	2	3	2	2	2	2	2	2	2	2	2	2	2	2	2	2
Story34	2	2	2	2	3	2	2	2	2	2	2	2	2	2	2	2	2	2	2	2	2	2	2	3	2	2	2	2	2	2	2	2	2	2	2	2	2	2
Story33	2	2	2	2	3	2	2	2	2	2	2	2	2	2	2	2	2	2	2	2	2	2	2	3	2	2	2	2	2	2	2	2	2	2	2	2	2	2
Story32	2	2	2	2	3	2	2	2	2	2	2	2	2	2	2	2	2	2	2	2	2	2	2	3	2	2	2	2	2	2	2	2	2	2	2	2	2	2
Story31	2	2	2	2	3	2	2	2	2	2	2	2	2	2	2	2	2	2	2	2	2	2	2	3	2	2	2	2	2	2	2	2	2	2	2	2	2	2
Story30	2	2	2	2	3	2	2	2	2	2	2	2	2	2	2	2	2	2	2	2	2	2	2	3	2	2	2	2	2	2	2	2	2	2	2	2	2	2
Story29	2	2	2	2	3	2	2	2	2	2	2	2	2	2	2	2	2	2	2	2	2	2	2	3	2	2	2	2	2	2	2	2	2	2	2	2	2	2
Story28	2	2	2	2	3	2	2	2	2	2	2	2	2	2	2	2	2	2	2	2	2	2	2	3	2	2	2	2	2	2	2	2	2	2	2	2	2	2
Story27	2	2	2	2	3	2	2	2	2	2	2	2	2	2	2	2	2	2	2	2	2	2	2	3	2	2	2	2	2	2	2	2	2	2	2	2	2	2
Story26	2	2	2	2	3	2	2	2	2	2	2	2	2	2	2	2	2	2	2	2	2	2	2	3	2	2	2	2	2	2	2	2	2	2	2	2	2	2
Story25	2	2	2	2	3	2	2	2	2	2	2	2	2	2	2	2	2	2	2	2	2	2	2	3	2	2	2	2	2	2	2	2	2	2	2	2	2	2
Story24	2	2	2	2	3	2	2	2	2	2	2	2	2	2	2	2	2	2	2	2	2	2	2	3	2	2	2	2	2	2	2	2	2	2	2	2	2	2
Story23	4	4	4	4	5	4	4	4	4	4	4	4	3	3	3	3	4	4	4	4	4	4	4	5	4	4	4	4	4	4	4	3	3	3	3	4	4	4
Story22	4	4	4	4	5	4	4	4	4	4	4	4	3	3	3	3	4	4	4	4	4	4	4	5	4	4	4	4	4	4	4	3	3	3	3	4	4	4
Story21	4	4	4	4	5	4	4	4	4	4	4	4	3	3	3	3	4	4	4	4	4	4	4	5	4	4	4	4	4	4	4	3	3	3	3	4	4	4
Story20	4	4	4	4	5	4	4	4	4	4	4	4	3	3	3	3	4	4	4	4	4	4	4	5	4	4	4	4	4	4	4	3	3	3	3	4	4	4
Story19	4	4	4	4	5	4	4	4	4	4	4	4	3	3	3	3	4	4	4	4	4	4	4	5	4	4	4	4	4	4	4	3	3	3	3	4	4	4
Story18	4	4	4	4	5	4	4	4	4	4	4	4	3	3	3	3	4	4	4	4	4	4	4	5	4	4	4	4	4	4	4	3	3	3	3	4	4	4
Story17	4	4	4	4	5	4	4	4	4	4	4	4	3	3	3	3	4	4	4	4	4	4	4	5	4	4	4	4	4	4	4	3	3	3	3	4	4	4
Story16	4	4	4	4	5	4	4	4	4	4	4	4	3	3	3	3	4	4	4	4	4	4	4	5	4	4	4	4	4	4	4	3	3	3	3	4	4	4
Story15	4	4	4	4	5	4	4	4	4	4	4	4	3	3	3	3	4	4	4	4	4	4	4	5	4	4	4	4	4	4	4	3	3	3	3	4	4	4
Story14	4	4	4	4	5	4	4	4	4	4	4	4	3	3	3	3	4	4	4	4	4	4	4	5	4	4	4	4	4	4	4	3	3	3	3	4	4	4
Story13	4	4	4	4	5	4	4	4	4	4	4	4	3	3	3	3	4	4	4	4	4	4	4	5	4	4	4	4	4	4	4	3	3	3	3	4	4	4
Story12	4	4	4	4	5	4	4	4	4	4	4	4	3	3	3	3	4	4	4	4	4	4	4	5	4	4	4	4	4	4	4	3	3	3	3	4	4	4
Story11	4	4	4	4	5	4	4	4	4	4	4	4	3	3	3	3	4	4	4	4	4	4	4	5	4	4	4	4	4	4	4	3	3	3	3	4	4	4
Story10	4	4	4	4	5	4	4	4	4	4	4	4	3	3	3	3	4	4	4	4	4	4	4	5	4	4	4	4	4	4	4	3	3	3	3	4	4	4
Story09	4	4	4	4	5	4	4	4	4	4	4	4	3	3	3	3	4	4	4	4	4	4	4	5	4	4	4	4	4	4	4	3	3	3	3	4	4	4
Story08	4	4	4	4	5	4	4	4	4	4	4	4	3	3	3	3	4	4	4	4	4	4	4	5	4	4	4	4	4	4	4	3	3	3	3	4	4	4
Story07	4	4	4	4	5	4	4	4	4	4	4	4	3	3	3	3	4	4	4	4	4	4	4	5	4	4	4	4	4	4	4	3	3	3	3	4	4	4
Story06	4	4	4	4	5	4	4	4	4	4	4	4	3	3	3	3	4	4	4	4	4	4	4	5	4	4	4	4	4	4	4	3	3	3	3	4	4	4
Story05	4	4	4	4	5	4	4	4	4	4	4	4	3	3	3	3	4	4	4	4	4	4	4	5	4	4	4	4	4	4	4	3	3	3	3	4	4	4
Story04	8	8	8	8	10	8	8	8	8	8	8	8	7	7	7	7	8	8	8	8	8	8	8	10	8	8	8	8	8	8	8	7	7	7	7	8	8	8
Story03	8	8	8	8	10	8	8	8	8	8	8	8	7	7	7	7	8	8	8	8	8	8	8	10	8	8	8	8	8	8	8	7	7	7	7	8	8	8
Story02	8	8	8	8	10	8	8	8	8	8	8	8	7	7	7	7	8	8	8	8	8	8	8	10	8	8	8	8	8	8	8	7	7	7	7	8	8	8
Story01	8	8	8	8	10	8	8	8	8	8	8	8	7	7	7	7	8	8	8	8	8	8	8	10	8	8	8	8	8	8	8	7	7	7	7	8	8	8

Figure 6.14: Maximum number of horizontal rebars per wall for core 1, wall model 1.

In Figure 6.15, the maximum number of compressive rebars in each fine core wall on all sides and stories are shown for core 1, wall model 1. The maximum number of compressive rebars is calculated from all ULS load combinations and all wind directions. The number of compressive rebars is determined by the wall thickness and maximum compressive force acting on each wall.

The results show that there are more compressive rebars in regions where the compressive forces are higher. In general, these regions are located around the vertices of the core due to the linear distribution of stress from horizontal loads over each side of the core.

Maximum Number of Compressive Rebars per Wall (ø25)

	South									East									North								West									
	S01	S02	S03	S04	S05	S06	S07	S08	S09	E01	E02	E03	E04	E05	E06	E07	E08	E09	E10	N01	N02	N03	N04	N05	N06	N07	N08	N09	W01	W02	W03	W04	W05	W06	W07	W08	W09	W10
Story41	2	2	2	2	3	2	2	2	2	3	3	3	2	2	2	2	3	3	3	2	2	2	2	3	2	2	2	2	3	3	3	2	2	2	2	3	3	3
Story40	2	2	2	2	3	2	2	2	2	3	3	3	2	2	2	2	3	3	3	2	2	2	2	3	2	2	2	2	3	3	3	2	2	2	2	3	3	3
Story39	2	2	2	2	3	2	2	2	2	3	3	3	2	2	2	2	3	3	3	2	2	2	2	3	2	2	2	2	3	3	3	2	2	2	2	3	3	3
Story38	3	2	2	3	3	3	2	2	3	3	3	3	2	2	2	2	3	3	3	3	3	3	3	3	3	3	3	3	3	3	3	2	2	2	2	3	3	3
Story37	3	3	3	3	3	3	3	3	3	3	3	3	2	2	2	2	3	3	3	3	3	3	3	3	3	3	3	3	3	3	3	2	2	2	2	3	3	3
Story36	3	3	3	3	3	3	3	3	3	3	3	3	2	2	2	2	3	3	3	3	3	3	4	3	3	3	3	3	3	3	3	2	2	2	2	3	3	3
Story35	3	3	3	3	4	3	3	3	3	3	4	3	3	2	2	2	3	3	4	4	3	3	3	4	3	3	3	3	4	4	3	3	2	2	3	3	4	3
Story34	3	3	3	3	4	3	3	3	3	4	4	3	3	3	3	3	3	4	4	3	3	3	4	4	4	3	3	3	4	4	3	3	3	3	3	3	4	4
Story33	3	3	3	4	4	4	3	3	3	4	4	3	3	3	3	3	3	4	4	4	4	4	4	4	4	4	4	4	4	4	3	3	3	3	3	3	4	4
Story32	4	4	4	4	4	4	4	4	4	4	4	3	3	3	3	3	4	5	4	4	4	4	4	5	4	4	4	4	4	4	3	3	3	3	3	3	4	4
Story31	4	4	4	4	5	4	4	4	4	4	5	4	3	3	3	3	4	5	5	4	4	4	4	5	4	4	4	4	5	5	4	3	3	3	3	4	5	4
Story30	4	4	4	4	5	4	4	4	4	5	5	4	3	3	3	4	4	5	5	4	4	4	5	5	5	4	4	4	5	5	4	3	3	3	3	4	5	4
Story29	4	4	4	4	5	4	4	4	4	5	5	4	4	3	3	4	4	5	5	5	5	5	5	5	5	4	4	4	5	5	4	4	3	3	4	4	5	5
Story28	4	4	4	5	5	5	4	4	4	5	5	4	4	4	4	4	4	6	5	5	5	5	5	6	5	5	5	5	5	6	4	4	4	4	4	4	5	5
Story27	5	5	5	5	6	5	5	5	5	5	6	4	4	4	4	4	5	6	6	5	5	5	5	6	5	5	5	5	6	6	4	4	4	4	4	4	6	5
Story26	5	5	5	5	6	5	5	5	5	6	6	5	4	4	4	4	5	7	6	5	5	5	6	6	6	5	5	5	6	6	5	4	4	4	4	5	6	6
Story25	5	5	5	6	6	6	5	5	5	6	7	5	4	4	4	5	5	7	7	6	6	6	6	7	6	6	6	6	7	7	5	4	4	4	4	5	7	6
Story24	6	6	6	6	6	6	6	6	6	7	7	5	5	4	4	5	5	7	7	6	6	6	6	7	6	6	6	6	7	7	5	5	4	4	5	5	7	7
Story23	2	2	2	2	3	2	2	2	2	3	3	3	2	2	2	2	3	3	3	2	2	2	2	3	2	2	2	2	3	3	3	2	2	2	2	3	3	3
Story22	2	2	2	2	3	2	2	2	2	3	3	3	2	2	2	2	3	3	3	2	2	2	2	3	2	2	2	2	3	3	3	2	2	2	2	3	3	3
Story21	2	2	2	2	3	2	2	2	2	3	3	3	2	2	2	2	3	3	3	2	2	2	2	3	2	2	2	2	3	3	3	2	2	2	2	3	3	3
Story20	2	2	2	2	3	2	2	2	2	3	3	3	2	2	2	2	3	3	3	2	2	2	2	3	2	2	2	2	3	3	3	2	2	2	2	3	3	3
Story19	2	2	2	2	3	2	2	2	2	3	3	3	2	2	2	2	3	3	3	2	2	2	2	3	2	2	2	2	3	3	3	2	2	2	2	3	3	3
Story18	2	2	2	2	3	2	2	2	2	3	3	3	2	2	2	2	3	3	3	2	2	2	2	3	2	2	2	2	3	3	3	2	2	2	2	3	3	3
Story17	2	2	2	2	3	2	2	2	2	3	3	3	2	2	2	2	3	3	3	2	2	2	2	3	2	2	2	2	3	3	3	2	2	2	2	3	3	3
Story16	2	2	2	2	3	2	2	2	2	3	3	3	2	2	2	2	3	4	3	3	2	2	3	3	2	2	2	2	3	3	3	2	2	2	2	3	3	3
Story15	2	2	2	2	3	2	2	2	2	3	4	3	2	2	2	2	3	4	4	3	3	2	3	3	3	2	3	3	4	4	3	2	2	2	2	3	3	3
Story14	3	2	2	3	3	3	2	2	3	4	4	3	2	2	2	2	3	5	4	3	3	3	3	3	3	3	3	3	4	4	3	2	2	2	2	3	4	3
Story13	3	3	2	3	3	3	3	3	3	4	4	3	2	2	2	2	3	5	5	4	3	3	4	3	3	3	3	4	4	5	3	2	2	2	2	3	4	4
Story12	3	3	3	3	3	3	3	3	3	4	5	3	2	2	2	2	3	5	5	4	4	3	4	3	4	3	4	4	5	5	3	2	2	2	2	3	5	4
Story11	4	3	3	3	3	4	3	4	4	5	5	3	2	2	2	3	3	6	6	5	4	4	4	3	4	4	4	4	5	6	3	2	2	2	2	3	5	5
Story10	4	4	3	4	3	4	3	4	4	5	6	3	3	2	2	3	3	6	6	5	5	4	5	3	5	4	4	5	6	6	3	3	2	2	3	3	6	5
Story09	5	4	4	4	3	4	4	4	5	6	6	3	3	2	2	3	3	7	7	5	5	5	5	4	5	4	5	5	6	7	3	3	2	2	3	3	6	6
Story08	5	5	4	4	3	4	4	5	5	6	7	3	3	2	3	3	3	7	7	6	5	5	5	4	5	5	5	6	7	7	3	3	2	2	3	3	7	6
Story07	5	5	4	5	4	5	4	5	5	7	7	3	4	3	3	4	4	8	8	6	6	5	6	5	6	5	6	6	7	8	3	4	3	3	3	3	7	7
Story06	6	5	5	5	4	5	5	5	6	7	8	3	4	3	3	4	4	9	8	7	6	6	6	5	6	6	6	7	8	8	4	4	3	3	4	3	8	7
Story05	6	6	5	5	4	5	5	6	6	8	8	4	4	3	3	4	4	9	9	7	7	6	6	5	6	6	6	7	9	9	4	4	3	3	4	4	8	8
Story04	4	4	4	4	4	4	4	4	4	5	5	3	3	3	3	3	3	5	5	5	4	4	4	4	4	4	4	4	5	5	3	3	3	3	3	3	5	5
Story03	4	4	4	4	4	4	4	4	4	5	6	3	3	3	3	3	4	6	5	5	4	4	5	5	5	4	4	5	5	6	4	3	3	3	3	3	5	5
Story02	4	4	4	5	4	5	4	4	4	5	6	4	4	3	3	4	4	7	5	5	5	4	5	5	5	4	5	5	5	7	4	4	3	3	3	4	6	5
Story01	6	4	3	4	4	4	4	4	6	7	6	4	3	2	2	3	4	7	7	6	5	4	4	4	4	4	5	6	7	7	4	3	2	2	3	4	6	7

Figure 6.15: Maximum number of compressive rebars per wall for core 1, wall model 1.

6.4.2.4 Climate Impact

To evaluate the climate impact of the different models, the total volume of concrete and reinforcement for each model needs to be calculated. The total volume is then multiplied by a factor to obtain the CO2e for stages A1-A5. In Figure 6.16 below, the CO2e of concrete for the different core and wall models are shown. The results show that thinner walls have a smaller climate impact compared to thicker walls and that a smaller core has a smaller climate impact than a larger core, as would be expected.

In addition, the wall thicknesses have a larger impact on the CO2e than the core dimensions. In example, Core 1 has a CO2e value of 462.6 ton for wall model 1 and 500.1 ton for wall model 2. The difference in CO2e between the different wall models is 37.5 ton. Core 2 with slightly larger dimensions has a CO2e value of 480.5 ton for wall model 1, resulting in a difference of 17.9 ton between wall model 1 for Core 1 and 2. This could however be affected by the difference in wall thicknesses between each wall model.

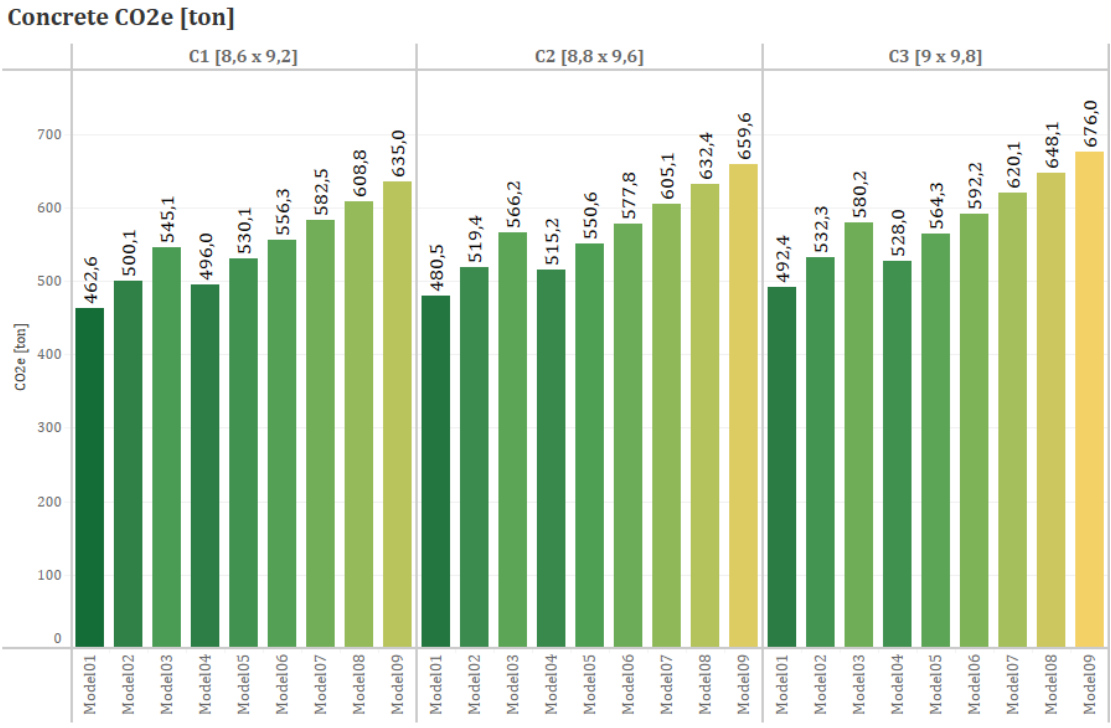

Figure 6.16: CO2e of concrete for the different models.

To evaluate the climate impact of reinforcement, the total volume of reinforcement for each model needs to be calculated. In Figure 6.17, the CO2e of compressive reinforcement for the different core and wall models are shown. The results show that thinner walls have a larger climate impact compared to thicker walls regarding compressive reinforcement. Additionally, it can be seen that climate impact of compressive reinforcement is minimally affected by the core dimensions. The change in wall thicknesses seem to have a larger effect on the CO2e for the thinner wall models, compared to the change of wall thicknesses for the thicker wall models where the difference in CO2e is minimal.

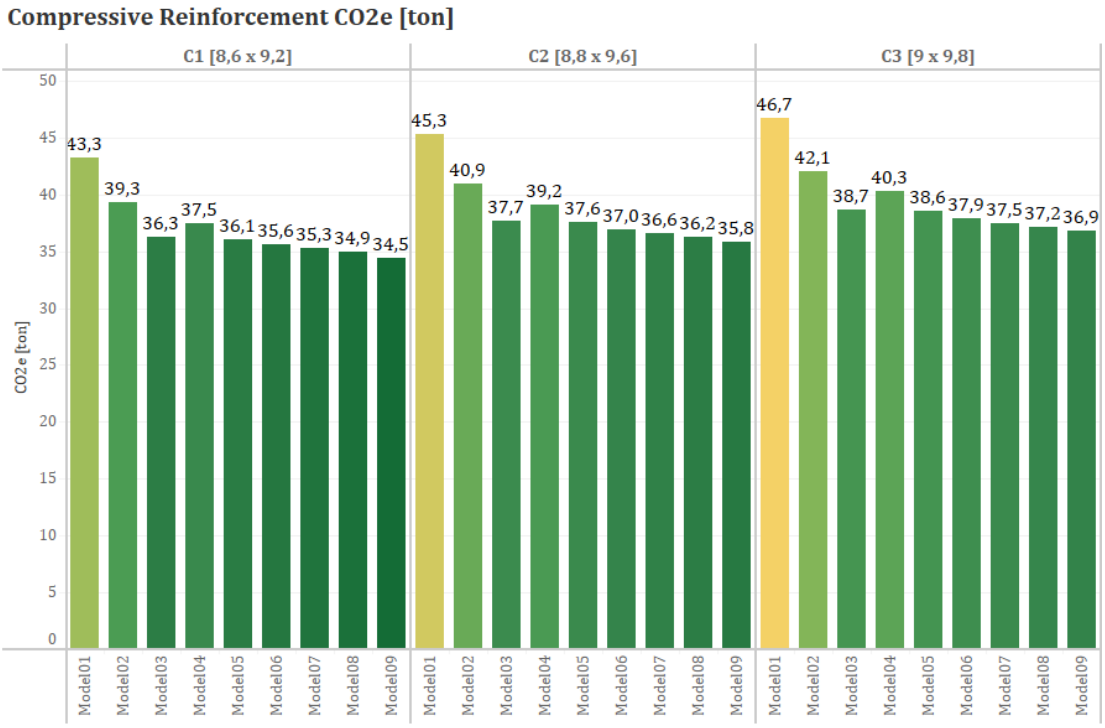

Figure 6.17: CO2e of compressive reinforcement for the different models.

In Figure 6.18, the CO2e of tensile reinforcement for the different core and wall models are shown. The results show that thinner walls have a larger climate impact compared to thicker walls regarding tensile reinforcement. Additionally, a smaller core seems to have a larger climate impact in contrast to a larger core. This is reasonable since a smaller core has a smaller lever arm, resulting in higher maximum stresses at the edges of the core where there is a need for tensile reinforcement.

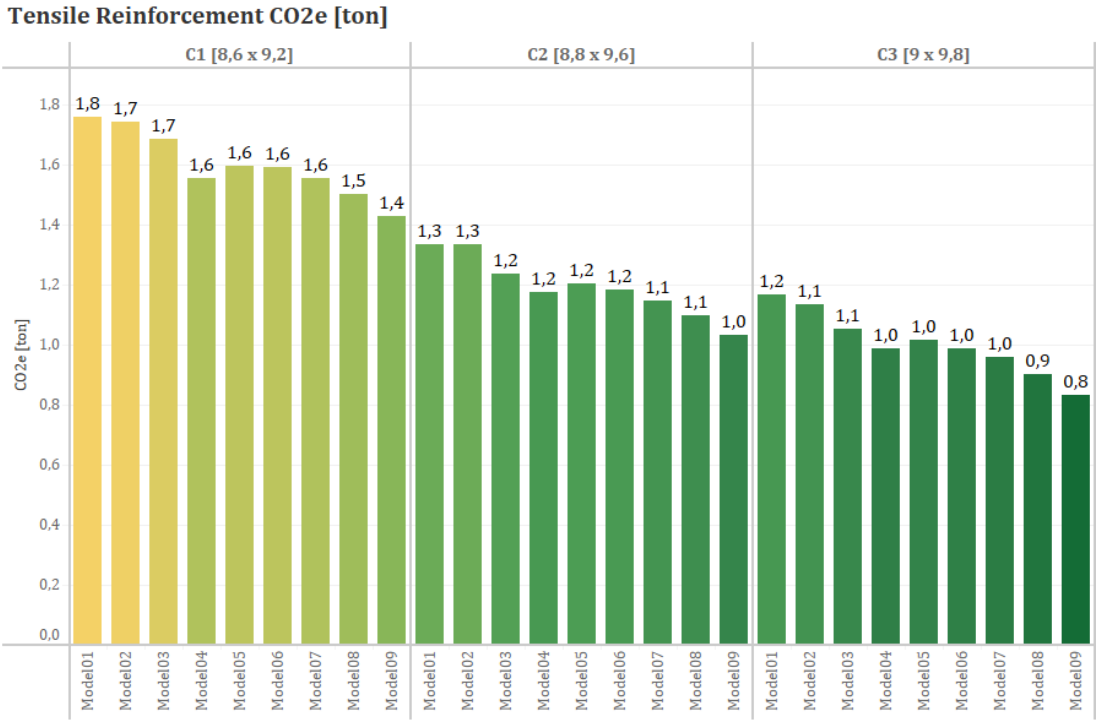

Figure 6.18: CO2e for tensile reinforcement for the different models.

In Figure 6.19, the CO2e of horizontal reinforcement for the different core and wall models are shown. Since the required amount of horizontal reinforcement only depends on the thickness of the walls, the CO2e of horizontal reinforcement for the different models follow the same pattern as the CO2e of concrete.

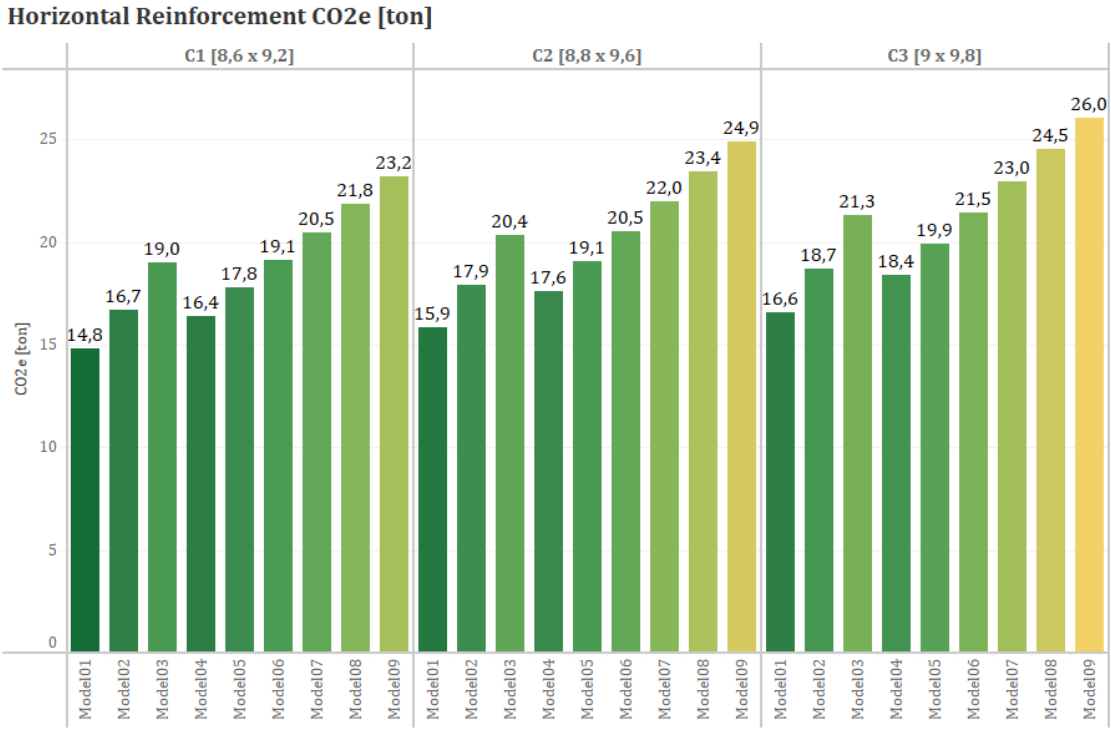

Figure 6.19: CO2e for horizontal reinforcement for the different models.

In Figure 6.20, the CO2e of the total reinforcement for the different core and wall models are shown.When summing all the required reinforcements, the CO2e for the different models looks differently than when displaying the CO2e for each reinforcement type.

The results show that a larger core has a larger climate impact than a smaller core, which is expected but needs to be put in relation to the structural performance of the core. When it comes to the climate impact of the wall thicknesses, the results show that wall models 4-5 have the lowest CO2e values for all core models. This suggests that wall thicknesses that aren't too thick or thin are preferrable in terms of CO2e of the total reinforcement.

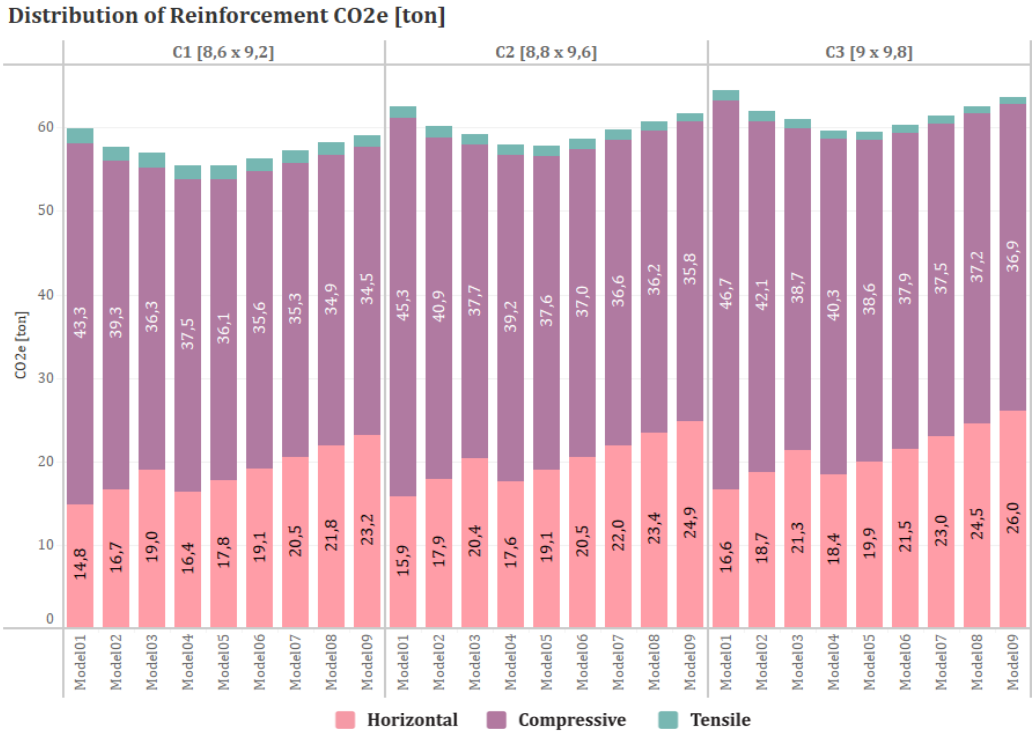

Figure 6.20: CO2e of total reinforcement for the different models.

In Figure 6.21, the total CO2e of the different models are shown, where the CO2e for concrete is shown in blue and CO2e for the total reinforcement is shown in red. The results show that the difference in CO2e of reinforcement in the different models has a minimal impact on the total CO2e. Rather, the difference in CO2e of concrete in the different models is the decisive factor.

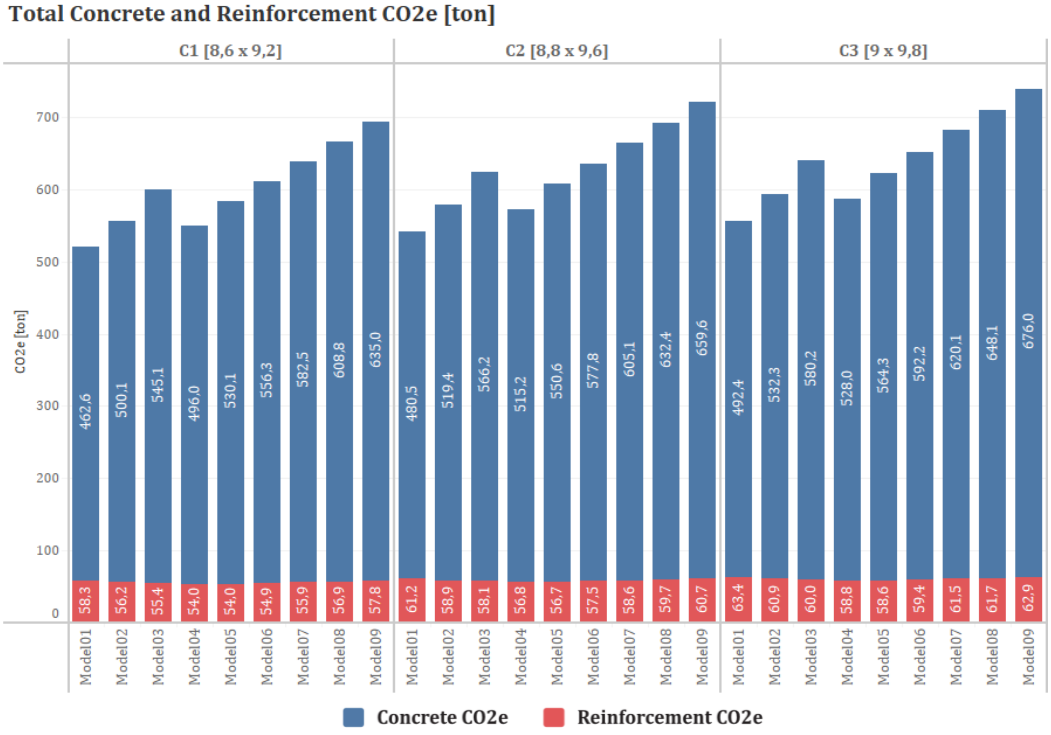

Figure 6.21: Total CO2e for the different models, including the CO2e of concrete and total reinforcement.

6.4.2.5 Conclusion from Results

To evaluate which core model and wall model is the best choice in regard to lowest climate impact, the models that fulfill the maximum allowed horizontal displacement have been selected in Figure 6.22 and Figure 6.23 below. The core and wall model that has the lowest climate impact is core 3, wall model 1. This also happens to be the model that has the largest CO2e of reinforcement, but smallest CO2e of concrete, resulting in the overall lowest CO2e.

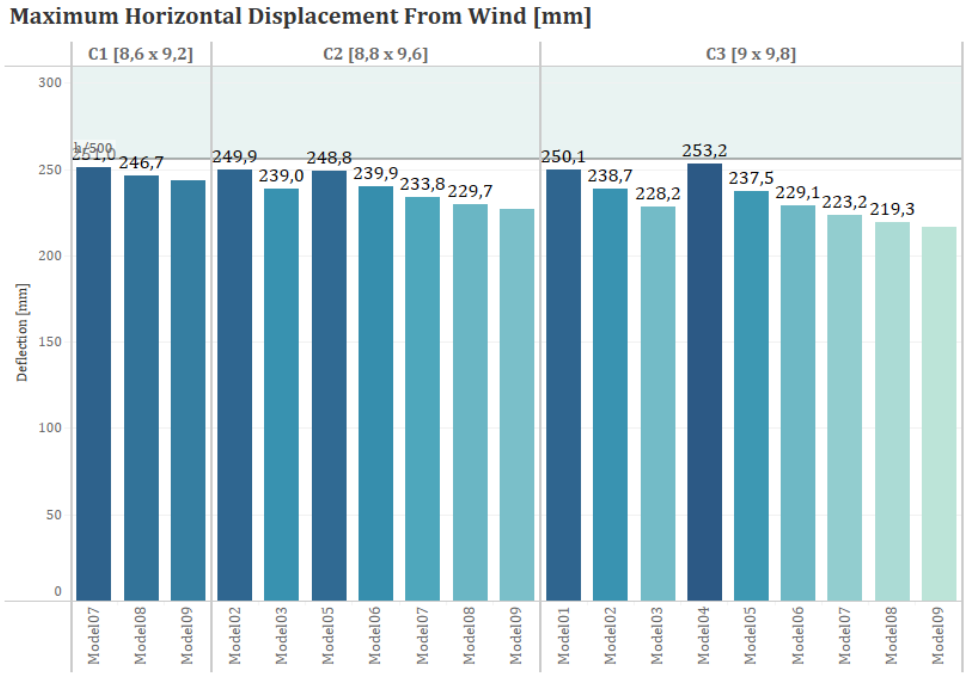

Figure 6.22: Maximum horizontal displacement of the models that fulfill the displacement requirement.

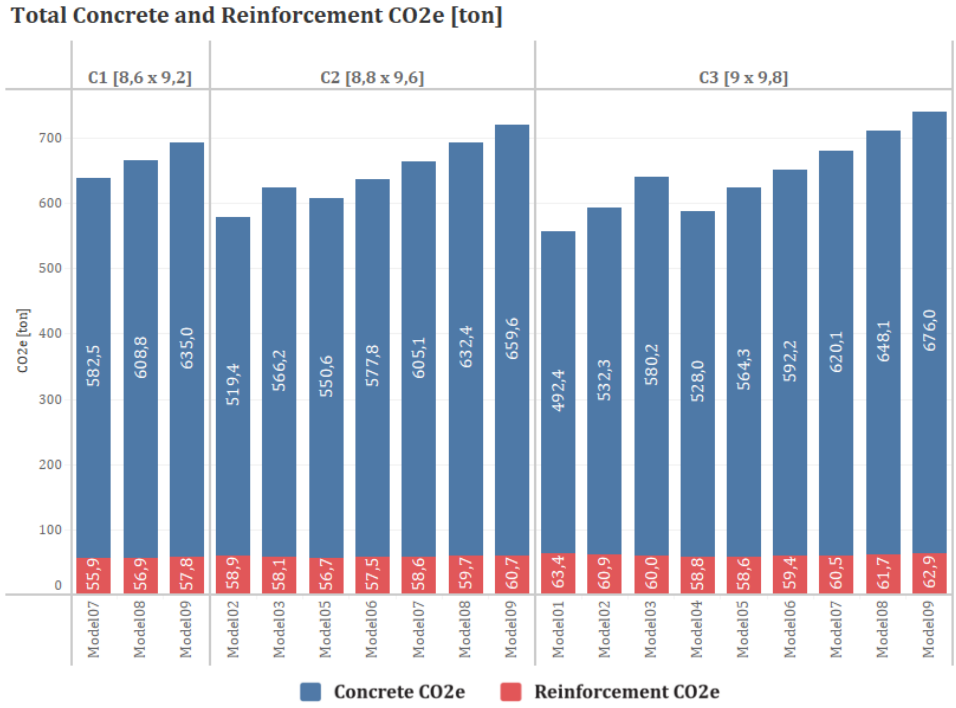

Figure 6.23: Total CO2e of the models that fulfill the displacement requirement.

7 Discussion

A discussion and evaluation of the results from the Rhino/Grasshopper tool and ETABS/VBA tool are presented in this chapter. The usability and limitations of the respective tools are also discussed.

7.1 Rhino/Grasshopper Tool

The Rhino/Grasshopper tool has proved its worth as a quick and easy design tool that interactively shows the behavior of a core in a high-rise building under wind-loading. The tool is particularly useful for visualizing how the building footprint, core dimensions and wind load parameters affect the structural behavior and performance of the building.

The Rhino/Grasshopper tool would benefit from certain adjustments as the core is modelled as too stiff. The core is modelled as four walls without any openings. This makes the core walls too stiff as there will always be door openings on the walls that reduce the stiffness of the core. The openings will also have link beams above them whose stiffness is significantly reduced. A solution to this would be to implement stiffness modifiers on the core walls that reduce the stiffness of the walls. Another solution could be to model openings on the walls, although the stiffness of the link beams would still need to be reduced to better resemble reality.

Additionally, the core wall thicknesses are currently uniformly modelled. This means that all walls have the same thickness regardless of which story the wall belongs to. In reality, the thickness of the core walls would likely decrease with increasing height to minimize unnecessary material usage. Since the cross sectional forces are the largest at the lower stories, thicker core walls are necessary at the lower stories compared to the higher stories.

The only load that is applied to the core in the Rhino/Grasshopper tool is wind. Although the wind is the governing load in high-rise buildings, the core will in reality be subjected to dead loads from slabs, columns and installations, as well as imposed loads and snow load. These loads act vertically and depending on the geometry of the building, they will affect the stability of the core.
It would however be interesting to explore if and how these loads affect the structural performance of the core.

7.2 ETABS/VBA Tool

The usefulness and efficiency of the ETABS/VBA tool can be evaluated in terms of saved time and user-friendliness. In the first iteration, 126 different structural designs were modelled and analyzed, which took the script around seven hours to complete. The time depends on several factors such as the size of the building, number of stories and how fine the mesh sizes are. By running the script during the night, no time effort is put into modelling and analyzing each iteration from the user. If this were to be done manually it would most likely take several

working days to complete, which proves the worth in terms of time efficiency of the tool.

In addition, the amount of data that is extracted from ETABS and stored in Excel is around a couple of million rows which the user doesn't have to handle. When the user links the Excel-file with all the data to Tableau, the results are immediately displayed in the graphs and tables that were presented in the previous chapter. This makes the data much easier to handle and understand, allowing the user to evaluate the structural performance of several designs to choose the optimal design in terms of low climate impact while fulfilling the maximum allowed horizontal displacement.

The core and wall model that had the lowest climate impact was core model 3 and wall model 1, which is the largest core with the smallest wall thicknesses. This core had the largest CO2e of reinforcement, but the lowest CO2e of concrete, resulting in the overall lowest CO2e. Generally, the CO2e of reinforcement had a minimal effect on the overall CO2e of the core compared to the CO2e of concrete. This suggests that the amount of concrete should be reduced as much as possible, even though this would increase the amount of reinforcement.

Furthermore, the wall thicknesses showed to have a larger impact on the overall CO2e of the models compared to the core dimensions. By decreasing the core dimensions from 9.0 x 9.8 m to 8.8 x 9.6 m between core 3 and 2, the total CO2e could be lowered by 15.9 ton. By decreasing the wall thicknesses from wall model 3 to wall model 2, the total CO2e could be lowered by 46 ton for core 2 and 47 ton for core 3. This suggests that the wall thicknesses should be reduced in firsthand in order to reduce the amount of concrete.

Despite the fact that a large core with thinner walls is an optimal design in terms of climate impact and structural performance, it is not an optimal design from an architect's or client's perspective. A larger core reduces the amount of profitable and usable space, thus an architect would rather want to minimize the core dimensions. From this perspective, an optimal design could be core 1, wall model 7 which has a total CO2e of 638.4 ton. This is an increase in CO2e by 82.6 ton from core 3, wall model 1. The tool allows both architects and structural engineers to reason about the climate impact of their respective optimal designs, where a design that is reasonable from both perspectives can be chosen.

The ETABS/VBA tool is developed for the early design stages, where decisions have the largest influence on the climate impact as well as costs of the building. The maximum allowed displacement at the top of the building is usually the dimensioning factor for 80-130 m tall buildings, which motivates a comparison between the CO2e of the cores and the maximum allowed displacement. However, for taller buildings, the acceleration of the building becomes increasingly important to consider. This is also relevant to consider for 80-130 m tall buildings as the horizontal displacements do not necessarily have to be the only parameters that govern the structural design. Therefore, the tool would benefit from involving the accelerations of the models to evaluate human comfort.

7.3 Further Studies

This sub-chapter discusses and suggests relevant aspects that may be of interest to investigate further in future studies.

7.3.1 Rhino/Grasshopper Tool

To make the Rhino/Grasshopper more precise, certain adjustments could be made to better resemble how a high-rise building in reality would perform. As previously mentioned, stiffness modifiers could be applied on the core walls to decrease the stiffness of the core. The stiffness modifiers could preferably be derived from a comparison study between the Rhino/Grasshopper tool and ETABS/VBA tool. The core in the ETABS/VBA tool is much more refined and closer to the behavior of a core in reality in contrast to the Rhino/Grasshopper tool. By conducting a parametric study between the two tools, a reduction factor for the stiffness in the Rhino/Grasshopper tool may be found. Stiffness modifiers would increase the reliability of the tool, resulting in core dimensions and wall thicknesses that are closer to the acceptable core dimensions and wall thicknesses in the ETABS/VBA tool.

7.3.2 ETABS/VBA Tool

As previously mentioned, factors other than horizontal displacements may govern the core dimensions. In early design stages, the eigenfrequencies and accelerations of the core are relevant to study to ensure that the building's dynamic performance is acceptable. For residential buildings, there may be requirements on low accelerations in early design stages that could govern the structural design of the core for 80-130 m tall buildings. Thus, the tool would benefit from including calculations on accelerations. The tool already outputs periods and eigenfrequencies from ETABS, but implementations are needed to calculate the corresponding accelerations.

Although the required amount of reinforcement for the different designs showed not to have a large impact on the overall CO2e, there is nevertheless room for improvement in how the tool calculates the compressive reinforcement amounts. The tool computes the compressive reinforcement amounts by interpolation between pre-calculated values for certain wall thicknesses. This could be directly implemented in VBA so that there is no additional work outside of the script and for more accurate results.

A limitation of the tool is that the configuration of the door openings cannot be altered for each iteration. This means that once the door openings are defined, all core models will have the same door opening configuration until the script is finished. It could be relevant to study different door opening configurations, but as the script is currently defined, this has to be done by updating the door openings between each time the script is run. This is relatively easy to do, but the tool could be improved in how the core dimensions and door opening configurations are defined in Excel and VBA.

An interesting aspect to study further is the columns at the perimeter of the building. There is a potential in optimizing their dimensions and concrete class based on differential settlements. Since the core and columns undergo long-term axial shortening at different rates, this affects the levelness of the slabs. By considering long-term effects of concrete, similar CO2e studies can be performed to evaluate the required amount of concrete against the corresponding CO2e. Also, other column types such as steel columns or precast concrete columns can be analyzed to compare the effect of CO2e of different materials.

Additionally, a slab thickness optimization could also be performed. A larger core results in smaller spans between the core and the facade, which would logically entail thinner slab thicknesses compared to a smaller core with larger spans. Since the results from this thesis concluded that it is the amount of concrete in the core that has the largest climate impact compared to the reinforcement, there is a possibility to minimize the amount of concrete in the slabs by reducing their thickness based on the size of the core. This could show that the climate impact of the core directly affects the climate impact of other parts of the building as well.

Lastly, if any further developments are to be made to the tool, a suggestion is to store the extracted data from ETABS in a database instead of Excel. The performance of Excel is significantly affected by storing one million rows in several worksheets, which made the tool slower than necessary. A suggestion would be to work with a database in Python and potentially even scripting in Python instead of VBA. This is a potential way forward, but the usability and easy access to Excel should not be neglected.

8 Conclusions

The two tools have been successfully developed as intended. The Rhino/Grasshopper tool is useful in obtaining an understanding of how different geometrical parameters affect the structural performance and behavior of the core of a high-rise building. The changes in the behavior of the core are updated in real time, making the tool particularly valuable for users without a background in structural engineering. Furthermore, preliminary structural optimization can be performed, where minimum core dimensions that fulfill the maximum allowed horizontal displacement are outputted. It is important to bear in mind that these dimensions are unconservative, but they could act as a guideline for dimensions in very early design stages.

The ETABS/VBA tool is a valuable asset when comparing the structural performance and climate impact of different core dimensions and wall thicknesses. The tool allows both structural engineers and architects to visualize the climate impact of different designs on a level that is appropriate for both professions. Although the tool is useful in minimizing the CO2e of the core of a high-rise building, there are other aspects, such as economical and practical aspects, to consider. Therefore, it is important that the user is aware of other aspects that may affect the individual project when using the tool. In example, a design that has a low climate impact but is more expensive may not be the obvious choice in a certain project. In any case, the tool allows the user to reflect upon how different design choices affect the climate impact of the design.

The ETABS/VBA tool is directly applicable and useful in projects in the construction industry without the need for further development. The tool is therefore ready to be used in projects and can also serve as an encouragement for structural engineers to consider implementing parametric design in the early design stages of their projects. The time it takes to implement a similar tool is most likely earned in the time that is saved in future projects, and the chances of more optimized and efficient designs are also increased.

One of the objectives of the thesis was to identify key parameters that affect the structural stability of high-rise buildings. For a tall building with one centrally placed core, the core dimensions and core wall thicknesses have been identified to have a large impact on the structural stability. Particularly, the core wall thicknesses have a larger impact on the structural stability and total CO2e of the core than the core dimensions have. In addition, the core dimensions are greatly affected by the wind direction. A rectangular core with the strong bending axis placed in the wind direction is the best choice when the wind blows perpendicular to the core. In contrast, a square core is the best choice when the wind blows diagonally or from several directions. For other structural systems in high-rise buildings, other key parameters can be more impactful, but these structural systems have not been examined in this thesis.

8.1 Design Recommendations

The following statements are recommendations regarding the design of cores in high-rise buildings based on the conclusions drawn from this thesis.

- A large core with thinner walls has less climate impact and better structural performance than a smaller core with thicker walls.
- The core wall thicknesses have a larger impact on the CO2e of the core than the core dimensions have.
- The CO2e of reinforcement has a minimal effect on the total CO2e of the core, therefore the amount of concrete in the core walls can advantageously be reduced by increasing the amount of reinforcement.

9 References

Abu-Zidan, Y., Mendis, P., Gunawardena, T., Mohotti, D., Fernando, S. (2022): Wind Design of Tall Buildings: The State of the Art. *Electronic Journal of Structural Engineering*, 1, 2022

Al-Emrani, M., Engström, B., Johansson, M., Johansson, P. (2013): *Bärande Konstruktioner Del 1*. Chalmers Tekniska Högskola, 2013:1, Gothenburg, Sweden, 2013

Ascher, K. (2011): *The Heights: Anatomy of a Skyscraper*. Penguin Books, USA, 2013

Boverket. (2019, February 20): *Introduktion till livscykelanalys (LCA)*. Retrieved January 3, 2024, from https://www.boverket.se/sv/byggande/hallbart-byggande-och-forvaltning/livscykelanalys/introduktion-till-livscykelanalys-lca/

Christensen P., Klarbring A. (2002): *An Introduction to Structural Optimization*. Springer, Linköping, 2002

Computers & Structures, INC. (2023): *ETABS*. Retrieved December 20, 2023, from https://www.csiamerica.com/products/etabs/enhancements/21

Condit, W. C., Dalziel, D.H., Bach, Ira K., Siegel, S.A. (1980): *Chicago's famous buildings: a photographic guide to the city's architectural landmarks and other notable buildings*. University of Chicago Press, Chicago, USA, 3rd Edition

Cortese, D. (2018, July 18). What is a Skyscraper?. The B1M. https://www.theb1m.com/video/what-is-a-skyscraper

Council on Tall Buildings and Urban Habitat (CTBUH). (n.d.). Tall Building Criteria. Retrieved August 24, 2023, from https://www.ctbuh.org/resource/height#tab-tall-supertall-and-megatall-buildings

Council on Tall Buildings and Urban Habitat (CTBUH). (2024). Sweden. Retrieved January 2, 2024, from https://www.skyscrapercenter.com/country/sweden

Fu, F. (2018): *Design and Analysis of Tall and Complex Structures*. Matthew Deans, Oxford, United Kingdom, 2018

Göteborgs Stad. (n.d.): *Om Centralstaden*. Retrieved January 3, 2024, from https://centralstadengoteborg.se/om-centralstaden

Jahan, A., Edwards, K. L., Bahraminasab, M. (2016, February 12): *Multi-criteria Decision Analysis*. Elsevier, 2016

Jayachandran, P. (2009): Design of Tall Buildings Preliminary Design and Optimization. *National Workshop on High-rise and Tall Buildings*, May 2009

Marshall, A. (2015, April 2). The world's first skyscraper: a history of cities in 50 buildings, day 9. The Guardian. Retrieved August 24, 2023, from https://www.theguardian.com/cities/2015/apr/02/worlds-first-skyscraper-chicago-home-insurance-building-history

Ottosen, N., Petersson, H. (1992): *Introduction to the finite element method*. Pearson Education, 1992

Poulos, H.G. (2017): *Tall Building Foundation Design*. Taylor & Francis Group, Florida, USA, 2017

Robert McNeel & Associates. (n.d.): *Features*. Retrieved January 3, 2024, from https://www.rhino3d.com/features/

Rutten, D. (2011, March 4): Evolutionary Principles applied to Problem Solving [Blog Post]. Retrieved November 18, 2023, from Evolutionary Principles applied to Problem Solving | I Eat Bugs For Breakfast (wordpress.com)

Savic, D. (2002): *Single-objective vs. Multiobjective Optimisation for Integrated Decision Support*. International Congress on Environmental Modelling and Software. https://scholarsarchive.byu.edu/cgi/viewcontent.cgi?article=3734&context=iemssconference

Taranath, B.S. (2005): *Wind and Earthquake Resistant Buildings – Structural Analysis and Design*. Marcel Dekker, New York, USA, 2005

The Concrete Centre (2014): *Tall Buildings Structural design of concrete buildings up to 300 m Tall*, MPA The Concrete Centre and Fédération international du béton (fib), London, United Kingdom

United Nations. (n.d.): *The 17 Goals*. Retrieved January 3, 2024, from https://sdgs.un.org/goals

Yeang, K. (2007): *Eco Skyscrapers*. (3rd Edition). The Images Publishing Group Pty Ltd.

A. Rhino/Grasshopper Tool

The following pages show how the Rhino/Grasshopper tool can be used.

A.1 Required Installations

To use the tool, an installation of Rhinoceros 3D is required. The tool was implemented in Rhino 7, thus this version of the program is recommended to use. Three plug-ins to Grasshopper need to be installed; Human, Octopus and Karamba3D. Human and Octopus can be downloaded from food4rhino.com and Karamba can be downloaded from karamba3d.com. A pro license for Karamba is required for the tool to work properly.

A.2 Overview of the Tool

The tool consists of a Grasshopper file named *Parametric High-Rise Building (RhinoGrasshopper Tool).SSi*. When opening the Grasshopper file, Rhino is also opened automatically. The script in Grasshopper is divided into different sections such as input data, wind calculations, structural analysis etc, see Figure A.1 for the different sections. The user only needs to interact with the Input, Optimization in Octopus and Results (Values), although the input and results are also displayed in Rhino.

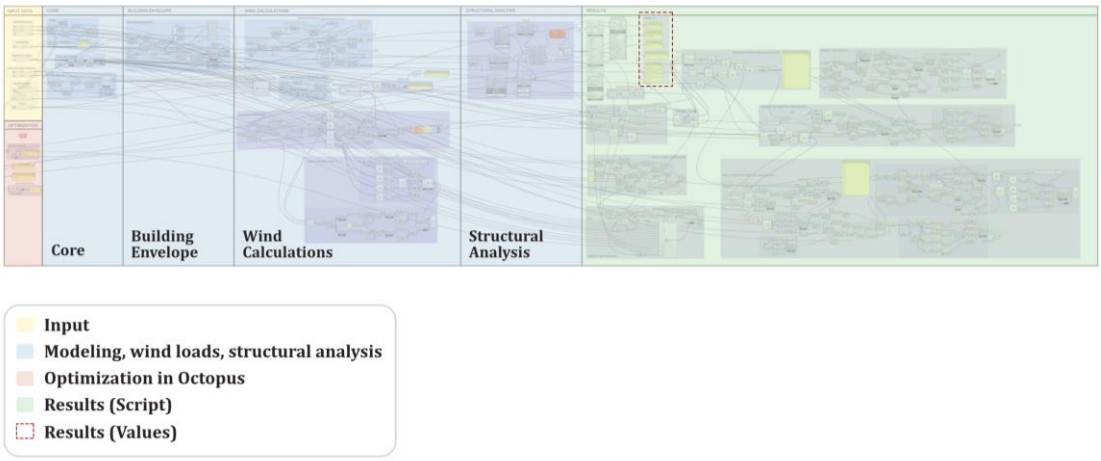

Figure A.1: The different sections of the Grasshopper file.

A.3 Input Data

There is a possibility of defining the input from either Rhino or Grasshopper. Figure A.2 shows where the input is given from Rhino, where the input panel is marked in red.

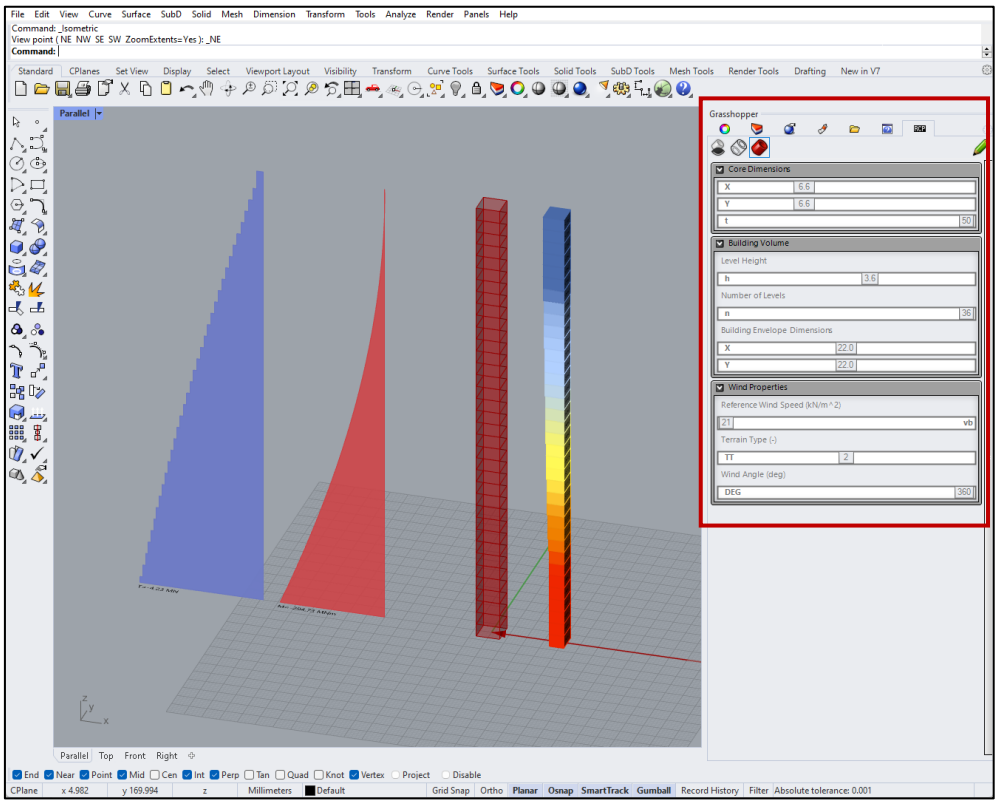

Figure A.2: The input panel in Rhino marked in red.

The user-defined input data is controlled by sliders with preset maximum and minimum values. The maximum and minimum values can be altered by the user if desired for a specific project. The sliders were previously presented in Table 4.1-4.5.

A.4 Optimization in Octopus

The optimization in Octopus can be found in the lower left section of the Grasshopper file. The pink component in Figure A.3 is the Octopus component. By double-clicking the Octopus component, a new window is opened and the optimization is run by pressing *Start*. The *G*-output of the Octopus component is connected to the genes, which in this case consist of the core wall thickness as well as the width and length of the core. The *O*-output is connected to the objectives, which in this case consist of the displacement residual and core area.

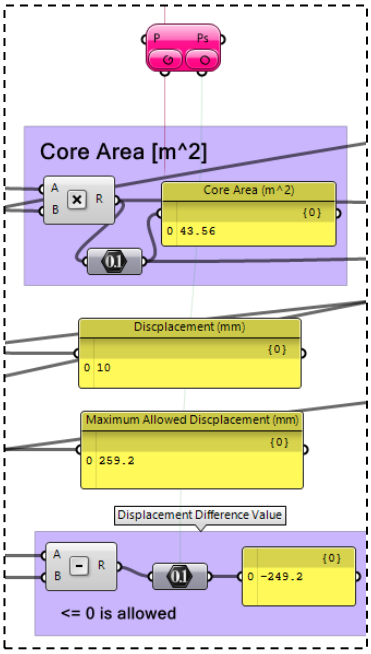

Figure A.3: Optimization in Octopus in the Grasshopper file.

B: ETABS/VBA Tool

The following pages show how the ETABS/VBA tool can be used.

B.1 Required Installations

To use the tool, an installation of ETABS is required. The tool was implemented in ETABS Plus v21, thus this version of the program is recommended to use. Excel needs to be installed on a Windows computer to be able to use VBA. If using a Mac computer, additional actions need to be taken to activate VBA in Excel. Lastly, Tableau needs to be installed with a license.

B.2 Overview of the Tool

The tool consists of a folder containing one file in ETABS, two files in Excel and one file in Tableau as seen in Figure B.1. The ETABS file needs to be opened before running the script in VBA. This specific ETABS file needs to be used in combination with the Excel file *Parametric_High-Rise_Building.SSi.* This is because the ETABS file has predefined load combinations, materials and piles. If using another ETABS file, some modifications to the script may have to be made for it to work properly.

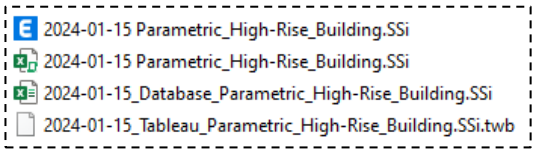

Figure B.1: The four different files that the ETABS/VBA tool consists of.

B.2.1 Excel

The Excel file named *Parametric_High-Rise_Building.SSi* is where the VBA script is embedded, the user-defined input data is given and the results are stored. The file consists of several worksheets which is where the input and output are stored. A selection of the worksheets is shown in Figure B.2 below.

Figure B.2: A selection of worksheets in the Excel file *Parametric_High_Rise_Building.SSi*.

The worksheets after *INPUT* are where the user defines geometrical properties of the building envelope and core, such as number of stories, core wall thicknesses, number of core openings, slab dimensions etc. The worksheets after *STORAGE* are where information such as labels, names and load combinations from ETABS are stored while the script is running. These worksheets do not contain any data relating to the results and the user does not need to bother about these worksheets. The worksheets after *RESULTS* store the results from each iteration. These are the worksheets where the contained data needs to be copied and stored in a separate Excel file to link the data to Tableau (see chapter B.3 for further instructions about the link between Excel and Tableau).

The worksheets after *PIERS* are related to the additional script where pier forces are computed for reinforcement calculations. These worksheets are only used if the additional script is run. The data stored in worksheets *Pier_forces_1-Pier_forces_10* need to be copied and stored in the separate database Excel file to link the data to Tableau.

Figure B.3 shows an extract of how the input regarding the core wall thicknesses for each wall model and story is defined in the worksheet *Models*.

Story	Model01	Model02	Model03	Model04	Model05	Model06	Model07	Model08	Model09
Story41	200	200	200	200	200	200	200	200	200
Story40	200	200	200	200	200	200	200	200	200
Story39	200	200	200	200	200	200	200	200	200
Story38	200	200	200	200	200	200	200	200	200
Story37	200	200	200	200	200	200	200	200	200
Story36	200	200	200	200	200	200	200	200	200
Story35	200	200	200	300	300	300	300	300	300
Story34	200	200	200	300	300	300	300	300	300
Story33	200	200	200	300	300	300	300	300	300
Story32	200	200	200	300	300	300	300	300	300
Story31	200	200	300	300	300	300	300	300	300
Story30	200	200	300	300	300	300	300	300	300
Story29	200	200	300	300	300	300	300	300	300
Story28	200	200	300	300	300	300	300	300	300
Story27	200	300	300	300	300	300	300	300	400
Story26	200	300	300	300	300	300	300	300	400
Story25	200	300	300	300	300	300	300	300	400
Story24	200	300	300	300	300	300	300	300	400
Story23	300	300	300	300	300	300	300	400	400
Story22	300	300	300	300	300	300	300	400	400
Story21	300	300	300	300	300	300	300	400	400
Story20	300	300	300	300	300	300	300	400	400
Story19	300	300	300	300	300	300	400	400	400
Story18	300	300	300	300	300	300	400	400	400
Story17	300	300	300	300	300	300	400	400	400
Story16	300	300	300	300	300	300	400	400	400
Story15	300	300	300	300	300	400	400	400	500
Story14	300	300	300	300	300	400	400	400	500
Story13	300	300	300	300	300	400	400	400	500
Story12	300	300	300	300	300	400	400	500	500
Story11	300	300	500	300	400	400	400	500	500
Story10	300	300	500	300	400	400	400	500	500
Story09	300	300	500	300	400	400	500	500	500
Story08	300	300	500	300	400	400	500	500	500
Story07	300	500	500	400	400	400	500	500	500
Story06	300	500	500	400	400	500	500	500	500
Story05	300	500	500	400	400	500	500	500	500
Story04	500	500	500	400	400	500	500	500	500
Story03	500	500	500	400	500	500	500	500	500
Story02	500	500	500	400	500	500	500	500	500
Story01	500	500	500	400	500	500	500	500	500

Figure B.3: An extract of the worksheet *Models* showing how the input regarding the core wall thicknesses for each wall model and story is defined.

Figure B.4 shows an extract of how the input regarding the core dimensions, core openings and local coordinates of the core is defined in the worksheet *Core*.

CORE DIMENSIONS			
	C1 [8,6 x 9,2]	C2 [8,8 x 9,6]	C3 [9 x 9,8]
Xcore	8,6	8,8	9
Ycore	9,2	9,6	9,8
CoreIndex	3		
TotCores	3		

DOORS		
	Door1	Door2
Length	1,2	1
Height	2,3	2,3

CORE OPENINGS (Local Coordinates)								
		Door Type	StartX/Y	XOpenS	YOpenS	ZOpenS	XOpenE	YOpenE
South	Open01	Door1	3,7	3,9	0	2,3	5,1	0
	Open02							
	Open03							
East	Open01	Door2	2	9	2,3	2,3	9	3,3
	Open02	Door2	6,2	9	6,5	2,3	9	7,5
	Open03							
North	Open01	Door1	4,9	5,1	9,8	2,3	3,9	9,8
	Open02							
	Open03							
West	Open01	Door2	7,2	0	7,5	2,3	0	6,5
	Open02	Door2	3	0	3,3	2,3	0	2,3
	Open03							

Figure B.4: An extract of the worksheet *Core* showing how the input regarding the core dimensions, core openings and local coordinates of the core is defined.

B.2.2 VBA and ETABS

As previously mentioned, the script in VBA is embedded in the Excel file named *Parametric_High-Rise_Building.SSi.* The script is written in several subs, where each sub performs a specific task. The sub *run_all* assembles all subs and runs the iterations of the core and wall models. The subs can be run directly in VBA by pressing *Run* or through macros in Excel. A selection of the macros in Excel is shown in Figure B.5 below. The sub *run_all_fine_walls* runs the additional script to obtain the pier forces. This script is computationally heavy as it divides the core walls into finer core walls.

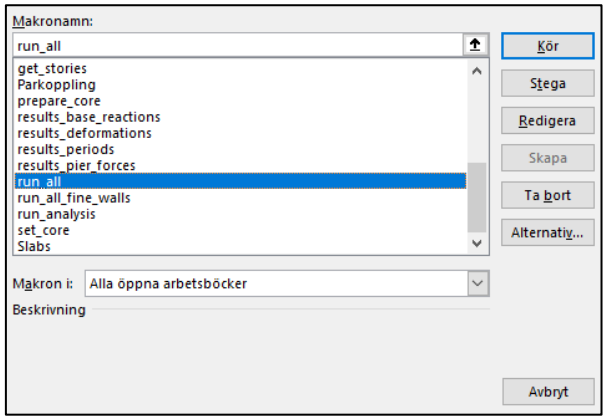

Figure B.5: A selection of the macros in Excel where the *run_all* macro is highlighted.

When the script in VBA is run, the building and core is automatically modelled in the running instance of ETABS as depicted in Figure B.6.

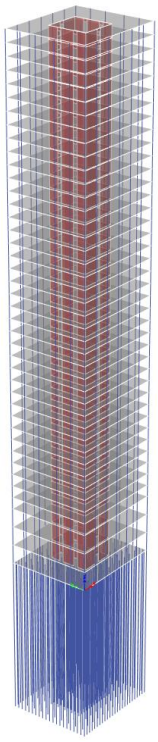

Figure B.6: The FE-model of the building and core in ETABS.

The script in VBA extracts the results from ETABS and stores the data in the worksheets after *RESULTS*. An extract from the worksheet *Deformations* is shown in Figure B.7, which is where the results regarding the deformations are stored.

RESULTS - DEFORMATIONS											
Core Model	Wall Model	Story	Name	Loadcase	Stepnum	ux	uy	uz	rx	ry	rz
C1 [8,6 x 9,2]	Model01	Story03	284	Wind	1	8,944791	0,032903	1,04127	-6,3E-07	0,000766	1,26E-05
C1 [8,6 x 9,2]	Model01	Story03	284	Wind	2	9,626255	9,603829	2,3128	-0,0008	0,00082	4,93E-06
C1 [8,6 x 9,2]	Model01	Story03	284	Wind	3	0,045827	10,19625	1,276802	-0,00086	-8,2E-07	-7,6E-06
C1 [8,6 x 9,2]	Model01	Story03	284	Wind	4	-9,53824	9,522445	0,08123	-0,0008	-0,00082	-1,3E-05
C1 [8,6 x 9,2]	Model01	Story03	284	Wind	5	-8,92268	-0,04024	-1,0411	3,67E-07	-0,00077	-1,8E-06
C1 [8,6 x 9,2]	Model01	Story03	284	Wind	6	-9,60795	-9,58449	-2,31216	0,000805	-0,00082	-3,1E-06
C1 [8,6 x 9,2]	Model01	Story03	284	Wind	7	-0,05294	-10,1793	-1,27671	0,000858	1,09E-06	-1,3E-06
C1 [8,6 x 9,2]	Model01	Story03	284	Wind	8	9,534158	-9,52634	-0,08153	0,000803	0,000822	1,18E-05
C1 [8,6 x 9,2]	Model01	Story40	182	Wind	1	185,595	0,737363	2,919244	-1E-05	0,001712	1,32E-05
C1 [8,6 x 9,2]	Model01	Story40	182	Wind	2	199,6779	187,0597	6,346247	-0,00171	0,001845	4,51E-06
C1 [8,6 x 9,2]	Model01	Story40	182	Wind	3	0,881299	198,6799	3,433495	-0,00181	1,15E-05	-8,1E-06
C1 [8,6 x 9,2]	Model01	Story40	182	Wind	4	-198,014	185,462	0,090982	-0,00169	-0,00182	-1E-05
C1 [8,6 x 9,2]	Model01	Story40	182	Wind	5	-185,558	-0,74869	-2,91953	8,49E-06	-0,00172	1,6E-06
C1 [8,6 x 9,2]	Model01	Story40	182	Wind	6	-199,648	-187,028	-6,34691	0,001714	-0,00185	-2E-06
C1 [8,6 x 9,2]	Model01	Story40	182	Wind	7	-0,89604	-198,652	-3,43376	0,001818	-9,7E-06	-3,9E-06
C1 [8,6 x 9,2]	Model01	Story40	182	Wind	8	198,0089	-185,468	-0,09093	0,001688	0,001825	9,6E-06
C1 [8,6 x 9,2]	Model01	Story39	183	Wind	1	180,3436	0,706615	2,914058	-2,4E-06	0,001732	1,79E-05
C1 [8,6 x 9,2]	Model01	Story39	183	Wind	2	194,0153	181,8211	6,33527	-0,00172	0,001857	5,18E-06
C1 [8,6 x 9,2]	Model01	Story39	183	Wind	3	0,843293	193,1241	3,427691	-0,00184	1,72E-06	-1,2E-05
C1 [8,6 x 9,2]	Model01	Story39	183	Wind	4	-192,424	180,2875	0,091095	-0,00172	-0,00185	-1,7E-05
C1 [8,6 x 9,2]	Model01	Story39	183	Wind	5	-180,303	-0,72	-2,91433	2,46E-06	-0,00173	-1,4E-07
C1 [8,6 x 9,2]	Model01	Story39	183	Wind	6	-193,982	-181,786	-6,33588	0,001724	-0,00186	-2,2E-06

Figure B.7: An extract from the worksheet *Deformations* showing how the results are stored.

B.3 Linking Excel to Tableau

To link the results in Excel to Tableau, the results need to be copied and stored in a separate Excel file (referred to as a database file). The database file is named *Database_Parametric_High-Rise_Building.SSi* and only consists of worksheets containing results. The names of the worksheets should not be changed, as this would require changes in the Tableau file. The specific Tableau file named *Tableau_Parametric_High-Rise_Building.SSi* needs to be used as this file contains pre-defined calculations and links between different labels. Figure B.8 shows where the database file in Excel needs to be linked to Tableau.

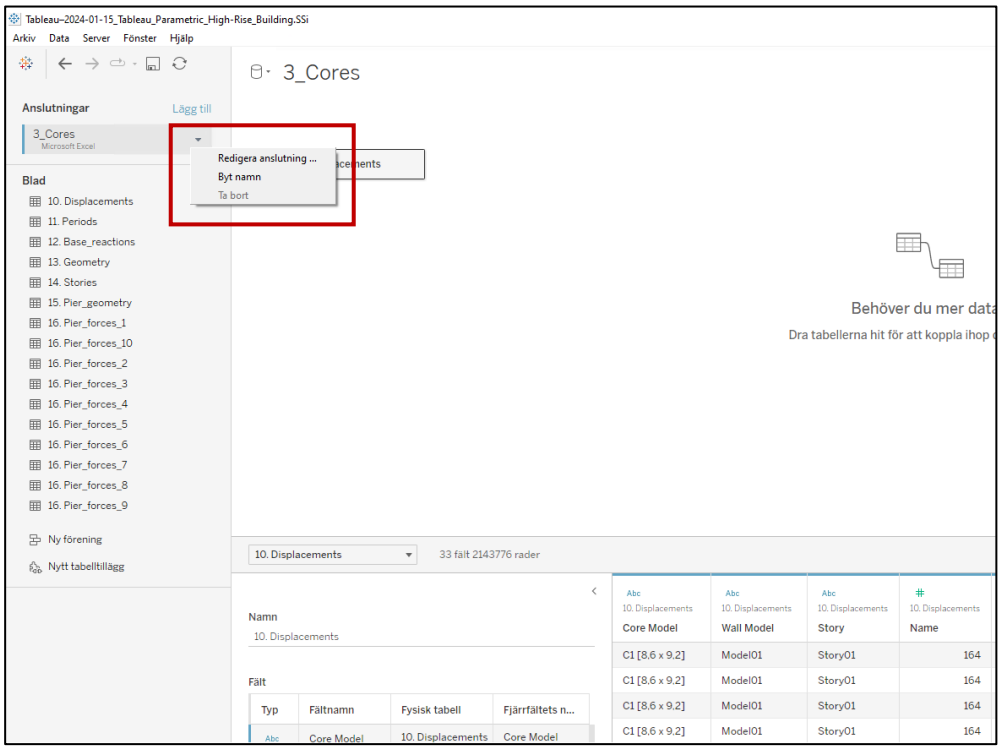

Figure B.8: An extract from the Tableau file showing where the database file in Excel needs to be linked to Tableau.

C: Hand Calculations

Moment and Deflection (129.6 m tall beam) - Rhino/Grasshopper Tool

```
# Input data
n = 36 # Number of levels [-]
h = 3.6 # Level Height [m]
XC = 7.1 # X-dimension of core [m]
YC = 7.1 # Y-dimension of core [m]
tC = 0.5 # Core wall thickness [m]
E =  33*pow(10,9) # Young's modulus for concrete type C30/37 [N/m^2]
w1 = 38.346*pow(10,3) # Wind load, max value at top of building calculated from GH-script [N/m]
w2 = 26.136*pow(10,3) # Wind load, max value at bottom of building calculated from GH-script [N/m]

# Calculate second moment of inertia around Y-axis [m^4]
Iy = (YC*pow(XC,3)/12)-((YC-tC*2)*pow((XC-tC*2),3)/12) # [m^4]

# Calculate Moment
My = ((w1*pow((n*h),2)/2)-((w1-w2)*pow((n*h),2)/6))/pow(10,6)

# Calculate deflection
u1 = ((w1*pow((n*h),4))/(8*E*Iy))*1000
u2 = (((w1-w2)*pow((n*h),4))/(30*E*Iy))*1000

u = u1-u2

print('Iy =', round(Iy,1), 'm\N{SUPERSCRIPT FOUR}')
print('My =', round(My,1), 'MNm')
print('Deflection = ', round(u,1), 'mm')
```

```
Iy = 96.4 m⁴
My = 287.9 MNm
Deflection =  389.0 mm
```

Moment and Deflection (21.6 m tall beam) - Rhino/Grasshopper Tool

```
# Input data
n = 6 # Number of levels [-]
h = 3.6 # Level Height [m]
XC = 7.1 # X-dimension of core [m]
YC = 7.1 # Y-dimension of core [m]
tC = 0.5 # Core wall thickness [m]
E =  33*pow(10,9) # Young's modulus for concrete type C30/37 [N/m^2]
w1 = 24.921*pow(10,3) # Wind load, max value at top of building calculated from GH-script [N/m]
w2 = 24.921*pow(10,3) # Wind load, max value at bottom of building calculated from GH-script [N/m]

# Calculate second moment of inertia around Y-axis [m^4]
Iy = (YC*pow(XC,3)/12)-((YC-tC*2)*pow((XC-tC*2),3)/12) # [m^4]

# Calculate Moment
My = ((w1*pow((n*h),2)/2)-((w1-w2)*pow((n*h),2)/6))/pow(10,6)

# Calculate deflection
u1 = ((w1*pow((n*h),4))/(8*E*Iy))*1000
u2 = (((w1-w2)*pow((n*h),4))/(30*E*Iy))*1000

u = u1-u2

print('Iy =', round(Iy,1), 'm\N{SUPERSCRIPT FOUR}')
print('My =', round(My,1), 'MNm')
print('Deflection = ', round(u,1), 'mm')
```

```
Iy = 96.4 m⁴
My = 5.8 MNm
Deflection =  0.2 mm
```

DEPARTMENT OF ARCHITECTURE AND CIVIL ENGINEERING
CHALMERS UNIVERSITY OF TECHNOLOGY
Gothenburg, Sweden 2023
www.chalmers.se

CHALMERS
UNIVERSITY OF TECHNOLOGY